UC Riverside

UC Riverside Electronic Theses and Dissertations

Title

The Production of High Levels of Renewable Natural Gas from Biomass Using Steam Hydrogasification

Permalink

https://escholarship.org/uc/item/6qh949sb

Author

Thanmongkhon, Yoothana

Publication Date

2014

Peer reviewed|Thesis/dissertation

eScholarship.org Powered by the California Digital Library
University of California

UNIVERSITY OF CALIFORNIA
RIVERSIDE

The Production of High Levels of Renewable Natural Gas from Biomass Using Steam Hydrogasification

A Dissertation submitted in partial satisfaction
of the requirements for the degree of

Doctor of Philosophy

in

Chemical and Environmental Engineering

by

Yoothana Thanmongkhon

August 2014

Dissertation Committee:
Dr. Joseph M. Norbeck, Chairperson
Dr. Robert C. Haddon
Dr. David Kisailus

Copyright by
Yoothana Thanmongkhon
2014

The Dissertation of Yoothana Thanmongkhon is approved:

_____

_____

_____

Committee Chairperson

University of California, Riverside

ACKNOWLEDGEMENTS

I would like to express my sincerest gratitude to my advisor, Professor Joseph M. Norbeck, for his consistent support, warm encouragement, insightful suggestions and scientific guidance during my research. The research turned to be interesting and successful under his instruction. I would also want to acknowledge Dr. Chan S. Park, my chief technical advisor, who introduced me to the field of renewable energy production. I thank him for giving me insightful new ideas about my research. Dr. Arun Raju and Dr. Kim, Postdoc in our group, gave me important guidance during my Ph.D. research. I am extremely grateful for his assistance. I express my earnest appreciation to my reading committee members, Professor Robert Haddon, Professor David Kisailus and my advance candidacy members, Professor Sharon Walker, Professor Gregory Beran, for their suggestions. I also wish to thank Junior Castillo and Sean Franco, who provided superb support and excellent work on the process demonstration unit of renewable natural gas production. They shared a plenty of time to involve in this project to help me complete this mission. I am grateful to my colleagues, Dr. Xiaoming Lu, Dr. Qian Luo, Dr. Xin Fan, Dr. Yang Li, Dr. Amornrat Suemanotham, Dr. Zhongzhe Liu and other members in our lab. They offered many valuable suggestion and useful discussions. I want to give my special thanks to my mother, my siblings and everyone in my family. Their endless love helped me overcome a lot of difficulties I met in my life. This study would not have been completed without their love and support.

Yoothana Thanmongkhon

ABSTRACT OF THE DISSERTATION

The Production of High Levels of Renewable Natural Gas from Biomass
Using Steam Hydrogasification

by

Yoothana Thanmongkhon

Doctor of Philosophy, Graduate Program in Chemical and Environmental Engineering
University of California, Riverside, August 2014
Dr. Joseph M. Norbeck, Chairperson

Renewable Natural Gas (RNG) has been identified as an important alternative fuel that can help to achieve a number of national goals related to the reduction of fossil fuels and to the reduction in carbon dioxide emission. RNG can be produced from various carbonaceous materials such as biomass and organic wastes via a gasification process. The CE-CERT steam hydrogasification technology combines hydrogen with steam under pressurized conditions to convert a wet feedstock to a methane enriched syngas which can be upgraded to RNG and used for electric power and as an alternative transportation fuel.

The main objective of this thesis is to develop a new process configuration of the steam hydrogasifier (SHR) using a water gas shift (WGS) reactor for the increased production of RNG in an economical manner. The producer gas from the SHR consists of H_2, CH_4, CO, CO_2 and steam. The WGS process converts CO using the existing steam in the product stream from the SHR to H_2 and CO_2. This results in a self-sustainable internal source of hydrogen that can be generated internally and of sufficient quantity to be recycled back to the SHR. In this study, a mixture gas comparable to the composition of

the producer gas from the SHR when using biosolids comingled with green waste was used as the input gas to the WGS reactor. A lab-scale WGS reaction system using a commercially available high temperature shift (HTS) catalyst was designed and built. The influence of temperature, space velocity, gas composition and particle size of catalysts on the conversion of CO using this system was investigated. It was found that at optimum conditions approximately 65% of the CO can be converted using the HTS catalyst operating at 350^{o}C and atmospheric pressure. The hydrogen produced at this condition was sufficient to be recycled back to the SHR. Also, the overall change of CH_4 production was negligible.

A mixture gas containing a wide range of H_2S was carried out in the shift reactor using a Sour Gas Shift (SGS) catalyst to determine the influence of sulfur impurities. The conversion of the mixture gas with 350ppm of sulfur was 55% at the reaction temperature of 450^{o}C and a space velocity of 2500h^{-1}, compared to 65% with no sulfur. The percent conversion of CO could be improved if the composition of CO_2 was decreased.

A larger scale HTS reactor was designed and built using the data from the experiments mentioned above. This was integrated into a bench scale Process Demonstration Unit (PDU) of the SHR with a capacity of 0.1TPD of dry feed. This process configuration demonstrated the production of high levels of RNG based for the CE-CERT technology using co-mingled biosolids and woody biomass as the feedstock. The reaction temperature of the SHR and WGS reactor were set at 750^{o}C and 350^{o}C, respectively, with an operating pressure at 150psi. A carbon conversion of 42% for the SHR and CO conversion of 60% of WGS were achieved at those conditions. The final product gas

contained over 85% of CH_4 after gas cleanup in which 85MJ/day or 32.6MJ/m^3 of energy was produced. This result clearly shows the viability of the process and provides critical design information to upscale to a pilot facility in the near future.

Table of Contents

Chapter 1 Introduction 1

1.1 Background 1

1.1.1 Traditional natural gas production 4

1.1.2 Hydraulic fracturing from shale gas 7

1.2 Renewable natural gas production 10

1.2.1 Renewable natural gas from biochemical processes 12

1.2.2 Renewable natural gas from thermochemical processes 15

1.3 Introduction of CE-CERT process for RNG production 18

1.4 Overview of water gas shift reaction and its application 20

1.4.1 Introduction to WGS reaction 20

1.4.2 WGS reaction in industrial applications 23

1.5 Energy recovery from biosolids 24

1.6 Thesis Objectives 26

Chapter 2 RNG Production from Steam Hydrogasification 29

2.1 Modeling of the RNG Production Process 29

2.1.1 Aspen simulation 29

2.1.2 Simulation results 32

2.2 Summary 44

Chapter 3 Development of WGS reactor for RNG process 46

3.1 Designing of Water Gas Shift Reaction System 46

3.1.1 Literature review of water gas shift catalysts 46

3.1.2 Selection of catalyst for the design and experiment 50
3.1.3 Laboratory scale setup of water gas shift reaction 51
3.1.4 Analysis Method 56
3.1.5 Conversion of WGS reaction 58
3.2 Investigation and optimization of WGS reaction 58
3.2.1 Experimental procedure 58
3.2.2 Experimental design and parameters 61
3.3 Result and Discussion 62
3.3.1 Influence of space velocity on the conventional WGS reaction 62
3.3.2 Influence of gas species on CO conversion in WGS reaction 64
3.3.3 Influence of reaction temperature, particle size and loading of catalyst 65
3.3.4 Reforming effects of CH_4 on WGS catalyst 71
3.3.5 Influences of gas composition on CO conversion 72
3.3.6 Influence of low steam to carbon ratio over HTS catalyst 78
3.4 An alternative process of RNG production for a high sulfur feedstock 79
3.4.1 Experimental setup for WGS reaction using sour gas shift catalyst 79
3.4.2 Influences of H_2S concentration on the performance of SGS catalyst 83
3.4.3 Influences of different gas distribution over sour gas shift reaction 86
3.5 Summary 92
Chapter 4 Process demonstration unit for RNG production 94
4.1 Thermochemical processes for RNG/SNG production from organic waste 94
4.2 Introduction of CE-CERT process demonstration unit (PDU) for RNG 96

4.2.1 Feedstock Pretreatment Unit (FPU) 96
4.2.2 Bubbling Fluidized Bed Gasifier 100
4.2.3 Design and construction of the water gas shift reactor 103
4.2.4 Product gas separation and analysis 105
4.3 Performance of PDU scale of RNG process 107
4.3.1 Computational result from a modified Aspen simulation model 107
4.3.2 PDU performance of SHR only operation 109
4.3.3 PDU performance of the SHR integrated with the WGS reactor 112
4.4. Summary 118
Chapter 5 Estimation of RNG Production by CE-CERT Technology 119
5.1 Process design methodology and evaluation 119
5.2 Availability of feedstock in Southern California 128
5.2.1 Biosolids availability 129
5.2.2 Biomass or green waste availability 131
5.3 Cost comparison with other RNG productions 134
5.4 Summary 137
Chapter 6 Conclusions and Recommendations 139
6.1 Conclusions 139
6.2 Recommendations 142
References 143
Appendices 153

List of Tables

Table 1-1 Typical Composition of Natural Gas 5

Table 1-2 A typical composition of untreated biogas in different plants 14

Table 2-1 Char fraction as a function of gasification temperature 31

Table 2-2 Composition of some feedstock used in the simulation 33

Table 2-3 Optimum H_2, H_2O and feed ratios and RNG HHV of various feedstocks 43

Table 3-1 Specification of ShiftMax®120 51

Table 3-2 Pressure drop in WGS reactor using different loading and particle size 70

Table 3-3 Chemical composition of some different feedstocks 73

Table 3-4 Composition of producer gas from SHR using different feedstocks 74

Table 3-5 Specification of ShiftMax®820 80

Table 3-6 Summary of the optimum condition from the lab-scale WGS reactor 93

Table 4-1 Composition of biosolids comingled with pine wood 99

Table 4-2 Specification of silica sand and ground silica 101

Table 4-3 Summary of the bubbling fluidized bed gasifier design parameters 101

Table 4-4 WGS fixed bed reactor design summary 105

Table 4-5 Composition of carbonaceous gas produced from SHR using comingled feed 112

Table 4-6 Overall performance of SHR only operation using comingled feed 112

Table 4-7 Percentage of gas component compared between input and output of WGS 117

Table 5-1 Unit operations specified in Aspen simulation 120

Table 5-2 Plant performance of three scenarios 126

Table 5-3 Gross biosolids production and availability for conversion in 2010 130

Table 5-4 Gross biosolids production and availability for conversion in CA 130

Table 5-5 Gross green waste production and availability for conversion in 2010 132

Table 5-6 Gross green waste production and availability for conversion in CA 132

Table 5-7 Technical available feedstock yields for RNG production in Southern CA ... 133

Table 5-8 Assumptions for the production cost calculation 134

Table 5-9 TPC of Steam Hydrogasification Process 135

Table 5-10 Comparison of the RNG producing processes 136

Table 5-11 Production cost of the different RNG producing processes 137

List of Figures

Figure 1-1 Prediction of global energy consumption in 2040 1

Figure 1-2 Projection of U.S. primary energy consumption and production in 2040 2

Figure 1-3 Annual average Henry Hub spot natural gas prices, 1990-2040..... 3

Figure 1-4 Simplified typical onshore treatment process 6

Figure 1-5 Conventional oil and gas production from the underground resources 7

Figure 1-6 Horizontal well in an underground rock layer with multiple fracture stages created by hydraulic fracturing 9

Figure 1-7 Practical potential RNG from the feedstock capability during 2035-2050..... 11

Figure 1-8 A typical key process stages of anaerobic digestion 13

Figure 1-9 General process of RNG production using a traditional gasification 15

Figure 1-10 Schematic diagram of RNG production using SHR system 19

Figure 1-11 Variation of equilibrium constant (K_p) for WGS reaction with temperature 21

Figure 1-12 Ammonia synthesis plant diagram: reforming, HTS, LTS 24

Figure 2-1 Gas composition from SHR using various feedstocks at 750^{o}C and 400 psi... 34

Figure 2-2 Influence of temperature on equilibrium composition of carbonaceous product gases from SHR using comingled feed (H_2O/Feed = 1.5, H_2/C_{Feed} = 1.0 at P = 400 psi) 36

Figure 2-3 Influence of pressure on equilibrium composition of carbonaceous product gases from SHR using comingled feed (H_2O/Feed = 1.5, H_2/C_{Feed} = 1.0 at T = 750^{o}C)..... 37

Figure 2-4 Simplified diagram of SHR configured with WGS reactor 38

Figure 2-5 Comparison of conversion between SHR and WGS at various H_2O/Feed mass ratio and H_2/C_{Feed} molar ratio equals to 1.0 (at T = 750ºC, P = 400 psi) 39

Figure 2-6 CH_4 yield and H_2 availability for recycle at various H_2O/Feed mass ratio and H_2/C molar ratio equals to 1.0 (at T = 750ºC, P = 400 psi) 40

Figure 2-7 Comparison of conversion between SHR and WGS at various H_2/C_{Feed} molar ratio and H_2O/Feed mass ratio equals to 1.5 (at T = 750ºC, P = 400psi) 41

Figure 2-8 CH_4 yield and H_2 availability for recycle at various H_2/C_{Feed} molar ratio and H_2O/Feed mass ratio equals to 1.5 (at T = 750ºC, P = 400psi) 41

Figure 2-9 CO conversion of WGS reaction at different temperature and pressure 42

Figure 2-10 Simulation results of SHR with WGS reactor using the co-mingling between biosolids and green waste as feedstock at the optimum condition 44

Figure 3-1 Schematic diagram of a lab-scale WGS reaction system 52

Figure 3-2 Configuration of internal WGS packed bed reactor 53

Figure 3-3 Experimental setup of the lab-scale water gas shift reaction 55

Figure 3-4 Cirrus ^{TM} Atmospheric Pressure Residual Gas Analyzer (RGA) 56

Figure 3-5 Temperature diagram for catalyst activation and process operation 60

Figure 3-6 CO conversion of various space velocities for the conventional WGS reaction at 350^oC 63

Figure 3-7 CO conversion of different gas composition in WGS reaction at 350^oC and space velocity of 4500 h^{-1} (S/C = 3 in (1) and S/C = 5 in (2)) 64

Figure 3-8 CO conversion of mixture gas, MG1, obtained from WGS reaction using various particle sizes and loading of catalyst at different temperature 66
Figure 3-9 Profile of the real time operation of WGS reaction using HTS catalyst at 350^{o}C and space velocity of 2500 h^{-1} 68
Figure 3-10 Gas distribution compared between input and output via WGS reaction at 350^{o}C and space velocity of 2500 h^{-1} 68
Figure 3-11 Mole of carbon balance of MG1 as dry basis compared between input and output via WGS reaction at 350^{o}C and space velocity of 2500 h^{-1} 69
Figure 3-12 Deviation of CH_4 flow rate compared between input and output of WGS system at different temperature 72
Figure 3-13 CO conversion of mixture gas, MG2, obtained from WGS reaction using various particle sizes and loading of catalyst at different temperature 75
Figure 3-14 Gas species as dry basis of MG2 compared between input and output via WGS reaction at 350^{o}C and space velocity of 4500 h^{-1} 76
Figure 3-15 CO conversion of WGS reaction at different temperature of a mixture gas produced from steam hydrogasification of coal 77
Figure 3-16 CO conversion of WGS reaction at 350^{o}C for different ratios of CO/CO_2 in mixture gas produced from steam hydrogasification 77
Figure 3-17 Gas species as dry basis of MG2 compared between input and output via WGS reaction at S/C = 1 (at 350-450^{o}C and space velocity of 4500 h^{-1}) 79
Figure 3-18 Schematic diagram of the RNG production using sour gas shift reactor 80
Figure 3-19 Schematic diagram of WGS reaction system using sour gas shift catalyst 82

Figure 3-20 CO conversion of MG1 contained the different concentration of H_2S operated at various space velocities (2500-10000 h^{-1}).....84
Figure 3-21 CO conversion of MG1 contained 350 ppm of H_2S at different temperature 85
Figure 3-22 CO conversion of mixture gases contained the different concentration of H_2S operated at 450^oC and space velocity of 2500 h^{-1} (20g of SGS catalyst) 86
Figure 3-23 CO conversion of MG2 contained 350 ppm of H_2S at 450^oC.....87
Figure 3-24 Gas distribution compared between input and output of sour gas shift reaction for MG2 contained 350 ppm of H_2S at 450^oC and space velocity of 2500 h^{-1} 88
Figure 3-25 CO conversion at different level of H_2S in feed gas for WGS reaction using HTS catalyst at 350^oC (at CO/CO_2 = 0.28 and 1.0) 90
Figure 3-26 Gas distribution compared between input and output of WGS reaction using HTS catalyst for MG1 contained 350 ppm of H_2S at 350^oC and space velocity of 4000 h^{-1} 91
Figure 3-27 Gas distribution compared between input and output of WGS reaction using HTS catalyst for MG2 contained 350 ppm of H_2S at 350^oC and space velocity of 4000 h^{-1} 91
Figure 4-1 Simplified diagram of SHR-WGS configuration.....96
Figure 4-2 Flow diagram of CE-CERT Hydrothermal Pretreatment (HTP) 97
Figure 4-3 Stirred batch type hydrothermal reactor.....98
Figure 4-4 Untreated and HTP treated samples of biomass comingled with biosolids.....99
Figure 4-5 Detail of the process diagram for SHR-PDU.....102

Figure 4-6 Detail of the water gas shift reactor for the PDU 104
Figure 4-7 Pictures of Process demonstration unit of RNG production at CE-CERT 107
Figure 4-8 Mass balance of the SHR-WGS process demonstration unit operated at 750^{o}C for gasification and 350^{o}C for water gas shift reaction underneath 150psi 108
Figure 4-9 Front panel display of SHR-PDU operating system 110
Figure 4-10 Real time of producer gas generated from SHR using biosolids comingled with pine wood as feedstock 111
Figure 4-11 Front panel display for SHR-WGS operating system 114
Figure 4-12 Real time operation of the demonstration unit of SHR-WGS using biosolids comingled with pine wood as feedstock 116
Figure 4-13, Comparison of the gas distribution between input and output of WGS reactor at 350^{o}C resulted from the operation of the PDU 117
Figure 5-1 Mass and energy balance of main processing units of SHR-WGS based process for RNG production in Case 2 127
Figure 5-2 Map of California with county lines defining Southern California 129

Chapter 1 Introduction

1.1 Background

Over 80% of the energy consumption in the world comes from fossil fuels (e.g. petroleum, natural gas and coal) [1]. Approximately 22% of the global energy used is Natural Gas (NG). The trend in energy usage by category is shown in Figure 1-1 [2, 3]. The consumption of natural gas is projected to grow by nearly 40% from 2010 through 2040 [3], and is the fastest growing fossil fuel compared to the others.

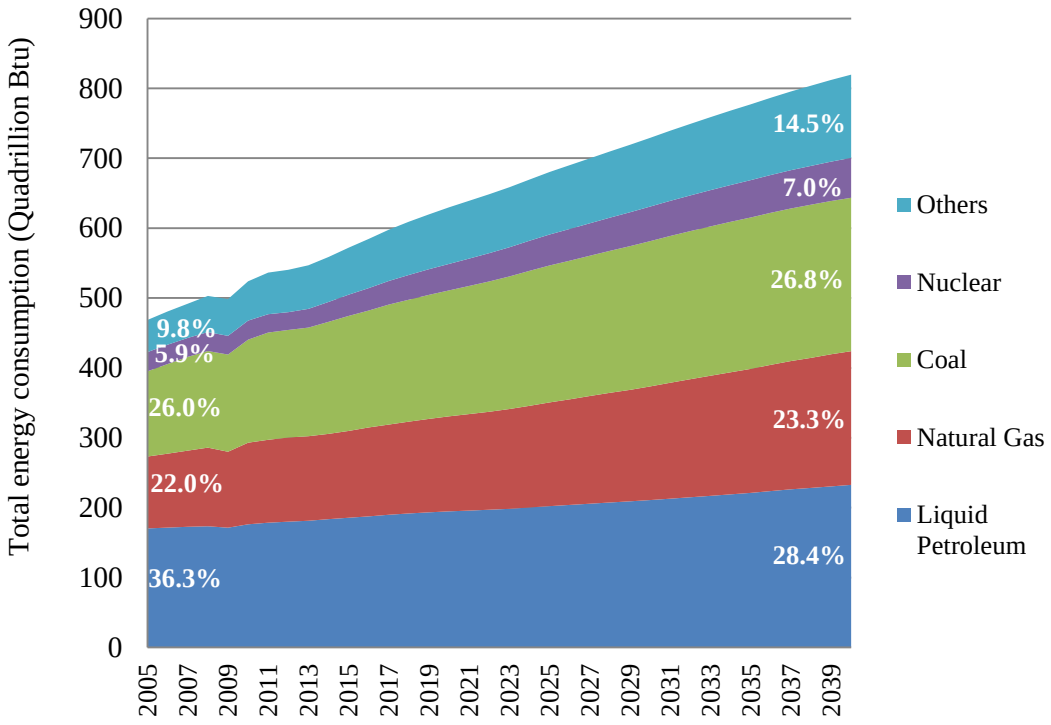

Figure 1-1 Prediction of global energy consumption in 2040

The total primary energy consumption in the United States will increase from 95 quadrillion Btu in 2012 to 106 quadrillion Btu in 2040 and NG will account for 30% of the total. See Figure 1-2 [4], US domestic consumption of natural gas is projected to increase from 25.6 to 31.6 trillion cubic feet (tcf) during 2012-2040. The largest share of the growth is for increased electricity generation. Demand for natural gas in the electric power sector will increase from 9.3 tcf to 11.2 tcf, with a portion of the growth attributable to the retirement of coal-fired power plant by 2021 [4].

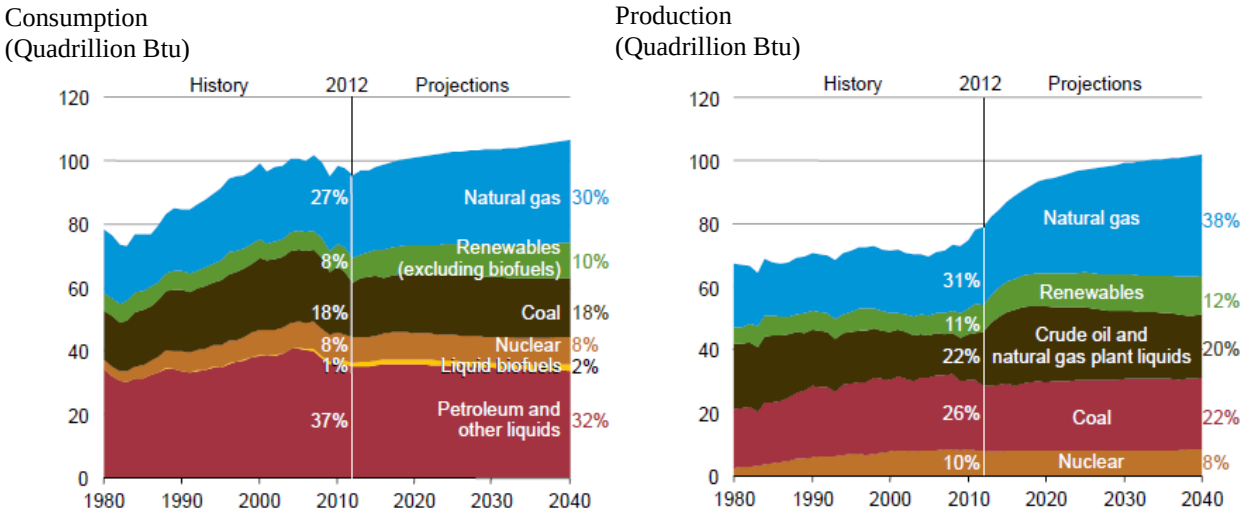

Figure 1-2 Projection of U.S. primary energy consumption and production in 2040

Natural gas production in U.S. is predicted to increase an average of 1% per year from 2011 to 2040 which should be sufficient to cover the domestic growth and even allow for some export [2, 3]. The growth in production is driven by the increase in the development on US shale gas resources and the application of horizontal drilling and

hydraulic fracturing. The domestic supplies are abundant and recent prices of natural gas have declined in the past several years. This has led the United States to reduce imports but lower prices have boosted purchases of U.S. natural gas and increase exports. Consequently, the United States is anticipated to becoming an overall net exporter of natural gas to 2018, as reported in the AEO2014 [4]. However, it is forecasted, based on annual average Henry Hub spot natural gas prices, that natural gas price is going to increase by an average of 2.4% a year, to $7.83 per million Btu in 2040. This trend is depicted in Figure 1-3 [2].

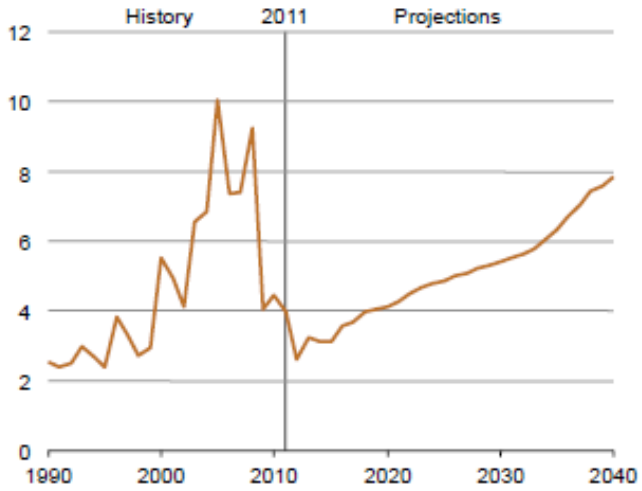

Figure 1-3 Annual average Henry Hub spot natural gas prices, 1990-2040

(2011 dollars per million Btu)

Natural gas is the cleanest and the most environmentally friendly fuel and has the lowest CO_2 emissions and pollutants per unit of energy. This makes it an attractive fuel source

in every country where the government is launching policies to mitigate greenhouse gas (GHG) emissions. The combustion of natural gas, depending on the quality of each fuel, results in at least 25-30% less CO_2 than oil and at least 40-50% less than coal [4,5]. Therefore, natural gas, either traditional or synthetic, is a reasonably promising fuel for new power generation plants and transportation [6].

The traditional process of natural gas production is discussed in the next section. This will be followed by a review of the sources of renewable natural gas and the technologies available to produce it which is the main focus on this thesis.

1.1.1 Traditional natural gas production

Natural gas is a fossil fuel formed when layers of buried plants, gases, and animals are exposed to intense heat and pressure over thousands of years. The energy that the plants originally produced from the sunshine is accumulated in the form of its chemical bonding. It is generally occurred as mixture gas found in the deep underground natural rock formation or associated with other hydrocarbon reservoirs and exists as a gas under atmospheric conditions. Natural gas is increasingly important as a primary energy source and continues to be favored as an environmentally attractive fuel because of its lower carbon intensity compared with coal and oil. It is the favorable fuel of choice for electric power generation, for industrial and domestic heating purposes, for feedstock of other chemicals, also as a transportation fuel (CNG or LNG).

Natural gas used by end consumers is composed almost entirely of CH_4. However, natural gas found at the wellhead, although still composed primarily of CH_4, is by no means as pure. Crude natural gas comes from three types of wells [7]: oil wells, gas wells, and condensate wells. Natural gas that comes from oil wells is typically termed 'associated gas'. This gas can exist separate from oil in the formation or dissolved in the crude oil. Non-associated gas is termed of the natural gas from gas and condensate wells, in which there is little or no crude oil. Gas wells typically produce raw natural gas by itself, while condensate wells produce free natural gas along with a semi-liquid hydrocarbon condensate. The typical composition of natural gas includes methane, ethane, propane and other hydrocarbons with a heavier molecular weight (in minor proportions) as displayed in Table 1-1 [8, 9]. Normally it also has low contaminants, such as nitrogen, CO_2, water, hydrogen sulfides and very small amounts of mercury primarily in elementary form.

Table 1-1 Typical Composition of Natural Gas

Name	Formula	Volume (%)
Methane	CH_4	70-90
Ethane	C_2H_6	0-20
Propane	C_3H_8	
Butane	C_4H_{10}	
Carbon dioxide	CO_2	0-8
Hydrogen sulfide	H_2S	0-5
Nitrogen	N_2	0-5
Oxygen	O_2	0-0.2
Rare gases	Ar, He, Ne, Xe	trace
Specific Gravity		0.57-0.62
Gross Heating Value (MJ/m^3), dry basis		36.0-40.2

Major transportation pipelines usually impose restrictions on the make-up of the natural gas that is allowed into the pipeline. Natural gas processing consists of separating all of the various hydrocarbons and undesired components from the pure natural gas to produce what is known as ‘pipeline quality’ dry natural gas. Practically, the processing is quite complex, shown in Figure 1-4 [10], but usually involves four principal processes to remove the impurities. These processes consist of the oil and condensate removal step, the water removal step, the separation of natural gas and liquids step, then the sulfur and CO2 removal step [7].

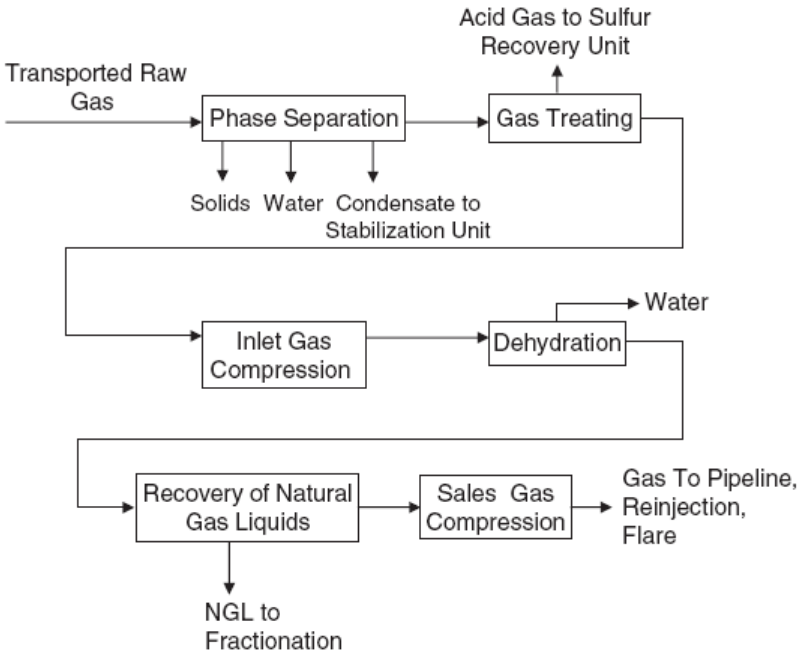

Figure 1-4 Simplified typical onshore treatment process

1.1.2 Hydraulic fracturing from shale gas

Shale gas refers to natural gas found in shale formations. Shales are fine-grained sedimentary rocks that can be rich sources of petroleum and natural gas. Over the last several years there have been a considerable increase in domestic natural gas production made plausible by two technologies that are used to tap into deep resources of natural gas that were thought to be inaccessible. The first is horizontal drilling, seen in Figure 1-5 [11], where a vertical hole can be branched into several horizontal cuts once the precise depth has been achieved. This is an important development because it largely mitigates the surface impact of drilling activities by providing access to more of the underground natural gas resources from fewer wells above ground [11].

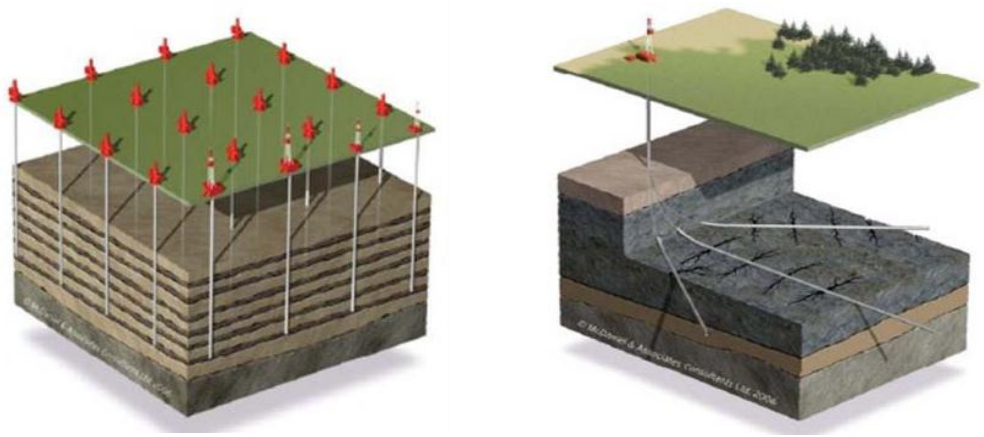

Traditional Well **Horizontal Drilling**

Figure 1-5 Conventional oil and gas production from the underground resources

The other technique that allows producers to safely recover natural gas and oil from deep shale formations is hydraulic fracturing. This procedure has been used by the oil and gas industry and has become a viable technology of natural gas and oil development worldwide since the 1940s. Hydraulic fracturing, generally known as "fracking" is a process for maximizing the extraction of oil and natural gas from underground resources. This technology uses hydraulic pressure to create fissures, or fractures, in shale rock formations to release natural gas and oil. The production of natural gas from shale formations has rejuvenated the natural gas industry in the United States, and shale production techniques could be applied globally [12].

Hydraulic fracturing, shown in Figure 1-6 [12, 13], takes place typically almost 1.5 miles below the earth's surface and many thousands of feet below freshwater formations. The process is minimally invasive and involves drilling a small hole (typically about 15'' in diameter), which is lined with multiple layers of steel encased in cement to seal off any fresh water supplies and to allow for the safe extraction of natural gas. Then pressurized liquids, commonly made up of 99.5% of water and sand and 0.5% of chemical additives, are injected to create small, often millimeter-thick fissures in the targeted sections of the shale rock formation. The newly created fractures are opened by the sand and kept from closing after the pressure is released in order to allow the natural gas and oil to flow into the wellbore and be collected at the surface. The fracturing fluids (water and chemical additives) are then returned back to the surface. Normally a hydraulic fracturing operation is only performed once during the life of a well [14].

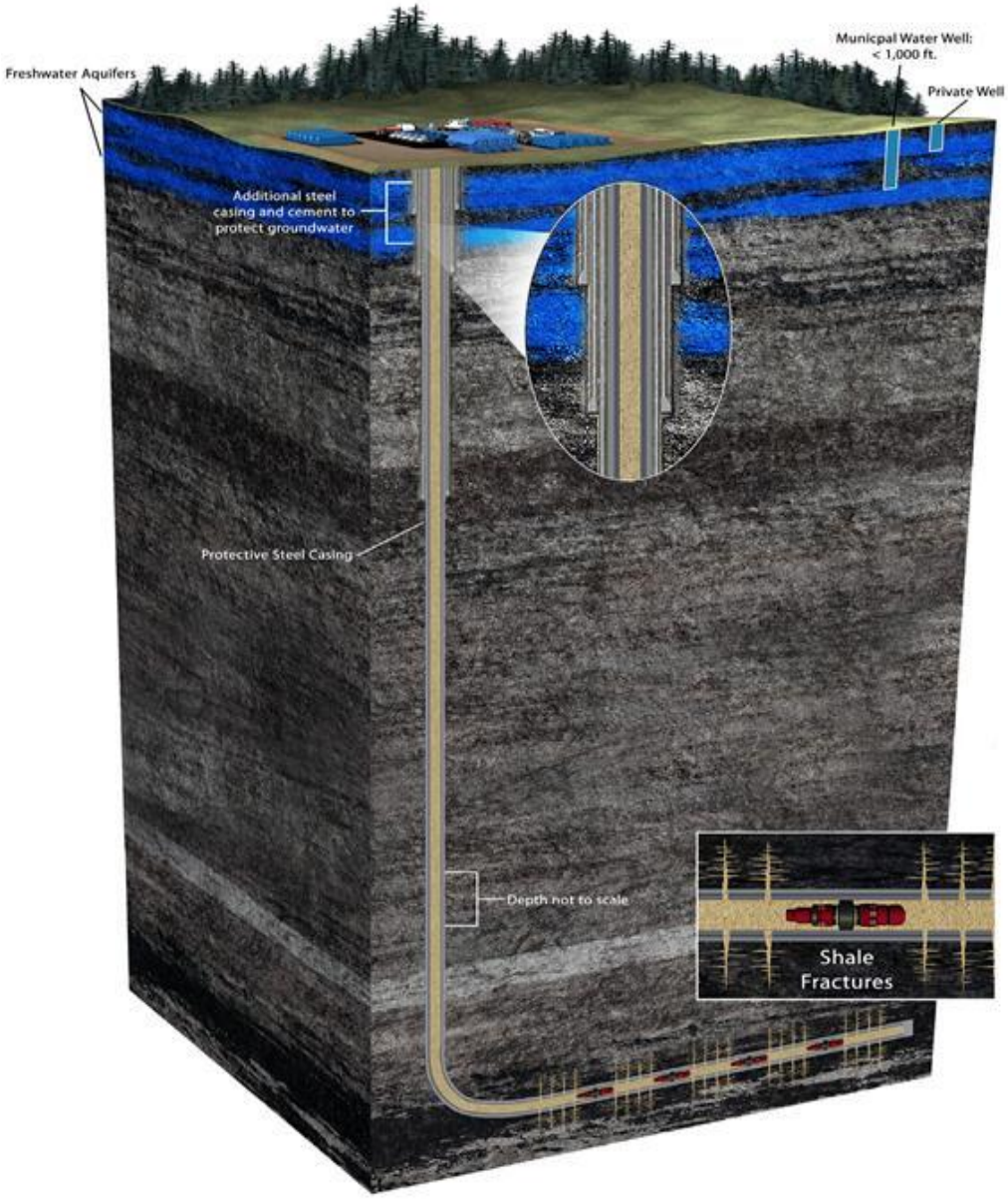

Figure 1-6 Horizontal well in an underground rock layer with multiple fracture stages created by hydraulic fracturing

Natural gas is considered a non-renewable resource because it cannot be replenished on a human time frame [15]. Biomass to fuel processes is viable because of abundant reserves in most places of the world and its environmental-friendly nature as a carbon sink [16-18]. Natural gas has the lowest carbon factor among the conventional fossil energy source (53 vs. 90-95 kgCO_2/MMBtu for other liquid fuels [19, 20]), but RNG from biomass has been identified as the lowest carbon fuel available (12-15 Kg CO_2/MMBtu [19, 20]) because of its carbon-neutralized aspects. Further utilization of any CO_2 from the process could generate negative carbon emissions. Today, U.S. has abundant cheap natural gas, but with expanded use as a transportation fuel and for electricity generation coupled with the challenges of global warming or climate change, renewable or substitute natural gas (RNG or SNG) has to be seriously considered to supplement or as a replacement to the conventional fossil fuel supply. It is also needed to reach 20% of biofuels replacement on petroleum following the goal of the United State biofuel consumption in 2020 [21-23].

1.2 Renewable natural gas production

Renewable Natural Gas or RNG is pipeline quality gas that is fully interchangeable with fossil natural gas and able to serve as 100% substitute for, or blended with, conventional gas streams applied in power generation or vehicle engines. Utilization of RNG presents an opportunity to convert marginal and zero-value waste products into a favorable transportation fuel. RNG is produced from a variety of organic wastes and/or biogas sources including landfill gas, solid waste, municipal wastewater, and agricultural

manure via purpose-built anaerobic digesters (AD) [24-26]. It can also be produced from biomass sources such as forestry and agricultural residue via the thermo-chemical process, i.e. thermal gasification (TG) [25, 27]. Estimates of the potential supply of RNG are dependent on various assumptions including future waste streams, biomass availabilities, conversion technologies, and process yields. A review of the current literature indicates that the practical RNG potential is approximately 4.8 trillion cubic feet per year or 40 billion gasoline gallon equivalents (GGE) per year. Figure 1-7 summarizes the revised estimates for total and practical biogas and biomass resources, the assumed yields and the resulting practical RNG potential that have been derived from a recent review of the literature [28].

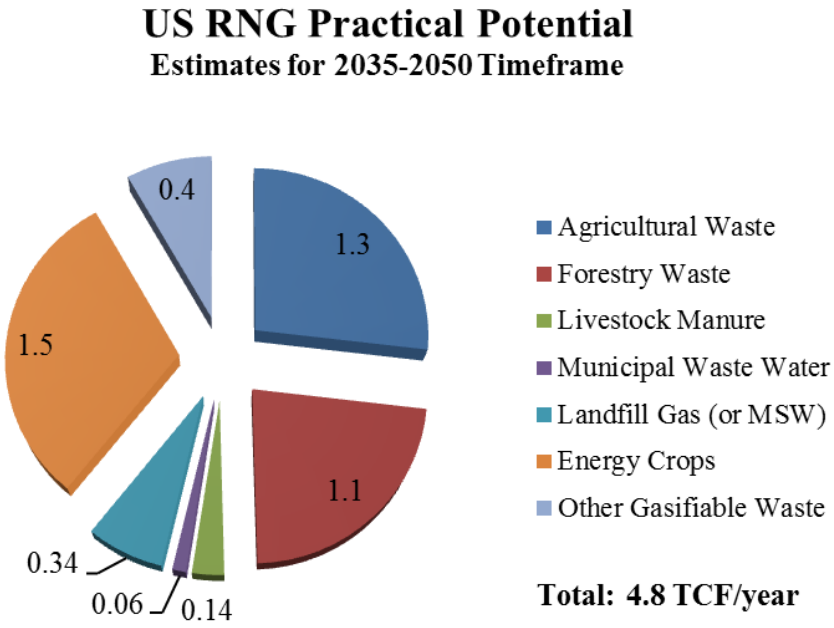

Figure 1-7 Practical potential RNG from the feedstock capability during 2035-2050

1.2.1 Renewable natural gas from biochemical processes

Anaerobic digestion is a process, where biodegradable organics materials are decomposed in an airtight container, and a biogas is accumulated after a certain period of time. This process is the most mature and popular technology used for the production of RNG from various kinds of feedstock such as biomass, food and municipal waste. An anaerobic conversion of any organic waste is biologically converted to CH_4, CO_2, and water. The stoichiometry of the reaction for anaerobic digestion is given below [29].

$$(C_nH_aO_{b)} + \left(n - \frac{a}{4} - \frac{b}{2}\right)H_2O \longrightarrow \left(\frac{n}{2} - \frac{a}{8} + \frac{b}{4}\right)CO_2 + (\frac{n}{2} + \frac{a}{8} - \frac{b}{4})CH_4$$

There are four key biological and chemical stages of anaerobic digestion as shown in Figure 1-8 and described below [30].

1. Hydrolysis is a process where complex organic molecules are broken down into simple sugars, amino acids, and fatty acids.
2. Acidogenesis is a stage for further breakdown of the remaining components by acidogenic (fermentative) bacteria. Here, volatile fatty acids (VFAs) are created, along with ammonia, CO_2, and hydrogen sulfide, as well as other byproducts.
3. Acetodenesis is a step where simple molecules created through the acidogenesis phase are further digested by acetogens to produce largely acetic acid, as well as CO_2 and hydrogen.

4. Methanogenesis is the terminal stage of anaerobic digestion. Here, methanogens use the intermediate products of the preceding stages and convert them into CH_4, CO_2, and water. These components make up the majority of the biogas emitted from the system. Methanogenesis is sensitive to both high and low pHs and occurs between pH 6.5 and pH 8. The remaining indigestible material the microbes cannot use and any dead bacterial remains constitute the digestate.

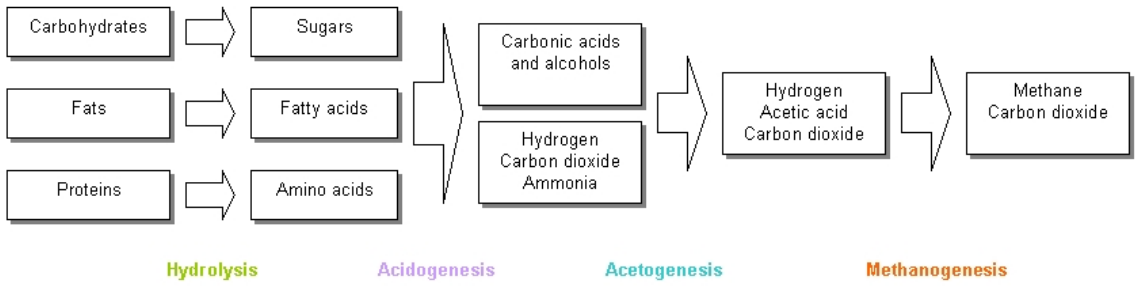

Figure 1-8 A typical key process stages of anaerobic digestion

The biogas plant technology is simple, but many practical details have to be considered in order to avoid interruptions and optimize production. Manure and organic waste are mixed in mixing tanks and from there pumped into the closed and stirred reactor tanks were it is heated and anaerobically digested. The digestion culture is self-sustaining after a start-up phase. The process is continuous, as a daily fractional extraction is replaced by new feed. The reactor productivity is significantly improved by the addition of organic waste. The average residence time is between 12 and 25 days depending on temperature, with shorter residence times for higher temperatures [30]. The operating temperatures

depend on the types of microrganisms used in the process. Thermophilic digestion processes that use theromophiles as the primary microorganisms operate around 55-60°C and mesophilic digestion that use mesophiles as the primary microorganisms and 35-40°C [31, 32].

The product gas is depended on the types of feedstock and operating conditions. Some typical biogas compositions are shown in Table 1-2 [33]. This biogas can be directly used as cooking fuel, in combined heat and power gas engines, or upgraded by purifying to natural gas-quality, termed of bio-methane, which is acceptable for injection into the existing pipeline structure. Most biogas is recovered from landfills, dairies and other livestock operation, or waste water treatment plants [34].

Table 1-2 A typical composition of untreated biogas in different plants

Component	Concentration	Farm biogas plant	Sewage Plant	Landfill
CH_4	%vol.	60-70	55-65	45-55
CO_2	%vol.	30-40	balance	30-40
N_2	%vol.	<1	<1	5-15
H_2S	ppm	10-2000	10-40	50-30

Based on the literature review [28], the amount of feedstock available for the production of RNG depends on several factors. About 180 million dry tons per year (or ~12%) of total biomass resources is available for current AD technologies. Also, about 4.5 billion GGE or 0.5 TCF of RNG per year is the practical potential from available resources for anaerobic digestion.

1.2.2 Renewable natural gas from thermochemical processes

RNG can also be produced from a series of biomass gasification and methanation processes, sometimes called Bio-SNG. Gasification is a thermochemical process normally used to convert organic or fossil based carbonaceous materials into CO, H_2 and CO_2. This is achieved by chemical reaction of the material at high temperatures, usually over 700°C, with a controlled amount of oxygen and/or steam [35]. The resulting gas mixture is called syngas or producer gas. Methanation, discovered in 1902, is a chemical process to synthesize CH_4 from a mixture of various gases from coal or biomass [36]. The main feedstock components that are fed into a methanation reactor are carbon monoxide and hydrogen to form methane and water following this stoichiometry.

$$CO + 3H_2 \Leftrightarrow CH_4 + H_2O \qquad \text{(Eq. 1-1)}$$

Figure 1-9 shows the general process of the RNG production via a traditional gasification which can be described following below [37].

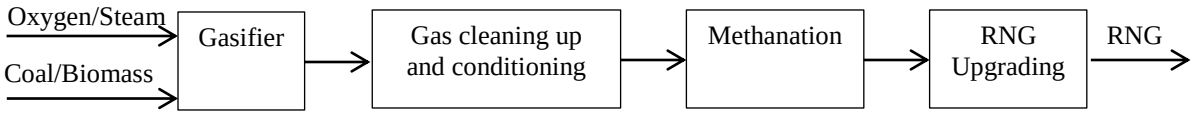

Figure 1-9 General process of RNG production using a traditional gasification

- *Gasifier*

The most common and important reaction process for converting coal or biomass to RNG is partial oxidation (POX). Steam, oxygen or air is used in the gasifier at high temperature in convert carbon (organic matter) into syngas. The gasification process primarily produces CO, H_2, CO_2, a small amount of CH_4, and higher hydrocarbons such as ethane and propane. The exact gas composition depends upon the operating conditions of the gasifier and the specific feedstock [38].

- *Gas conditioning and cleanup*

The syngas cleanup is done in two steps. First, the syngas from the gasifier is quenched and cooled, and the particulates and tar are removed. Then, the syngas is cleaned a second time to remove the acid gases H_2S and CO_2. The acid gas cleanup system uses either the Selexol or Rectisol process [39]. Both processes are based on physical absorption, which makes them more economical than the amine process which is used for CO_2 separation in power plants and based on chemical absorption.

- *Methanation*

CO and H_2 are converted to CH_4 and H_2O in a fixed bed catalytic reactor. The process is called methanation. Since methanation is an exothermic reaction, the increase in temperature is controlled by recycling the product gas or by using a series of reactors. Steam is added to the reaction to avoid coke formation in the reactor. After the steam and

other impurities are removed from the product gas by condensation and separation, the RNG is ready for utilization [40].

The other process of methane synthesis in a gasifier was originally developed in the early 1900s and there was a revived interest in the process during the 1970s and 80s because of increasing natural gas prices [41]. Via this process, hydrogen is used as a gasifying agent to directly produce methane from carbonaceous materials. This method is called Hydrogasification. The basic reaction is shown below.

$$C + 2H_2 \Leftrightarrow CH_4, \quad \Delta H \text{ at } 1000K = -89.9 \text{ kJ/mol} \qquad \text{(Eq. 1-2)}$$

Although this reaction is mildly exothermic, a significant amount of energy must be spent in bringing the reactants up to temperature and also to sustain the process. Methane production is favored at high pressures and temperatures ranging from 750-1000ºC [42]. A major barrier of the hydrogasification processes is the need to have an external source of hydrogen. Moreover, the much lower reactivity of carbon with hydrogen, compared to other gasifying agents such as oxygen or steam, resulted in this technology not to be very attractive [43].

Approximately 35 billion GGE or 4 TCF of RNG is the practical available mass from biomass sources suitable for thermal gasification [28]. The total practical potential of about 40 billion GGE or 4.8 TCF of RNG per year is available for both AD and TG conversion [28]. Resources such as woody biomass, agricultural crop waste, and energy

crops comprise about 80% of the current potential RNG inventory for gasification and compete with liquid biofuels production.

Thermochemical conversion technologies, such as combustion and gasification, are less suited for feedstock with high moisture content (e.g., municipal solid waste, food waste, biosolids from the waste water treatment facilities) when compared to anaerobic digestion. The University of California at Riverside's College of Engineering-Center for Environmental Research and Technology (CE-CERT) has developed a new process called Steam Hydrogasification. This process can utilize feedstock with high moisture content that would otherwise need to be dried in order to be used with conventional gasification and combustion processes.

1.3 Introduction of CE-CERT process for RNG production

The CE-CERT process can generate an energetic gaseous biofuels using Steam hydrogasification reaction (SHR) which is a key and innovative step in this process. One unique feature of the SHR is the use of a slurry feed which reduces the cost of drying the feedstock, typically required for most of conventional gasification technologies. This technology appears to be an attractive option for converting organic matters with high moisture, such as comingling of biomass and biosolids, MSW, food waste and algae, etc., into energetic products. Steam hydrogasification of carbonaceous material results in improved carbon conversion compared to normal hydrogasification [44, 45]. This process

can generate a product gas with a considerable amount of methane compared to that from the conventional partial oxidation technologies without external sources of oxygen or air as gasifying agents. Steam hydrogasifier (SHR) configured with a water gas shift (WGS) reactor presents a new process configuration to generate high quality gaseous fuel with a higher concentration of methane. The extra H_2 produced from WGS is then separated and recycle into the SHR in order to maintain the process with an internal self-sustainability of H_2. The basic overall reactions taking place during the process can be described below.

Steam hydrogasification:

$C + H_2O + 2H_2 \rightarrow CH_4 + H_2O + \text{others (CO, } CO_2, C_2+ \text{ etc)}$ (Eq. 1-3)

Water gas shift reaction:

$H_2O + CO \rightarrow CO_2 + H_2$ (Eq. 1-4)

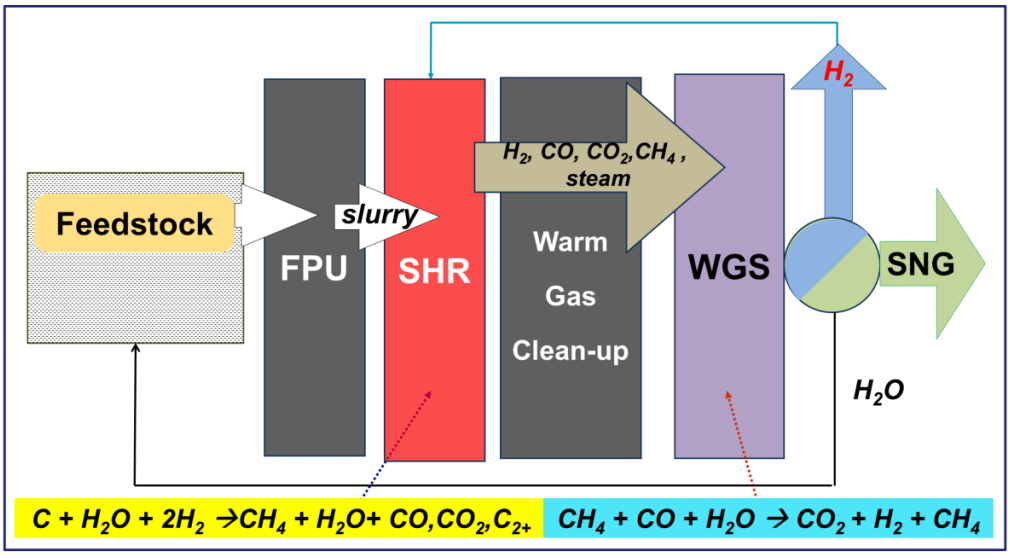

Figure 1-10 Schematic diagram of RNG production using SHR system

Figure 1-10 shows the process diagram involving the SHR process to produce RNG. A slurry made of the carbonaceous feedstock and water, along with the recycled hydrogen, is fed to the SHR operated at a favorable temperature and pressure. The SHR generates a high methane content product gas that is further subjected to warm gas cleanup unit in order to remove undesired impurities such as sulfur species. The gas cleanup unit needs to be performed at a temperature above the dew point of water. This will allow the excess steam co-existing with other product gases from the SHR to be directly fed into the WGS reactor. The amount of H_2 has been increased by the shift reaction using the presence of CO and steam in the clean gas feed. Methane is believably assumed to be inert and properly maintained in this reactor. This product gas is then cooled down to eliminate the moisture from the stream and the excess of H_2 is separated for recycle into the SHR. By this process, the issue of external hydrogen supply has been completely managed. Thus, the RNG with a high level of methane can be achieved after the upgrading by purifying process.

1.4 Overview of water gas shift reaction and its application

1.4.1 Introduction to WGS reaction

The water gas shift, WGS, reaction is an exothermic and reversible process in which water in the form of steam is reacted with carbon monoxide to obtain hydrogen and carbon dioxide following this chemical reaction.

$$H_2O + CO \Leftrightarrow CO_2 + H_2 \quad (\Delta H_o = -41.2 \text{ kJ/mol}) \qquad \text{(Eq. 1-5)}$$

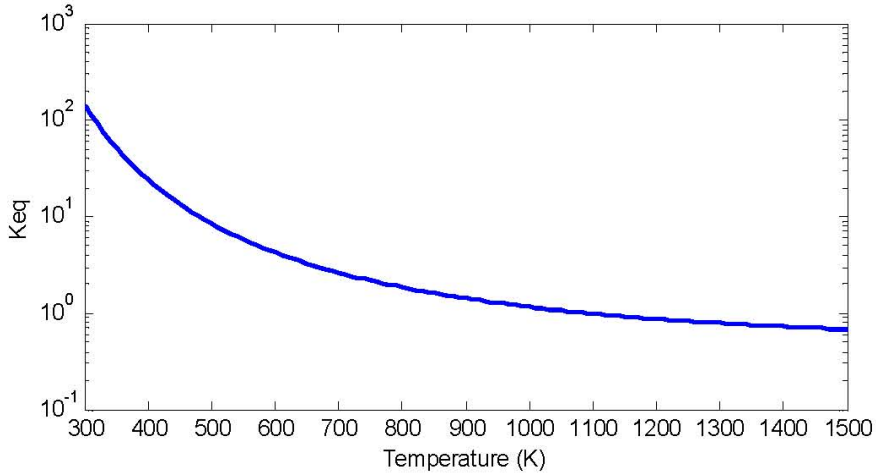

Figure 1-11 Variation of equilibrium constant (K_p) for WGS reaction with temperature

In Figure 1-11, the equilibrium constant, K_p, of the water gas shift reaction is defined by the below equation [46].

$$K_p = \frac{P_{H2}\, P_{CO2}}{P_{CO}\, P_{H2O}} \qquad \text{(Eq. 1-6)}$$

Due to its moderate exothermic reaction, the WGS reaction is unfavorable at elevated temperatures. However, the reaction is reversible and the exothermic nature increases the temperature. The forward rate is strongly inhibited by the products, H_2 and CO_2. This is illustrated by the continuous decreasing equilibrium constant as temperature, in Kelvin, given by equations as seen below [47].

$$K_p = \begin{cases} \exp[(4604/T)-4.3701] & \text{at about } 250^oC \\ \exp[(4546/T)-4.2939] & \text{at about } 440^oC \\ \exp[(3971/T)-3.670] & \text{at } 750\text{-}1050^oC \end{cases} \quad \text{(Eq. 1-7)}$$

To achieve a sufficiently high reaction rate, it is necessary to operate at higher temperature even though the equilibrium composition is not favorable under such conditions. The reaction proceeds without any change in the number of moles therefore the equilibrium composition would be independent on the operation pressure.

Three technical processes based on WGS reaction have been developed in the past 50 years. The reaction is sensitive to operation temperature and catalysts are required in order to obtain a high conversion of CO. A High Temperature Shift (HTS) reactor is able to be operated in the temperature ranging of 350-600^{o}C. An iron-based catalyst is typically used for industrial production [48]. An equilibrium CO concentration of 3-5% at the outlet has been achieved with this system. The average life time of the HTS catalysts is around 3 years. The catalyst activity declines with time because of the exposure of steam. A Low temperature shift (LTS) reactor operates between 190-300^{o}C and usually consists of a copper-based catalyst. This technology can achieve an equilibrium CO concentration as 0.1-0.3%. The life time of the LTS catalysts is average 2-4 years, depending on the operating conditions and the purity of the feed. Both types of catalysts

require a sulfur-free gas to avoid poisoning on the catalysts [48]. A sour gas shift, Co-Mo based, catalyst has been developed for industrial applications for the conversion of raw gases containing sulfur and traces of hydrocarbons produced from coal or crude oil gasification without cleanup. This catalysts are normally activated using hydrogen at 400-500^{o}C containing 1-6 vol.% of H_2S. The operating temperature is 230-450^{o}C with typical life time of 2 years [48]. A number of noble metal supported catalysts have been investigated for the shift activity, for example, Pt-based or Au-based, catalyst. The reactivity has been studied at the temperature ranging of 270-380^{o}C. However, most of these studies are for laboratory use only [49].

1.4.2 WGS reaction in industrial applications

Two stage CO conversion systems employing WGS using Fe/Cr oxide catalysts and methanation using nickel based catalysts between the stages was the common and economical technology for ammonia synthesis gas up to the late 1950s. Most of these plants employed a Fe/Cr oxide high temperature shift catalyst as well in the second stage converter at temperatures as low as 320^{o}C. The conventional HTS catalysts worked extremely well in these applications. The success of these catalysts at low temperature led to its use as a second, lower temperature bed. This became the basis for the next evolution in ammonia plant design. The two stage converter systems easily and consistently reduced the CO level to 3000–4000 ppm compared to the single stage converters that could not reduce the CO to much less than 1% [50]. Today WGS takes place with a series of adiabatic converters. The effluent from the reformer system is

converted in two steps with the second at a significantly lower temperature in order to shift the equilibrium towards the favored hydrogen product as shown in Figure 1-12 [50].

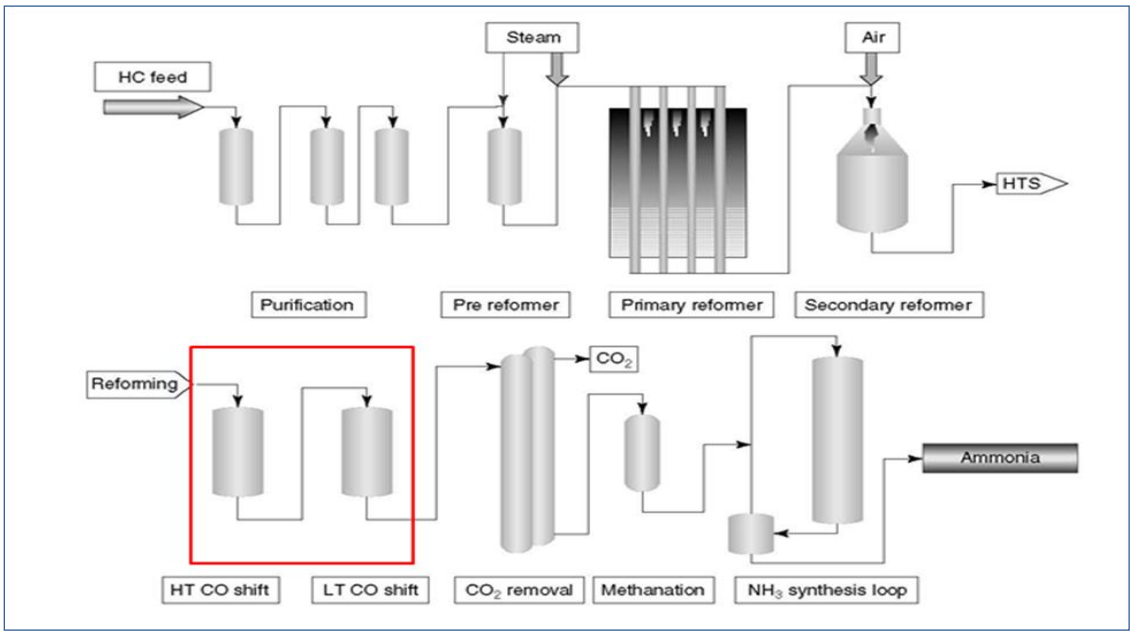

Figure 1-12 Ammonia synthesis plant diagram: reforming, HTS, LTS

1.5 Energy recovery from biosolids

Biosolids, or sewage sludge, is the by-product from municipal waste water treatment facilities. It contains various carbon residues, high water content and numerous metal elements. More than 16,500 publicly owned wastewater treatment works (POTWs) in US, has generated over 8 million dry tons of biosolids annually [51]. About 60 % of annual biosolids is disposed through land applications such as fertilizer in agriculture or direct landfill after drying [52]. Biosolids disposal exhibits a rising challenge as a result

in environmental concerns. In particular, high accumulation of toxic heavy metals in soil and groundwater caused by land applications and landfill leachate has become a major concern [53, 54]. Presently, the increase of biosolids has led to higher legal restrictions regarding disposal with environmental-friendly and cost-effective management [55-57]. Benefits of energy recovery from biosolids have become very attractive.

There are many studies published regarding clean energy production using biosolids or sewage sludge as feed. Wen-Tien Tsi [58] characterized the energy recovery using only dried biosolids from different waste water treatment plant in Taiwan and estimated the potential of waste-to-energy via thermochemical process during 2004-2010. It was reported that 1,100 TJ/year or almost 1.9 x 10^5 barrels of oil equivalent could be recovered. Nipattummakul et al. [59] studied the production of H_2 and Syngas using sewage sludge via steam gasification. It revealed that increasing of reactor temperature resulted in promotion of H_2 with the yield of 0.076 g_{gas} g_{sample}^{-1} at 1000 °C was. Steam gasification enhanced the H_2 yield three times as compared to air gasification. Sewage sludge yielded more H_2 than that from paper and food wastes. Saw et al. [60] found that the syngas produced from the biosolids, using a dual fluidized bed steam gasifier, had higher H_2 content (28%) compared with that from pure wood (23%) and the H_2 content increased with the percentage of biosolids loadings in mixed feed. The syngas yield and the cold gas efficiency of the gasification using wood and biosolids decreased dramatically by 53% and 43%, respectively. There are a large number of studies using biosolids in gasification, most of them have still required drying of the feedstock.

One of the most attractive benefits of the SHR process is the capability of using wet materials in the system. The CE-CERT gasification research group has developed an alternative approach for biosolids energy recovery using the SHR [61]. Biomass, municipal solid waste, woody or green waste can be co-mingled with biosolids waste stream to form a homogeneous slurry using as a raw feed for the steam hydrogasification process to generate energetic gaseous products. With more than 90% of moisture content in biosolids [62], the co-mingling of woody biomass or another form of carbonaceous material is able to achieve a desired mass ratio between dry feed and water. Compared to other gasification technologies, steam hydrogasification offers an advantage for biosolids removal by the elimination of the feedstock dying process that causes high cost and energy consumption. Wood or green waste mixed with biosolids has been chosen as one of the target feedstock as a potential commercial application for this process. The feedstock is readily available with ease of accessibility, low or moderate seasonal variation and homogeneity characteristics of the feedstock. Therefore, biosolids co-mingled with woody biomass, or green waste, can be a potential source of feedstocks for producing an environmental sustainable source of high quality of RNG.

1.6 Thesis Objectives

The major goal of this dissertation is to develop an efficient and economical process for production of Renewable Natural Gas from sustainable feedstock (biosolids co-mingled with green waste was chosen as example) using the CE-CERT steam hydrogasification

process. The research will investigate the effect, and evaluate the performance, of different commercial catalysts used in the WGS reaction. A demonstration unit for RNG production will be built and tested. A computational model for analysis of performance and economic viability of a commercial scale RNG production facility will be studied. The following objectives will be accomplished as part of the research effort.

1. The first objective of this thesis is to study the water gas shift reaction using commercial high temperature and sour gas shift catalysts for production of hydrogen and RNG from biomass-derived syngas. Their catalytic performances will be investigated via a laboratory scale WGS reactor. The WGS reactor will be operated using conditions obtained from modeling. The simulation model Aspen Plus will be used to assist in determining the flow rate and composition of the product gas stream from the SHR within the capability of the lab-scale facility. Experiments will be conducted under various experimental conditions such as pressure, temperature, steam/gas ratio, and amount of catalysts loading. The presence of CO, CO_2, CH_4, H_2 and steam in the WGS reactor is needed to relate with the steam hydrogasification feed parameters, i.e., H_2/C mole ratio and H_2O/Feed mass ratio those will be included in the analysis. The highest CO conversion at the optimum conditions will be determined. The optimal results will be used to assess the overall performance, characteristics and process conditions of RNG production.

2. The second objective is to develop a simulation model for the RNG production process using the CE-CERT technology and biomass feedstock. The Aspen Plus simulation software will be used to manipulate and study the production behavior of RNG process. The optimal operation parameters based on the experimental results will be used to simulate the overall process model in order to scale up the WGS reactor connected with the SHR to work as a Process Demonstration Unit (PDU) of RNG production. It is significant to note that the sustainability of hydrogen within the system is needed to be maintained under all operating conditions which is a critical characteristic of the CE-CERT technology. Finally, the performance of the demonstration unit of RNG will be evaluated.

3. The production of RNG also can be produced via an anaerobic digestion system. This is considered a very mature technology and is used to generate biogas, sometimes called bio-methane. This biological process is carried out by bacteria, in a humid environment and the absence of air, in which organic material is broken down into a stable fertilizer and useful methane. The third objective of this research is to compare the production cost of natural gas using the CE-CERT gasification technology with those obtained using the conventional anaerobic digestion facilities.

Chapter 2 RNG Production from Steam Hydrogasification

2.1 Modeling of the RNG Production Process

The CE-CERT gasification technology can produce an energetic gas that contains a high percentage content of methane. This is a consequence of steam-gasifying carbonaceous matter in a hydrogen environment. The water gas shift reaction combined with steam hydrogasification has the potential to produce an even higher percentage of renewable natural gas (methane), RNG, when using renewable carbonaceous feedstock. The CE-CERT gasification laboratory has developed a process demonstration unit (PDU) for RNG production from sustainable organic materials such as food waste, biosolids or biomass. A computer simulation of the overall gasification process would be very valuable tool to determine: (1) specific conditions of the reactor such as temperature, water/carbon ratio, and optimum amount of hydrogen; (2) an estimate of the maximum conversion of RNG possible for economic analyses; and (3) the specific design of the reactor that will be used for commercial applications.

2.1.1 Aspen simulation

Simulation can provide useful guidelines for the design of both laboratory scale reactors and commercial facilities. Critical information such as feed composition, reaction temperature and pressure, and flow rates can be optimized via simulation models. This can minimize “trial and error” experiments and costs. The Aspen Plus software package will be used for this purpose and discussed further below.

A process model using Aspen Plus (ASPEN Inc., 2011) has been developed and used to estimate overall process behavior, energy and mass balances. The Peng–Robinson equation of state within Aspen Plus was used to estimate the physical properties for gasification and further downstream unit operations. It is a recommended standard method by Aspen Plus when high temperature and pressure of hydrocarbon gas processing is involved [63]. This model simulates the steam hydrogasification process with a decomposition unit and a gasification unit. These are based on built-in Aspen reactor blocks and are used to calculate the equilibrium composition in the reactor under the specific conditions by means of Gibbs free energy minimization of the species present. The decomposition block breaks the non-conventional feedstock such as biomass or coal into its basic elements such as C (solid), H_2, O_2 and N_2 on the basis of yield using the RYIELD block. The gasification block calculates the equilibrium product gas composition using the RGIBBS block. The feedstock is assumed to be completely well-mixed with water and in a slurry form. The feed is injected into the gasifier along with hydrogen at a predetermined H_2/C by mole and H_2O/Feed by mass ratios. The composition and flow rates of the feed, the operating conditions of the reactors and the carbon conversion definitions are determined by the user [64]. All data obtained from experiment and the results of the simulation were largely in agreement with each other. The major assumptions used in this Aspen model are listed below.

1. Process is steady state and isothermal.
2. No heat and mass loss during the whole simulation process.
3. No tar generated in the steam hydrogasification process.

4. The char remaining is combusted and used as a source of energy to provide the process heat for the SHR.

According to previous preliminary research [65], higher gasification temperatures lead to higher carbon conversion efficiency (as expected) but also decreased the amount of char which is available as a heat source for the process. Char production from the SHR is assumed to be a function of gasification temperature even though there is some influence of H_2, H_2O or steam in the feed. From the earlier study in this research group, the fractions of leftover char generated from steam hydrogasification at the temperatures range between 650 to 850^oC are listed in Table 2-1 [66]. The gasifier was set at an operating pressure at 400 psi.

Table 2-1 Char fraction as a function of gasification temperature

SHR Temperature (^oC)	Leftover char (%)
650	35.2
700	21.7
750	17.9
800	13.8
850	9.2

It was decided to use a built-in module in Aspen of an isothermally equilibrium reactor to model the water gas shift reaction as given below.

$$H_2O + CO \Leftrightarrow CO_2 + H_2 \quad (\Delta H_o = -41.2 \text{ kJ/mol}) \qquad \text{(Eq. 2-1)}$$

The overall simulation process uses FORTRAN routines (calculator blocks) developed by our gasification group. The results from Aspen Plus are exported to an EXCEL worksheet where the overall mass and energy balances, product yields, carbon conversion and process thermal efficiency are calculated. Since the process heat required by the SHR is provided by a regenerator and the WGS is an exothermic reaction no further external heat is necessary. Chemical conversion efficiency and overall thermal efficiency used in the simulations are defined by the equations shown below.

- Chemical conversion efficiency in SHR = $(C_{feedstock} - Cco_2 - C_{char})/C_{feedstock}$
- Chemical conversion efficiency in WGS = $(CO_{in} – CO_{out})/CO_{in}$
- Overall thermal efficiency = Thermal energy of RNG/Thermal energy of feedstock input.

2.1.2 Simulation results

The results from the Aspen simulation of the product gas distribution and performance of RNG production via the CE-CERT gasification process using different feedstock are presented below.

- *Characteristics of the different feedstock*

The chemical composition of each feedstock such as coal, green waste (pine wood was used as an example) and comingled feedstock of biosolids and green waste used in these simulations are given in Table 2-2 [67].

Table 2-2 Composition of some feedstock used in the simulation

	Compound	Bituminous coal	Green waste	Biosolids	Biosolids mixed with Green waste
Proximate	Volatile Matter	40.00	86.39	60.25	80.98
	Fixed Carbon	49.45	13.33	10.00	16.67
	Ash	10.55	0.28	29.75	2.35
Ultimate	C	68.85	47.55	36.68	48.37
	H	4.74	6.31	5.39	5.95
	O	13.43	45.80	20.83	42.72
	N	1.04	0.05	5.79	0.46
	S	1.39	0.01	1.56	0.16

HHV of bituminous coal: 26.5 MMBTu/ton

HHV of green waste (pine wood): 18.1 MMBTu/ton

HHV of biosolids: 15.3 MMBTu/ton

HHV of comingled feed of biosolids and green waste: 18.2 MMBTu/ton

- *Composition of producer gas from SHR*

The composition of the dry gas produced from the SHR at the optimum feed ratio for H_2, H_2O and dry feedstock is given in Figure 2-1. The operating conditions for the SHR in the simulation model were set to 750^oC and 400psi. The gas distribution show that the content of CH_4 in the producer gas from coal is about 30% and greater than that generated from biomass. This is a consequence of the higher carbon content for coal. Molar percentage of CH_4 obtained from the co-mingling of green waste and biosolids is approximately 25% which is slightly higher than the fraction of CH_4 converted from pure feed of green waste or biosolids itself, 22% and 20% respectively.

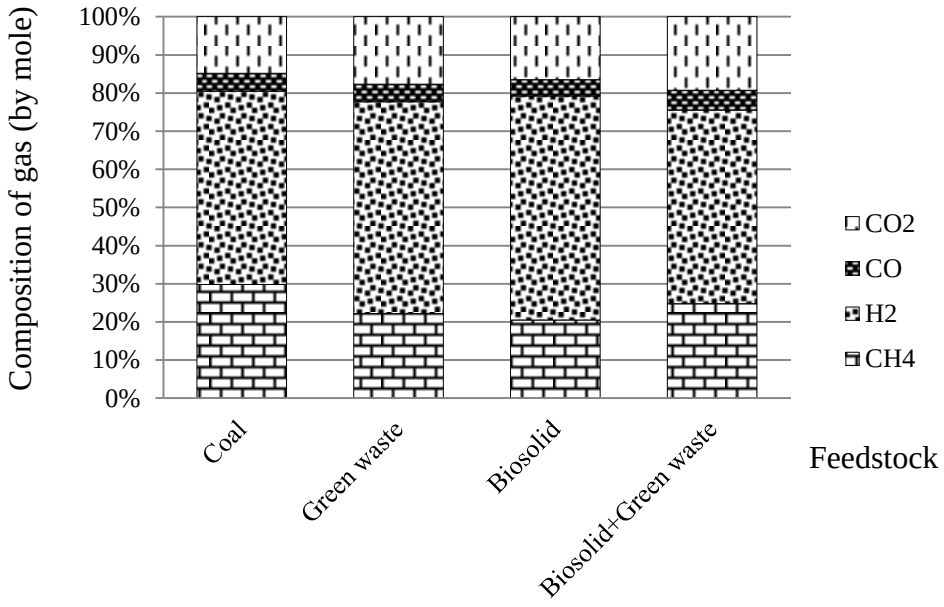

Figure 2-1 Gas composition from SHR using various feedstocks at 750^oC and 400 psi

The intent is to use biosolids (sewage sludge) from local waste water treatment facilities, co-mingled with woody biomass or green waste obtained from local municipal solid waste facilities. This appears to be a viable sustainable feedstock for the production of renewable fuel at low cost.

- *Temperature and pressure effects on product gas distribution in SHR*

An estimate of the composition of carbonaceous gases using the equilibrium model is presented in this section. The results are presented as a function of temperature and pressure. The analysis is performed with the assumption that all carbon in the product gas exists in the form of CH_4, CO and CO_2. The percentages of each component are shown in Figure 2-2 as a function of temperature; and Figure 2-3 as a function of pressure. The concentrations have been normalized to 100%. H_2O and H_2 that co-existed in the product gas are excluded in this analysis. A specific feed condition of H_2O/Feed mass ratio of 1.5 and H_2/C_{Feed} molar ratio of 1.0 was used for all of these calculations.

The concentration of CH_4 decreases with increasing gasification temperature whereas the concentration of CO and CO_2 increases. This is shown in Figure 2-2. This is expected since the hydrogenation of carbon which is the primary pathway to produce CH_4 is mildly exothermic. The steam carbon reaction ($2C+3H_2O \rightarrow 3H_2+CO+CO_2$) [68], and the reverse Water Gas Shift (RWGS) reaction of CO is endothermic which enhances the formation of CO at higher temperature. The fraction of CO_2 is relatively constant after 850^{o}C. The results may not totally represent the actual behavior in the gasifier especially at lower

temperatures because an equilibrium model was used. Small amounts of char and tar may exist which is not included in this simulation. The lower the temperature of the gasifier the longer gas residence time is required in order to reach the desired carbon conversion. This will lead to a larger sized gasifier and higher investment costs. It is this type of information that is helpful for experimental design and process evaluation in the future.

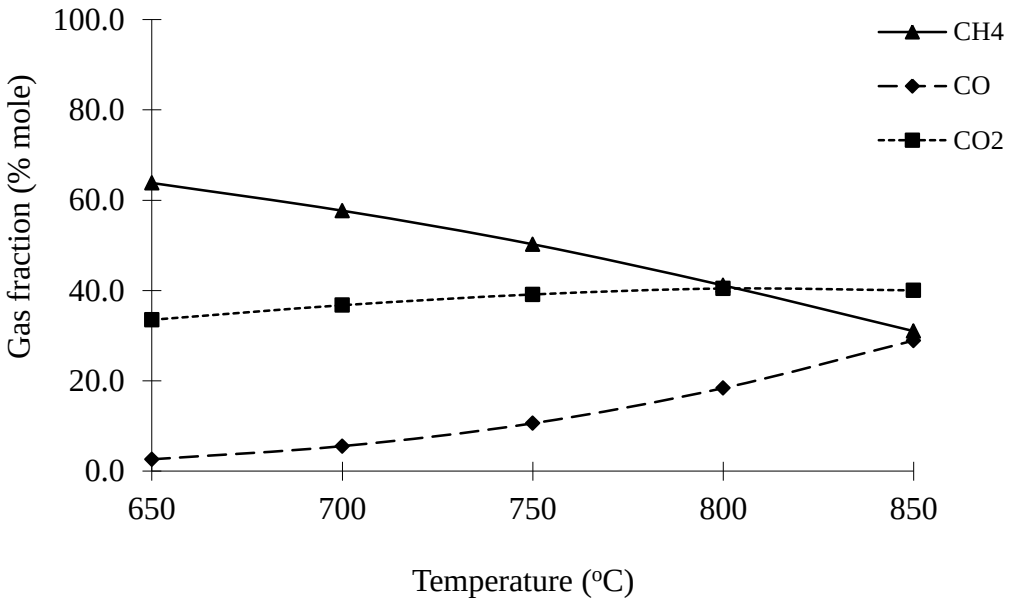

Figure 2-2 Influence of temperature on equilibrium composition of carbonaceous product gases from SHR using comingled feed (H_2O/Feed = 1.5, H_2/C_{Feed} = 1.0 at P = 400 psi)

The influence of pressure on the equilibrium composition of carbonaceous gases is presented in Figure 2-3. It shows that operation pressure plays a significant role on product gas distribution in SHR; particularly at lower pressures. It shows that the methane concentration could be increased with increasing pressure. The important result

from this simulation is that steam hydrogasification should be operated at relatively low temperature and high pressure. This would enhance CH_4 formation. A pressure and temperature of 400psi and 750ºC, respectively, was selected to be the operating conditions of the SHR. This is based on a series of experiments conducted in our laboratory [69, 70] and the modeling calculations presented here. These results provide the composition of the upstream fed that will be introduced into the laboratory scale WGS reactor which will be discussed further in the next chapter.

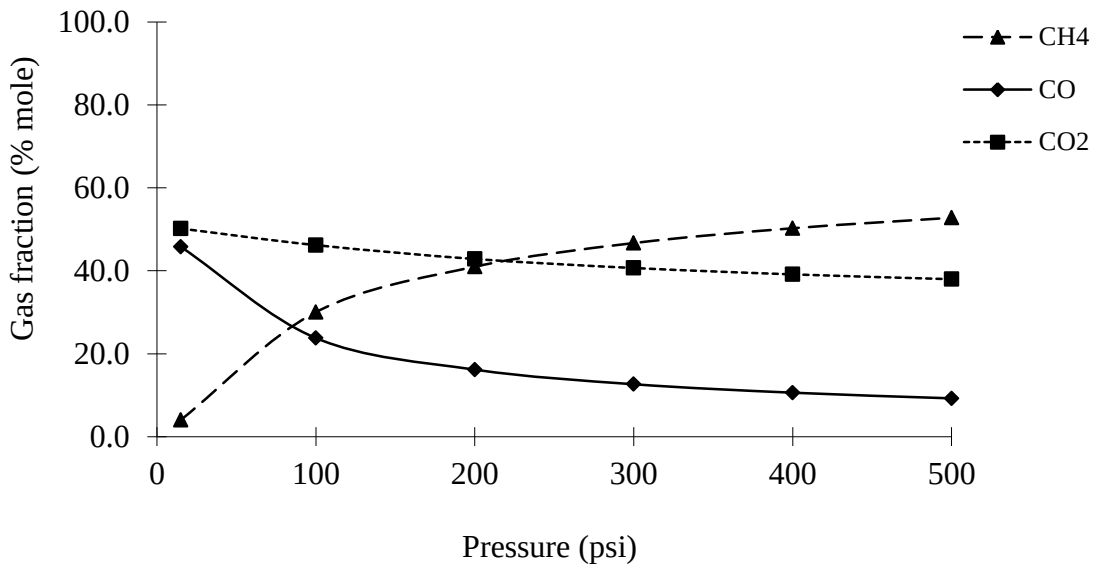

Figure 2-3 Influence of pressure on equilibrium composition of carbonaceous product gases from SHR using comingled feed (H_2O/Feed = 1.5, H_2/C_{Feed} = 1.0 at T = 750ºC)

- *Influence of H_2O and H_2 in feed on the operation of SHR and WGS*

The proper feed rate of H_2O and H_2 need to be determined in order to optimize the hydrogasification efficiency and maximize the methane yield downstream. One of the important characteristics of the CE-CERT process is that a sufficient hydrogen supply can be obtained by recycling the excess produced from the shift reactor. This eliminates the need for an external source of H_2. The availability of sufficient H_2 must be ensured at the desired operating conditions of the SHR. Additionally, CH_4 should be maximized in order to maximize the overall efficiency of the RNG process. This overall process discussed above is shown in Figure 2-4.

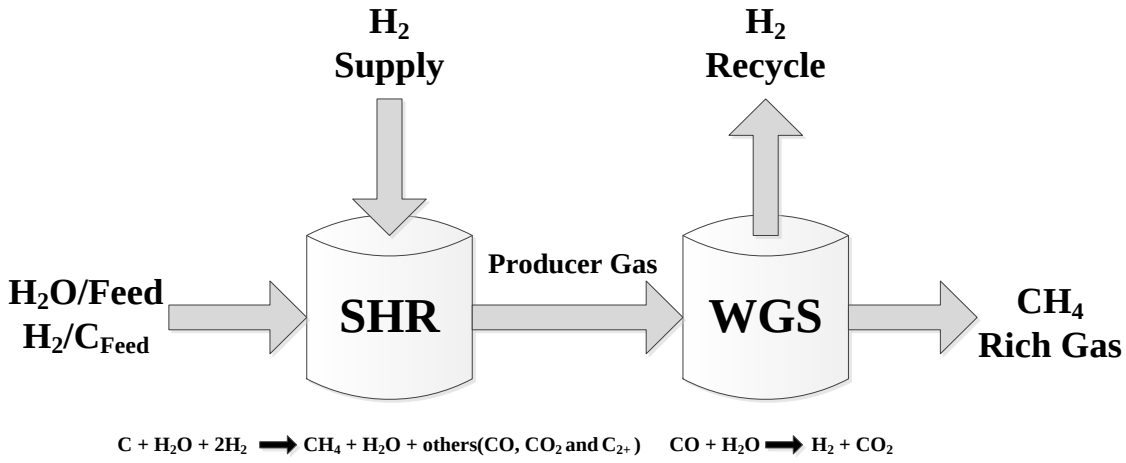

Figure 2-4 Simplified diagram of SHR configured with WGS reactor

A lower H_2O/Feed mass ratio leads to enhance carbon conversion in the SHR. This is shown in Figures 2-5 and 2-6. There are various trade-offs that need to be considered and understood. CH_4 production is promoted with a lower steam content in the SHR

while CO conversion in the WGS is decreased slightly. The reaction rate of carbon is influenced by the total amount of water in the SHR. If the H_2O/Feed mass ratio is too high it can result in a lower conversion efficiency. Higher gasification efficiency can be achieved by increasing the residence time which leads to higher costs for the reactor. In addition, increasing the water in the feed is unproductive for CH_4 yields and a higher input of energy is required to maintain the operation temperature. One of the key reasons for water in the process is to help achieve the pumpability of the resultant slurry in order to easily deliver feedstock into the pressurized gasifier. The appropriate H_2O/Feed mass ratio was selected to be 1.5. The excess H_2 supplied by the WGS reactor at this ratio is sufficient to recycle sufficient hydrogen to the SHR

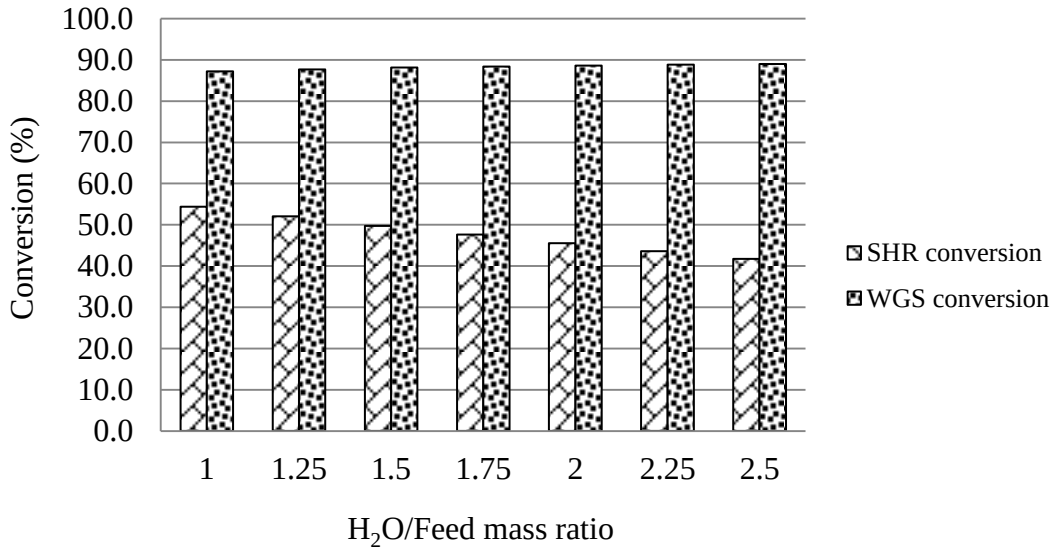

Figure 2-5 Comparison of conversion between SHR and WGS at various H_2O/Feed mass ratio and H_2/C_{Feed} molar ratio equals to 1.0 (at T = 750ºC, P = 400psi)

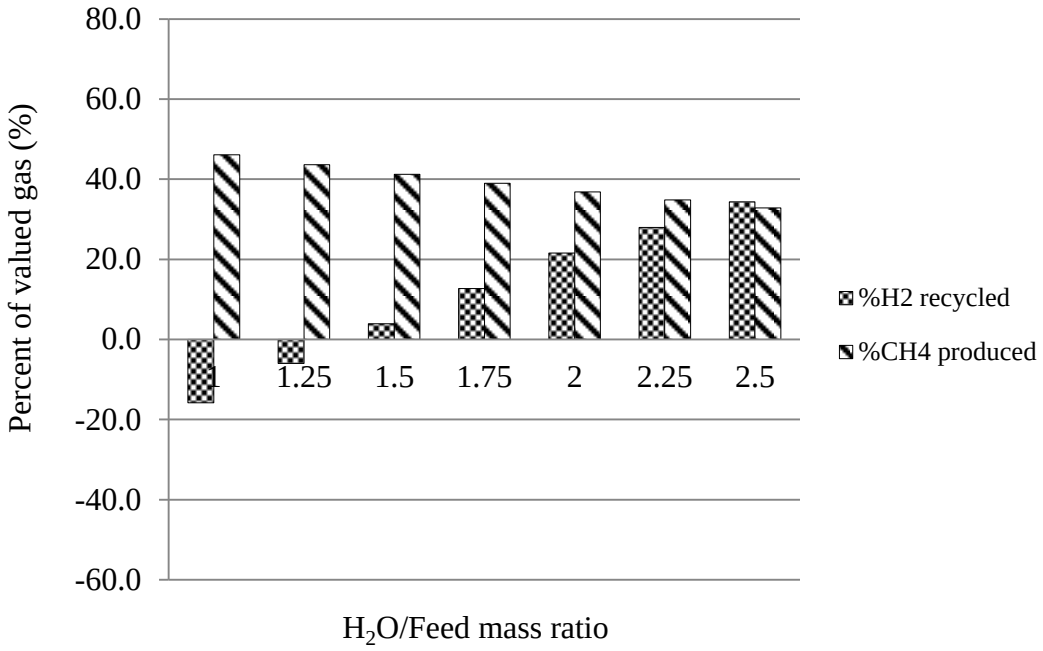

Figure 2-6 CH_4 yield and H_2 availability for recycle at various H_2O/Feed mass ratio and H_2/C_{Feed} molar ratio equals to 1.0 (at T = 750ºC, P = 400psi)

The chemical conversion efficiency for the SHR without the WGS and with the WGS is shown in Figure 2-7. The CH_4 yield and availability of H_2 are shown in Figure 2-8. The product gas from the SHR increases with an increase in the H_2 carbon feed ratio. The greater the H_2 input, the higher the gas conversion is obtained. An increase in the H_2/C_{Feed} molar ratio results in an increase in the CH_4 yield. The higher the concentration of H_2 shifts the chemical equilibrium within the system and promotes the hydrogenation of carbon and retards the formation of CO and CO_2 [71]. However, the H_2 sustainability can only be maintained when the H_2/C_{Feed} molar ratio is no larger than 1.

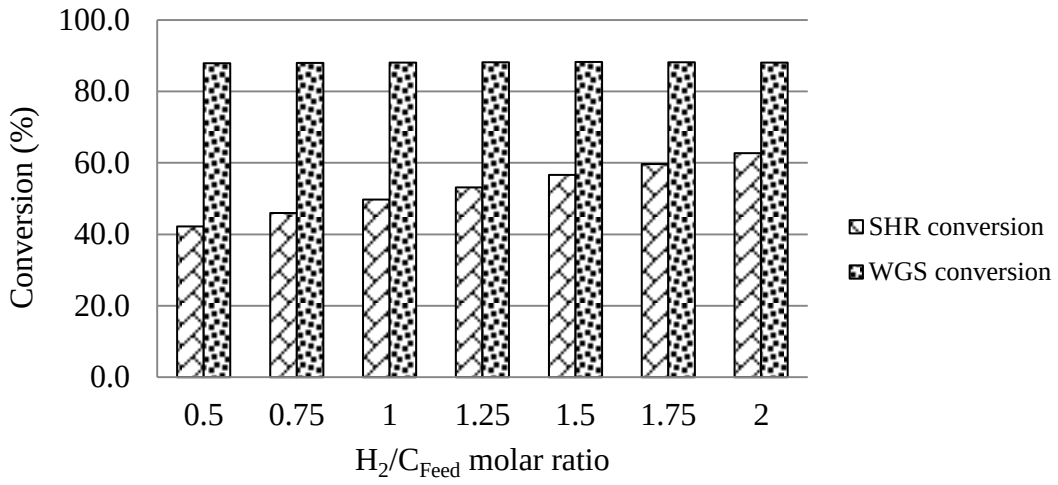

Figure 2-7 Comparison of conversion between SHR and WGS at various H_2/C_{Feed} molar ratio and H_2O/Feed mass ratio equals to 1.5 (at T = 750ºC, P = 400psi)

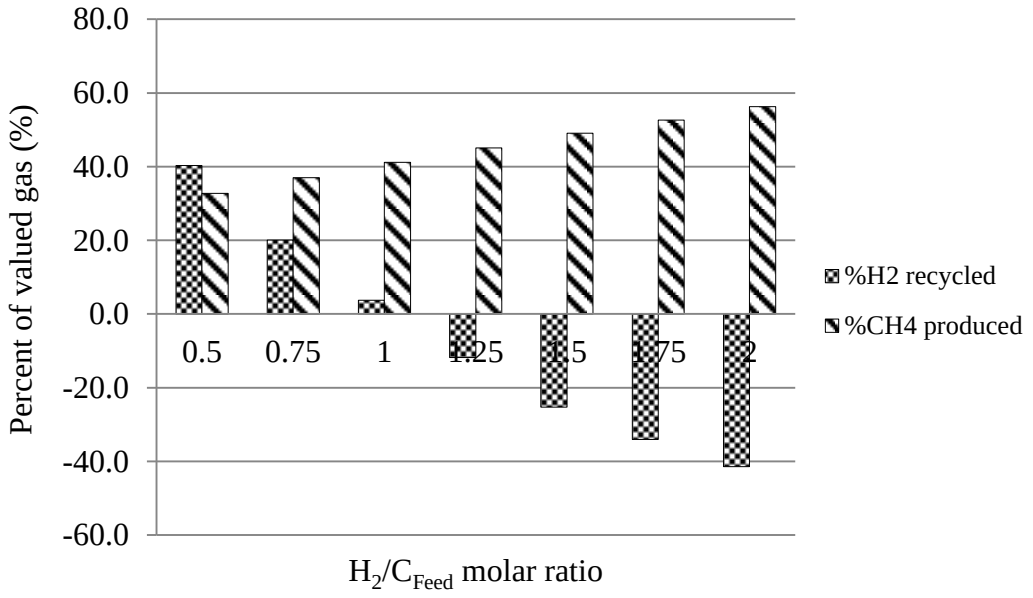

Figure 2-8 CH_4 yield and H_2 availability for recycle at various H_2/C_{Feed} molar ratio and H_2O/Feed mass ratio equals to 1.5 (at T = 750ºC, P = 400psi)

- *Temperature and pressure effect on CO conversion efficiency in WGS*

The CO conversion efficiency as a function of operational temperature and pressure of the WGS reactor is shown in Figure 2-9. The CO conversion via the shift reactor can achieve over 90% at 300^{o}C and decreased with an increase in temperature increase due to the equilibrium [72]. There was no impact of the operating pressure on the conversion.

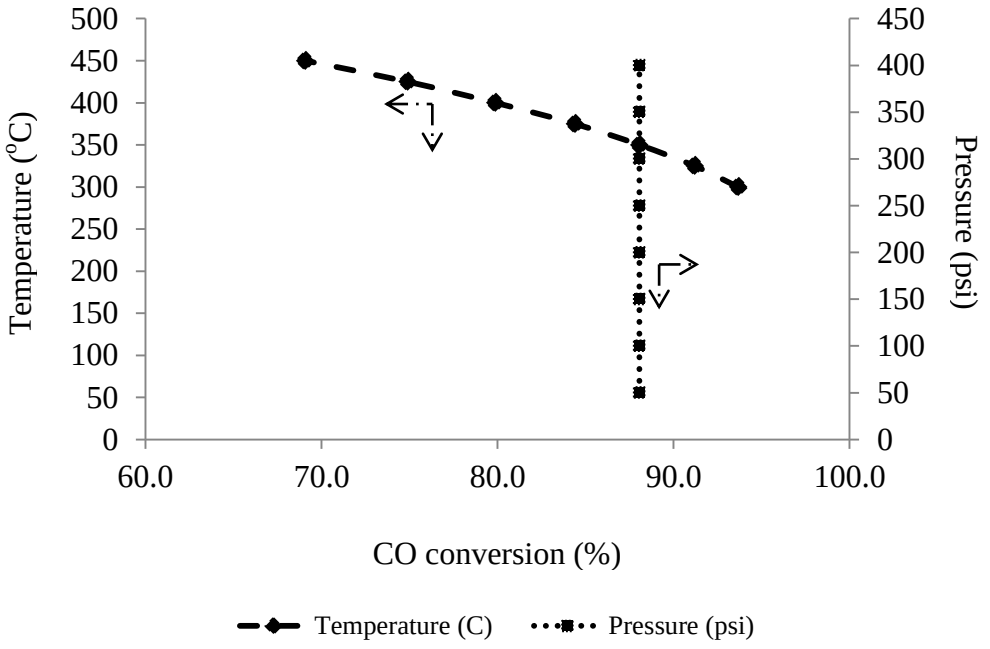

Figure 2-9 CO conversion of WGS reaction at different temperature and pressure

A high H_2O/feedstock mass ratio can guarantee that sufficient H_2 is available but results in a lower production of CH_4. The CH_4 yield increases with a high molar ratio of H_2/C but can result in not a sufficient Hydrogen for sustained operation.

Numerous simulations were done to determine the best operation conditions, optimal H_2/C ratio, and H_2O/feed ratio to obtain maximum RNG production at a 1 ton/day of feed rate. Table 2-3 presents the performance for production of RNG using biosolids co-mingled with green waste compared to other feedstock. The SHR and WGS reactor are operated at 750^oC with 400 psi and 350^oC with 150 psi, respectively.

Table 2-3 Optimum H_2, H_2O and feed ratios and RNG HHV of various feedstocks

Feedstock	H_2/C molar ratio	H_2O/Feed mass ratio	Carbon conversion (%)	Thermal Energy in RNG (GJ/day)
Biosolids+green waste	1	1.5	49.7	16.3
Biosolids	1	1.2	49.3	11.7
Green waste	1	1.5	49.6	13.7
Bituminous Coal	1	2.0	56.4	22.3

The overall process flow sheet using Aspen for comingled feedstock at the optimal operating condition determined above is given in Figure 2-10.

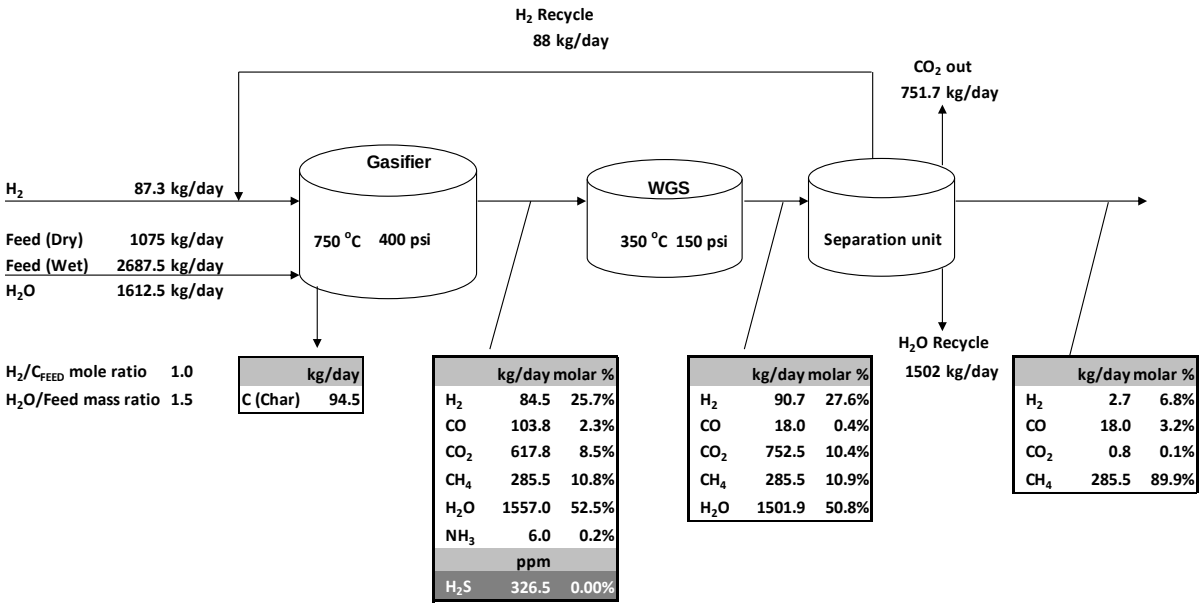

Figure 2-10 Simulation results of SHR with WGS reactor using the co-mingling between biosolids and green waste as feedstock at the optimum condition

2.2 Summary

A H_2/C molar ratio of 1.0 and a H_2O/feedstock mass ratio of 1.5 has been determined based on simulation results for comingled feedstock of biosolids with green waste. Gasification temperature and pressure was set at 750^{o}C and 400psi, respectively. The composition of dry gas stream generated from SHR consisted of 54% of H_2, 23% of CH_4, 5% of CO and 18% of CO_2. A sufficient H2 supply for recycling back to the SMR was achieved using a WGS reactor operated at 350^{o}C. Finally, RNG with a HHV of 16.3 GJ/day was produced at a feedstock flow rate of 1.0 ton/day.

The details of a lab-scale of water gas shift reactor will be presented in the next chapter. This will be used to investigate the reaction behavior and optimize the conversion of CO contained in the gas stream from the SHR and ensure that the availability of H_2 for recycling back to the SHR. A commercial High Temperature Shift (HTS) catalyst supplied by Clariant Corporation was used for the shift reaction. It is shown to be operational within the temperature range of 320-380^{o}C with an average reaction temperature maintained at 350^{o}C. In this study, WGS will be mainly considered for conducting the experiment. Based on these computations, the composition of the process gas from SHR is calculated and scaled down to be compatible with the gas conditions of the laboratory facility.

Chapter 3 Development of WGS reactor for RNG process

3.1 Designing of Water Gas Shift Reaction System

3.1.1 Literature review of water gas shift catalysts

A brief review of three classes of water gas shift catalysts is presented here. Each has different operating and thermal characteristics, chemical composition and commercial application. This was a necessary step in designing the WGS system for the Steam Hydrogasification technology.

- *High temperature shift catalyst*

High temperature shift (HTS) catalysts operate in the temperature range of 310-450^{o}C.They are called ferrochrome catalysts because of their chemical composition [73]. The inlet temperature is normally maintained at about 350^{o}C to prevent the catalyst bed temperature from going too high such that the catalyst is damaged. The maximum outlet temperature can be approximately 550^{o}C and can result in the CO concentration down to 3-5%. These catalysts are required to be activated prior to use by the partial reduction of Fe_2O_3 (Hematite) to Fe_3O_4 (Magnetite) following the below equations (Eq. 3-1 and Eq. 3-2) using the process gases and steam [73].

$3Fe_2O_3 + H_2 \Leftrightarrow 2Fe_3O_4 + H_2O$ ($\Delta H_o = -16.3$ kJ/mol) (Eq. 3-1)

$3Fe_2O_3 + CO \Leftrightarrow 2Fe_3O_4 + CO_2$ ($\Delta H_o = +24.8$ kJ/mol) (Eq. 3-2)

Over reduction can cause damage to the HTS catalyst. H_2 or a mixture of H_2-N_2 should not be used to reduce this catalyst because the strong exothermic reduction to metallic Fe can exist as described by equations (Eq. 3-3 to Eq. 3-7). It should be noted that only Fe_3O_4 is the active phase species in the WGS reaction scheme [73].

$Fe_3O_4 + H_2 \Leftrightarrow 3FeO + H_2O$ (ΔH_o = - 63.8 kJ/mol) (Eq. 3-3)

$Fe_3O_4 + CO \Leftrightarrow 3FeO + CO_2$ (ΔH_o = - 22.6 kJ/mol) (Eq. 3-4)

$FeO + H_2 \Leftrightarrow Fe + H_2O$ (ΔH_o = - 24.5 kJ/mol) (Eq. 3-5)

$FeO + CO \Leftrightarrow Fe + CO_2$ (ΔH_o = - 12.6 kJ/mol) (Eq. 3-6)

$Fe_3O_4 + 4H_2 \Leftrightarrow 3Fe + 4H_2O$ (ΔH_o = - 149.4 kJ/mol) (Eq. 3-7)

The ratios of H_2O/H_2 and CO_2/CO determine the relative stabilities of the Fe_2O_3 and Fe_3O_4 phases. Under normal operating conditions, the ratio of H_2O/H_2 should be over 0.4 and that of CO_2/CO should be above 1.2 at which the Fe_3O_4 is more stable [74]. Either FeO or metallic Fe is unable to be formed. However, the formation of metallic Fe by operating at a low ratio of H_2O/H_2 can initiate the highly exothermic Methanation and Boudouard reactions (Eq. 3-8 and Eq. 3-9) and can result in temperature runaway on the HTS catalyst [73].

$CO + 3H_2 \Leftrightarrow CH_4 + H_2O$ (ΔH_o = -206.2 kJ/mol) (Eq. 3-8)

$2CO \Leftrightarrow C + CO2$ (ΔH_o = -172.5 kJ/mol) (Eq. 3-9)

The Fe_3O_4 can be re-oxidized to Fe_2O_3 following the reverse of Eq. 3-1 if the catalyst is exposed to steam in the absence of reductant gases like H_2 or CO. This will lead to an

overall lower catalytic activity. The HTS catalyst can also be deactivated by the presence of sulfur present in the product gas. The decrease of active sites due to the occupancy of sulfur species on the catalyst surface hinders the catalytic activity of the WGS reaction described by Eq. 3-10. The Fe-Cr based catalyst can tolerate sulfur up to 1000ppm [73].

$Fe_3O_4 + 3H_2S + H_2 \Leftrightarrow 3FeS + 4H_2O$ (ΔH_o = -75.0 kJ/mol) (Eq. 3-10)

- Low temperature shift catalyst

The low temperature shift (LTS) reaction occurs at 200-250^oC and the catalyst is a mixture of ZnO, CuO and Cr_2O_3/Al_2O_3 at varying composition depending on the manufacturer. The active species in the catalyst is the copper metal crystallites. ZnO and Cr_2O_3 provide the structural support for the catalyst. Al_2O_3 is inactive but helps in the dispersion and minimizes pellet shrinkage. The Cu-based catalyst is very susceptible to thermal sintering hence high temperature operation needs to be avoided [73]. The reaction temperature of the LTS catalyst is limited by the dew point of the mixture gas at operating conditions. The LTS catalyst has to be activated and it usually is exposed to the process gases with dilute H_2 [73]. Then, CuO is reduced to copper by the reaction described below (Eq. 3-11).

$CuO + H_2 \Leftrightarrow Cu + H_2O$ (ΔH_o = - 80.8 kJ/mol) (Eq. 3-11)

A LTS reactor is installed in series after the HTS reactor to reduce CO in low temperature applications. The exit concentration of CO can be reduced as low as 0.1%. One major

disadvantage is that LTS catalyst is easily poisoned by sulfur in gas stream following the irreversible reaction in Eq. 3-12.

$2Cu + H_2S \rightarrow Cu_2S + H_2$ (ΔH_o = -59.4 kJ/mol) (Eq. 3-12)

A fixed bed reactor of ZnO is used to prevent the deactivation by sulfur and to eliminate any undesired species before the shift reactor [73]. A major advantage of the LTS catalyst is its selectivity with few side reactions occurring [74].

- *Sour gas shift catalyst*

It is necessary to consider a sulfur resistant catalyst for the WGS reaction as a consequence of the concern of LTS catalysts in acidic environments. These catalysts usually consist of cobalt and molybdate formulation and are less active than the Cu-Zn based (LTS) catalyst operating with a cleaned feed gas. These are used during the gasification of high sulfur feedstock, such as, coal, heavy fuel oil, oil shale or even biomass where concentrations of sulfur are up to 3% [73]. Only a HTS catalyst can be operated at higher sulfur content however, either the higher amount of catalyst or the increasing of H_2O/CO ratio is needed to obtain the desired conversion due to its lower catalytic activity, about 50% [74]. The Co-Mo based catalyst is primarily active in the sulfide form in which an activation step is needed based on the equations below (Eq. 3-13 and Eq. 3-14) [50].

$$CoO + H_2S \Leftrightarrow CoS + H_2O \quad \text{(Eq. 3-13)}$$

$$MoO_3 + 2H_2S + H_2 \Leftrightarrow MoS_2 + 3H_2O \quad \text{(Eq. 3-14)}$$

The minimum content of sulfur should be about 300ppm when a sour gas shift catalyst is used. If the catalyst is adequately pre-sulfided, satisfactory activity at low levels of sulfur, 35ppm, can still be obtained [76]. The commercial sour gas shift catalyst operates at a temperature of 250-350^{o}C and a pressure of 1-40 Bar with 1% of CO content at the exit of the reactor.

3.1.2 Selection of catalyst for the design and experiment

According to a literature review of performance and availability of shift catalysts in the marketplace, the high temperature shift (HTS) catalyst supplied by the SÜD-CHEMIE catalyst group was selected for the lab-scale system. The commercial name of the catalyst is "ShiftMax®120" which is well-known for the combination of high activity and good physical robustness. The composition and physical characteristic of the catalyst is given in Table 3-1 [77, 78].

Table 3-1 Specification of ShiftMax®120

Composition	Content (wt.%)
Fe_2O_3	80
Cr_2O_3	8.5
CuO	2
Bulk density (kg/l)	1.23
Size (mm)	6x6
Shape	Tablets

The operational pressure of this catalyst is between atmospheric and 600 psig (42kg/cm^2). The normal operating temperatures at the inlet of the reactor are 316^{o}C up to 382^{o}C as it becomes deactivated. A temperature rise will be observed through the bed of catalyst since the water gas shift reaction generates heat, [79].

3.1.3 Laboratory scale setup of water gas shift reaction

A lab-scale reaction system was designed and constructed for determining the optimum design of WGS reactor to be implemented with the SHR process in the next stage. The structure of this WGS reactor is similar to a conventional continuous fixed bed reactor system, and consists of feed gas, input gas flow controller, reactor, cooling gas unit, product collector, back pressure regulator, output gas flow meter and gas sampler. The schematic diagram of a lab-scale WGS reaction system is shown in Figure 3-1.

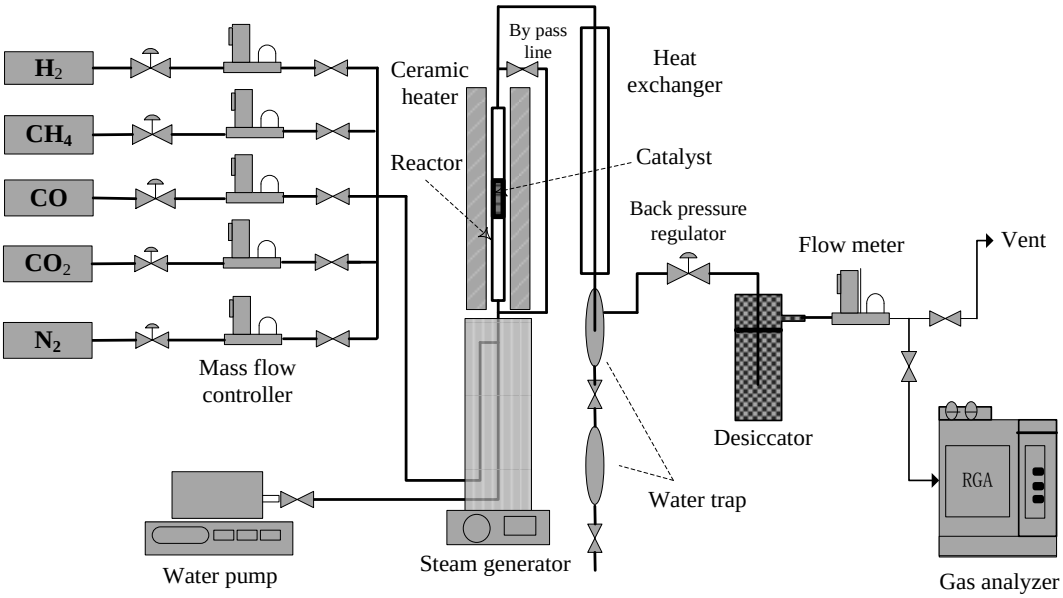

Figure 3-1 Schematic diagram of a lab-scale WGS reaction system

High purity grade H_2, CH_4, CO, CO_2, and N_2 gases were used. If not specified, all of the supplied gases were purchased from Praxair Inc. Multiple mass flow controllers (MFCs) were used to set and manipulate total mass flow rate of the input gases during the experiments. All of the MFCs were properly calibrated before running the experiments. The calibration of each pure gas was completed using Bios DryCal Primary Gas Flow Calibrator which was calibrated by the manufacture. Check valves were installed following all MFCs to prevent any backward flow from the system. All the gases were converged to a single line. The mixture gas set to be representative of the composition of

the producer gas from the SHR. Furthermore, a by-pass line was also added to the system in order to confirm the composition of the input gas without reaction.

The fixed bed reactor was made of 316 stainless steel tubing with inside diameter of 11 mm. and length of 760 mm. It was covered with a ceramic fiber heater (Watlow VC401A12A) in order to provide sufficient heat during the reaction. The HTS catalyst was loaded at the center of the reactor. Stainless steel wool and glass beads were used to support the whole catalyst bed. Two flat layers of glass wool of 9 μm were put on the top and the bottom of the bed. These layers helped distribution of the gas flow inside of the reactor and kept the catalyst particles from moving. Figure 3-2 shows the configuration of packed bed in the shift reactor.

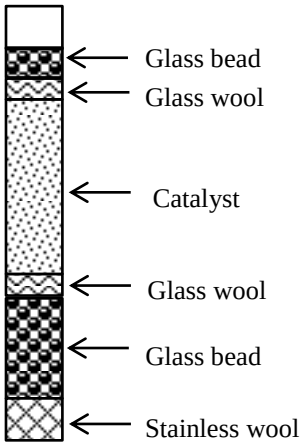

Figure 3-2 Configuration of internal WGS packed bed reactor

Two K-type thermocouples were used to measure the temperature at the inlet and outlet of the packed bed in the reactor. Another TC was placed on the reactor outside wall. It was used to provide feedback for reactor temperature control. The reaction temperature was controlled by LabVIEW software with a PID-type temperature controller. Two pressure transducers monitored the operating pressure between the inlet and outlet of the reactor. All reaction parameters such as temperature, pressure and flow rate of product gas were collected every second through the LabVIEW data acquisition (DAQ) system.

Water was introduced to the system in the form of steam using a steam generator. It was made of a stainless steel tube, 1/8 in. dia. shaped as a coil to increase its heat surface area. A ceramic heating system was installed for heating up and controlling the temperature of the steam and input gas. This was coupled to a high pressure feed water pump (Series I of Isocratic Pump for Chromatography from Scientific Systems, Inc.) with the maximum capacity of 40 ml/min. The amount of water delivered was controlled by changing the scale of the pump.

A heat exchanger made from a double tube, composed of 1/4 in. tubing as inner and 1/2 in. tubing as outer, was used for cooling the product gases after the reaction was completed. Excess water remaining from the reaction was condensed and separated by a set of water traps after cooling down the product gas. A back pressure regulator (BPR) was installed in order to sustain the system pressure. Moisture in the gas stream was eliminated using a desiccator made of silica gel to keep the product dry. Finally, the total

flow rate of output gas was measured by a mass flow meter (MFM) before venting. The product gas was collected by a tedlar gas sampling bag through a port connector. The composition of the product gas was determined by a Residual Gas Analyzer (RGA) or Non-Dispersive Infrared Analyzer (NDIR) for online analysis. The lab-scale WGS reaction system is shown in Figure 3-3

Figure 3-3 Experimental setup of the lab-scale water gas shift reaction

3.1.4 Analysis Method

A Cirrus ^{TM} Atmospheric Pressure Residual Gas Analyzer (referred to as RGA, MKS Instruments, Inc.) was used to analyze the composition of the product gas. The RGA, shown in Figure 3-4, can determine gaseous components using a quadruple mass spectrometer. This method has several advantages for analysis of the mixture gas [80, 81] Firstly, the RGA can analyze multiple components in a mixture gas at the same time, which provides fast online analysis results. Secondly, it can track gas composition over a wide dynamic range from percentage to ppb levels. Finally, it is so convenient for operation and maintenance because of its bench-top configuration.

Figure 3-4 Cirrus ^{TM} Atmospheric Pressure Residual Gas Analyzer (RGA)

This RGA is an atmospheric pressure system. Generally, the inlet gases should be injected into the RGA at the pressure equal to 1 bar. The RGA provides near real-time analysis of gaseous products by continuous scanning of mass spectra with an interval of 3-4 seconds. The sensitivity of the RGA to a particular gas species is expressed as the

peak intensity per unit measure as shown in Eq. 3-15, and it is assumed to be relatively unaffected in a wide range of RGA background.

$$S_C = \frac{I_C}{P_C} \qquad \text{(Eq. 3-15)}$$

Where

S_c: RGA sensitivity to a gas species

I_c (torr): major intensity of a gas species in mass spectra

P_c (torr): partial pressure of a gas species in mixture gases.

The RGA records the mass spectra data in intensity with units of torr. The major products analyzed with the RGA are H_2, CH_4, CO, and CO_2. The relative concentration of a gas species in the product gas is proportional to the intensity of this gas species following Eq. 3-15 and based on a constant sensitivity. The sensitivity of a gas species in the mixture gas is obtained by calibration using a certified calibration gas. Calibration is required before each sample. The product gas analyzed is identified by detecting the key fragment ions produced. Hence, analysis for CO and CO_2 are taken for the molecular peak of m/z=28, m/z=44 in the mass spectra pattern while the CH_4 analysis is taken for m/z=15 not m/z=16. This is because both mass spectra patterns of CO and CO_2 have fraction of the fragmental peak in the m/z=16 due to the ionization of oxygen element.

3.1.5 CO conversion of WGS reaction

CO conversion is used to define the activity of the WGS catalyst. The calculation is defined by Eq. 3-16.

$$CO\ conversion\ (\%) = \frac{mass\ flow\ rate\ CO_{in} - mass\ flow\ rate\ CO_{out}}{mass\ flow\ rate\ CO_{in}} \times 100 \qquad \text{(Eq. 3-16)}$$

The inert methane in the product gas should be unreacted in the WGS reaction and its amount which is determined by the water, hydrogen and feed mass ratio of the operating SHR should be relatively constant. Some other reactions, especially steam methane reforming and methanation, may also take part in the system. These assumptions and the overall CO conversion of the system will be determined by experiment with the goal of obtaining an optimized WGS system with the highest RNG production.

3.2 Investigation and optimization of the WGS reactor system

3.2.1 Experimental procedure

- *Start-up procedure*

The particle size of the commercial HTS catalyst was too large to put into the reactor. The catalyst was pulverized by a mortar grinder, and sieved, by mesh 100-200, to obtain a smaller particle size. This size, between 75-150 µm, was chosen since it had been

proven to be small enough to ignore the effect of inter-particle mass transfer limitation from a previous study in the literature [82].

A certain amount of HTS catalyst was loaded into the fixed bed reactor, depending on the space velocity. The catalyst is usually in the oxidized state and needs to be reduced before it becomes reactive. The activation procedure for the HTS catalyst was provided in the supplier's manual [79] and was done after setting up the reactor filled with catalyst and completing a leakage test at approximately 100psi. This procedure was done at atmospheric condition with a fully open of back pressure regulator.

The reactor was heated from ambient to 175^{o}C with a N_2 purge to eliminate moisture in the packed bed. A 2-2.5^{o}C/min temperature ramp was controlled carefully to avoid the catalyst sintering. The temperature was then continuously increased to 225-275^{o}C to perform the activation. At this temperature, the catalyst bed was ready to be activated by activation gases and steam at a minimum steam/carbon mass ratio of 25:1. Flow rates of N_2, H_2 and CO were set at 100, 60 and 30sccm, respectively, and fed into the system. Steam was introduced into the reactor at 1 ml/min using an HPLC feed water pump. The space velocity should be kept at a minimum of 200 $Nm^3/h/m^3$of bed [79]. This step typically takes about 30-60 minute to be completed. Then, the temperature of the WGS reactor can be raised to the required experimental conditions. The temperature profile and activation steps used are presented in Figure 3-5.

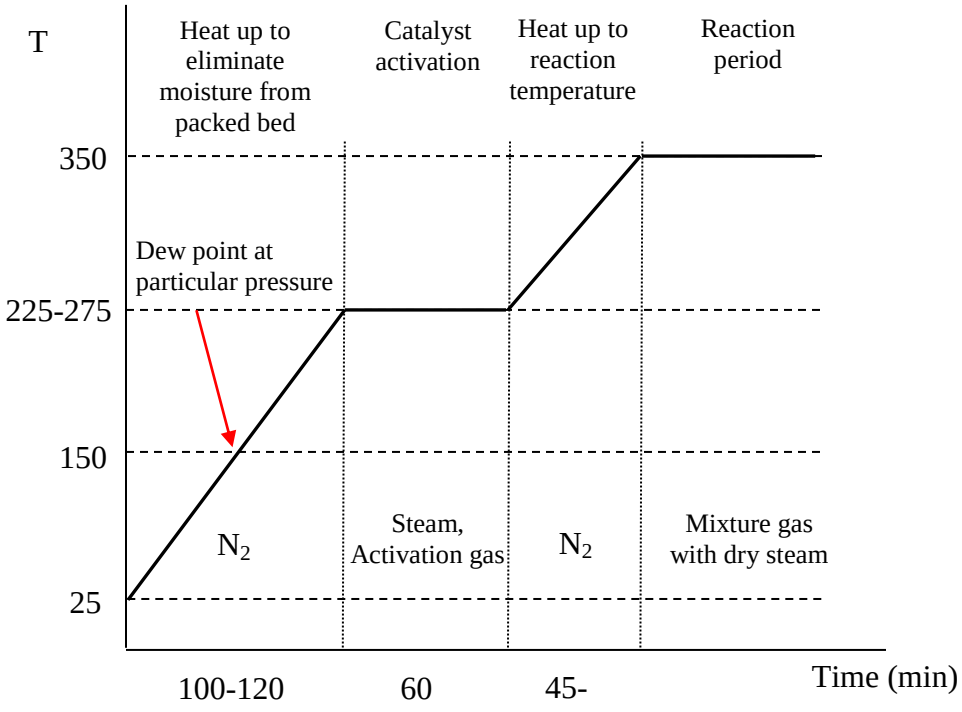

Figure 3-5 Temperature diagram for catalyst activation and process operation

- *Experiment protocol of the product gas sampling*

The gas and water mixture, in the form of steam, were adjusted to the specific flow rate after the activation step and when the appropriate reaction temperature was achieved. The input stream was fed to the system to investigate the behavior of the WGS reactor. The hot stream from the reactor was cooled down to condense the excess water and eliminate moisture from the product stream by water traps. The total flow rate of the output gas was determined by a mass flow meter. Samples of product gas were collected by a tedlar gas collecting bag every 30 min beginning after 1 hour of the introduction of the upstream (mixture gas and steam) into the system at the reaction conditions. The products were then analyzed by the RGA.

- *Shutdown procedure*

The mixture gas was replaced by N_2 flow of 100sccm when the test was completed in order to purge the system of the remained toxic gases. Meanwhile, the water pump output was increased to 1 ml/min to produce more input steam. More input steam helps to eliminate carbon deposition on the catalyst bed. This operation was continued for about 30 min then the heater was turned off. N_2 purging continued until the temperature of the rector was lower than 100^{o}C in order to protect the active catalyst from oxidation. The back pressure regulator was set to maintain a pressure of about 10 psi for sealing the catalyst bed in the reactor. Finally, the shut off valve of N_2 and the other process gas was turned off.

3.2.2 Experimental design and operational parameters

The overall characteristics and performance of the shift reactor were determined with the goal of achieving the highest CO conversion in the laboratory scale system. The experimental conditions are summarized below.

- Commercial available catalysts supplied by Clariant Corporation:

  - High Temperature Shift (HTS) catalyst, ShiftMax®120

  - Sour Gas Shift (SGS) catalyst, ShiftMax®820

- Temperature: 300 – 450^{o}C

- Pressure: Atmospheric

- Particle size of catalyst: 75μm – 1.3mm

- Catalyst loading: 5 – 20g

- Various concentration of mixture gas (H_2 ,CH_4 ,CO and CO_2), in particular CO_2

Input gas Component	% gas composition of MG1 (From simulation)	% gas composition of MG2 (From experiment)
H_2	54	66
CH_4	23	20
CO	5	7
CO_2	18	7

- Total flow rate of mixture gas (both MG1 and MG2): 30 – 200sccm

- Steam to C ratio: 3 – 5:1 (Only mole of C in CO and CO_2 were included [50])

The experimental results of the above parameters will be used to scale up the WGS reactor for implementation with the RNG demonstration unit. The optimum conditions based on these experiments will be useful for evaluating the overall mass and energy balance of the RNG production via Aspen Plus process simulation outlined in the previous chapter.

3.3 Results and Discussion

3.3.1 Influence of space velocity on the conventional WGS reaction

Prior to evaluating the performance of the lab-scale setup, the conventional WGS reaction using the Fe-Cr based, ShiftMax®120, catalyst was run to assure the reliability of the built system. The stoichiometry of the water gas shift reaction is shown below.

$H_2O + CO \Leftrightarrow CO_2 + H_2$ ($\Delta H_o = -41.2$ kJ/mol) (Eq. 3-17)

The reaction temperature was approximately 350^oC set at the inlet of the catalytic packed bed. The molar ratio of steam to carbon (S/C) was maintained at 3:1 to avoid carbon deposition on the catalyst as observed in several previous publications [83, 84]. Figure 3-6 presents the comparison between conversion of CO and space velocity of the wet gas. About 85-90% of conversion was achieved in a range of space velocities between 4500 to 9000 h^{-1}. This met the expectations for the lab-scale system and confirmed its use to perform further studies on the catalytic activity of the WGS system. Experiments were then carried out using simulated producer gases expected from the SHR to observe the reaction behavior and assure the availability of H_2 provided by the shift reaction.

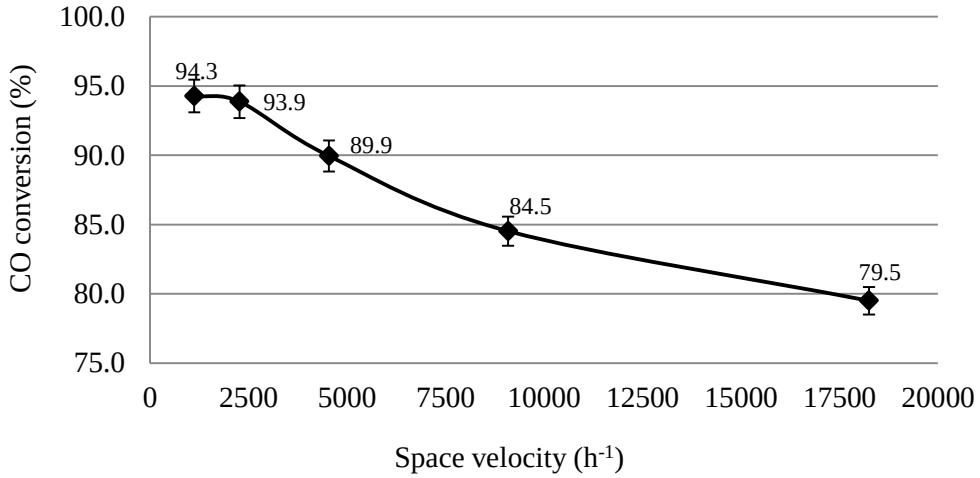

Figure 3-6 CO conversion of various space velocities for the conventional WGS reaction at 350^oC

3.3.2 Influence of gas species on CO conversion in WGS reaction

Other components, i.e., H_2, CO_2 and CH_4, were added into the feed gas to observe the influence of each species on the CO conversion in WGS reaction using HTS catalyst with 75-150μm of particle size. The results are presented here. The total flow rate of the input gas was set at 100sccm balanced by inert Argon instead of N_2 to avoid the intervention with CO on the RGA analysis. S/C ratio was set at 3 for each test except the last one which was increased to 5 which corresponds to the steam content used in the Aspen simulation presented in Chapter 2.

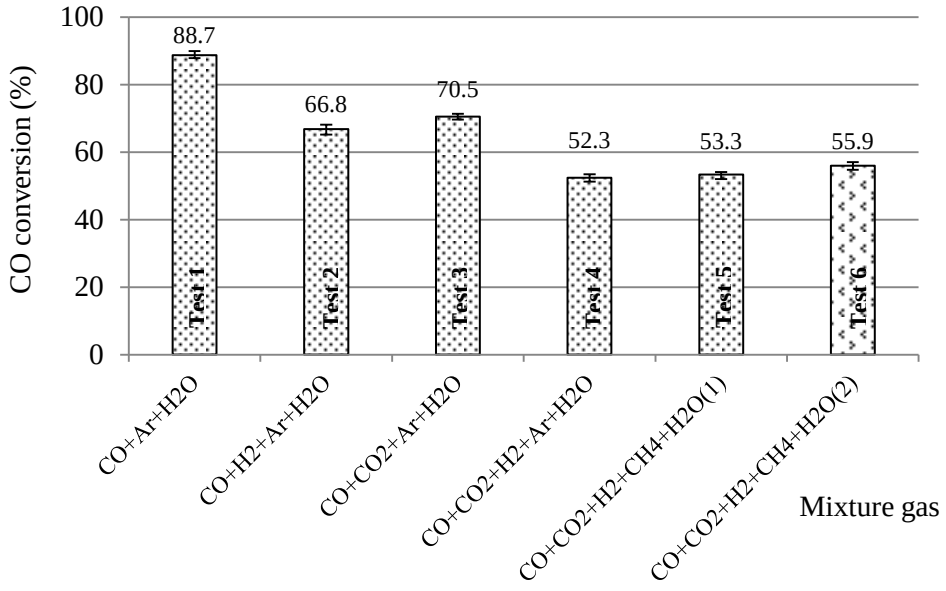

Figure 3-7 CO conversion of different gas composition in WGS reaction at 350^{o}C and space velocity of 4500 h^{-1} (S/C = 3 in (1) and S/C = 5 in (2))

Figure 3-7 shows the conversion of CO at 350^{o}C and SV of 4500 h^{-1} using different gas compositions. Argon slightly decreased the conversion compared to using pure CO because the overall SV was higher and the CO concentration was lower. The incremental addition of H_2 and CO_2 in the stream (experiments 2, 3 and 4) lowered the conversion to 67%, 70% and 52%, respectively. This was a consequence of the backward shift in the equilibrium. The conversion from the conditions in experiment 2 was lower than that of experiment 3 because the higher concentration of H_2 in the mixture gas had a larger inhibition on the reaction than CO_2. The conversion, about 53%, experiment 5 of was different from that of experiment 4 when Argon was replaced by CH_4. So, methane acted like inert in this experiment. The conversion slightly increased with the further addition of steam performed (experiment 6) helped push forward the WGS reaction.

3.3.3 Influence of reaction temperature, particle size and loading of the catalyst

The mixture gas, MG1, simulates the upstream SHR outlet gas composition when woody or green waste co-mingled with biosolids is used as the feedstock. This was discussed in Chapter 2. This was used as input to determine the conversion of the WGS system at different temperature, amount of catalyst and particle size. S/C was set at 5 similar to the proportion of stream discharged from the SHR. The results are summarized in Figure 3-8.

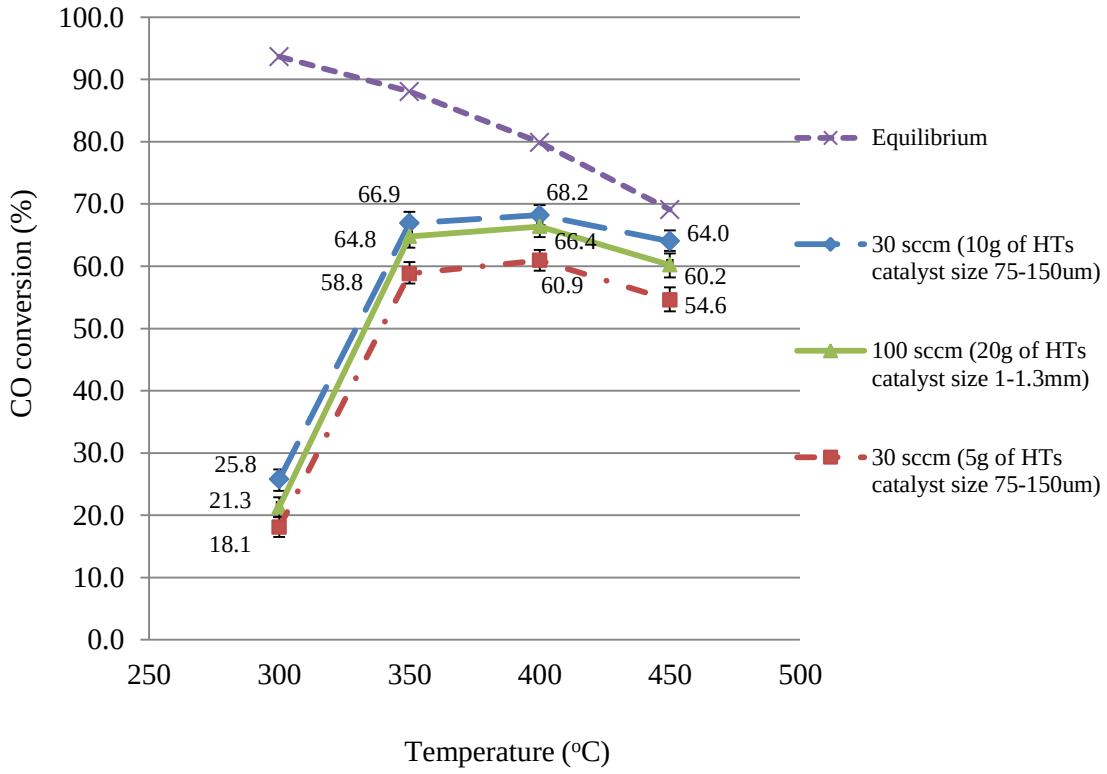

Figure 3-8 CO conversion of mixture gas, MG1, obtained from WGS reaction using various particle sizes and loading of catalyst at different temperature

The data show that the WGS system using the HTS catalyst performed well at the reaction temperature around 350-400^{o}C and declined slightly at higher temperature. About 60% of CO conversion was achieved using 5g of 75-150µm catalyst at 350-400^{o}C. The conversion increased to 70% when the amount of the catalyst was doubled. In order to determine the highest conversion rate possible the amount of the catalyst and feed rate were varied. The size of the catalyst needed to be increased to avoid a pressure drop across the packed bed. Twenty grams (20g) of catalyst with a mesh size of between 1-1.3mm resulted in a CO conversion of approximately 65-66% and a relatively low

pressure drop. This is shown in Table 3-2. The conversion was slightly lower with the larger particle size because of the smaller contact surface of catalyst or channeling limitations [85]. Consequently, the void fraction of the bed is larger and the pressure drop is lower. The CO conversions shown in Figure 3-8 were lower than the equilibrium line provided by an Aspen simulation. This is a consequence of the exothermic reaction raising the temperature at the outlet of the reactor which resulted in a non-isothermal process [86]. The best result obtained from the various experiments was a 65% CO conversion using 1-1.3 mm size of HTS catalyst at the calculated space velocity about 2000-2500 h^{-1} and temperature of 350^{o}C.

The profile of real time operation collected during the reaction of WGS at the optimum conditions is presented in Figure 3-9. The difference in temperature at the inlet and outlet of the catalyst bed was about 35-40^{o}C due to the exothermic reaction. The pressure drop across the bed was lower than 1-2 psi. The dry gas distribution profile is shown in Figure 3-10. The flow rates of H_2 and CO_2 downstream were increased while that of CO was decreased when compared to the upstream values. It should be a proportional ratio of 1:1 because of the equimolar reaction [50, 73]. The volumetric flow rates were converted to a molar basis and shown in Figure 3-11. This was done to determine the average carbon balance between the input and output gas streams. CH_4 was fairly constant as expected and supports the assumption that it has poor activity on the Fe-Cr based catalyst [87, 88]. The flow rate of H_2 increased approximately 7%. As a consequence, the amount of produced H_2 was sufficient to be recycled back to the SHR.

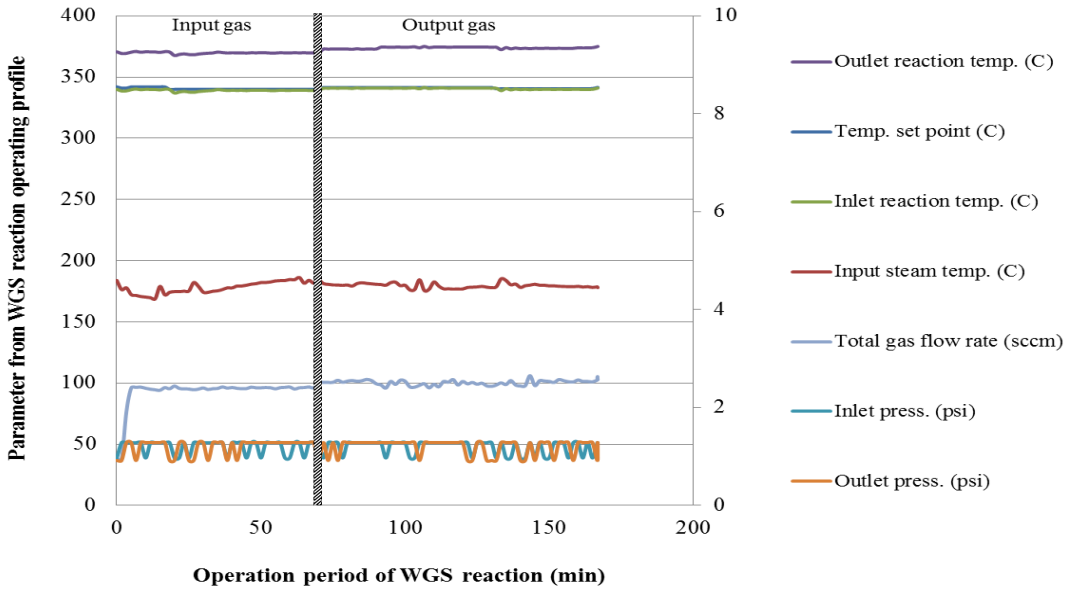

Figure 3-9 Profile of the real time operation of WGS reaction using HTS catalyst at 350^{o}C and space velocity of 2500 h^{-1}

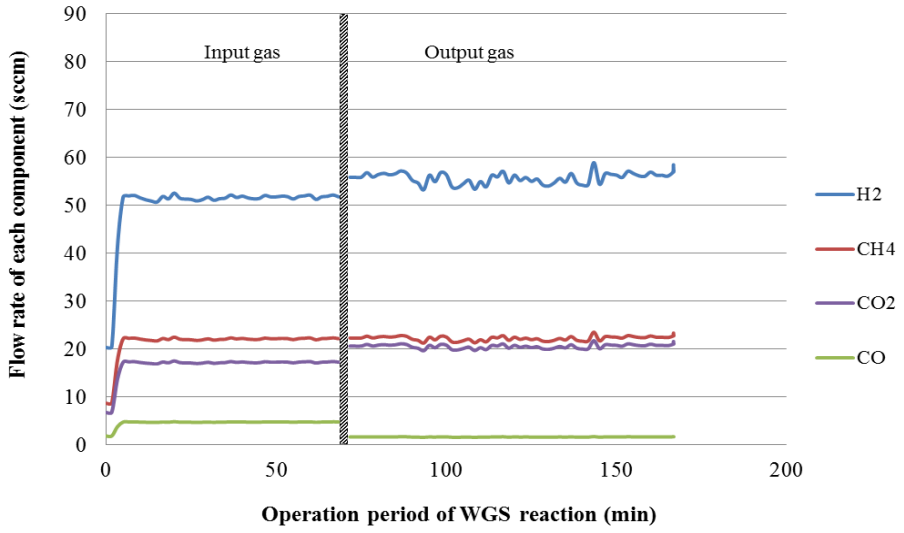

Figure 3-10 Gas distribution compared between input and output via WGS reaction at 350^{o}C and space velocity of 2500 h^{-1}

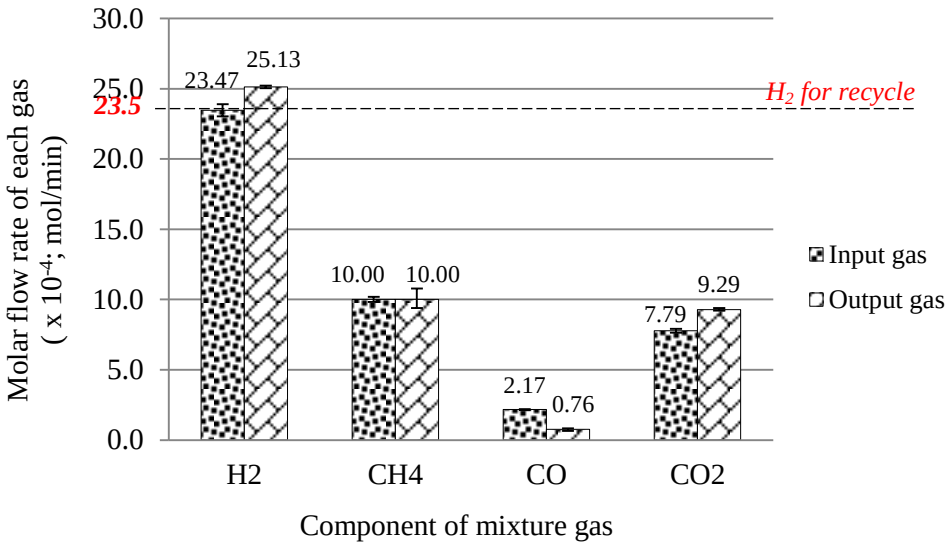

Figure 3-11 Mole of carbon balance of MG1 as dry basis compared between input and output via WGS reaction at 350°C and space velocity of 2500 h^{-1}

As previously mentioned, the particle size of the catalyst influences the pressure drop in the catalytic reactor. The expected pressure drop can be determined theoretically using the bed geometry and void fraction. Therefore, the volume of the reactor will be inversely related with the pressure drop across the bed. Assuming that turbulent flow is fully developed in the reactor, which is usually the case in most of commercial plants, the pressure drop can be estimated by the correlation derived by Ergun. The simplified equation is shown as Eq. 3-18 [73].

$$\Delta P = 1.75 \frac{(1-e)G^2 h}{e^3 d_e \rho} \qquad \text{(Eq. 3-18)}$$

ρ is the gas density

h is the height of catalyst bed; $h = 4V_b/\pi D^2$

V_b is bulk volume of catalyst; $V_b = V_s(1\text{-}e)$

V_s is solid volume of catalyst

e is the void fraction

G is the mass flow rate for unit cross section of bed; $G = 4M/\pi D^2$

d_e is equivalent diameter of catalyst particle; $d_e = \frac{6 \text{ x volume of particle}}{\text{surface area of particle}}$

However, the actual pressure drop in the fixed bed reactor is usually greater than that calculated. The actual pressure drop (See Table 3-2) was monitored and recorded by the Labview program during the experiments. Twenty grams (20g) of catalyst at a 1-1.3mm particle size results in both sufficient conversion and pressure drop. The parameters obtained by these experiments are helpful for designing a larger shift reactor to be used for the demonstration unit of a renewable natural gas process. This will be presented in the next chapter.

Table 3-2 Pressure drop in WGS reactor using different loading and particle size

Amount of catalyst (g)	10	10	20	20
Particle size	75-150μm	75-150μm	75-150μm	1-1.3mm
Space velocity (h^{-1})	9000	4500	4500	2200
Pressure drop (psi)	12-15	7-10	25-30	1-2

3.3.4 Reforming effects of CH_4 on the WGS catalyst

Another issue needed to be addressed is the stability of methane in the shift reaction. Methane in the producer gas is significant and the reforming of methane (Eq. 3-19 and Eq. 3-20) is an undesired result as the goal is to maximize its amount in the product. The reforming process occurs in a higher temperature range, e.g., 850^{o}C, over a Ni-based catalyst [73, 89]. In this section, the reforming activity of CH_4 over the Fe-Cr based catalyst will be investigated.

$CH_4 + H_2O \Leftrightarrow CO + 3H_2 \quad (\Delta H_o = +206 \text{ kJ/mol})$ (Eq. 3-19)

$CH_4 + 2H_2O \Leftrightarrow CO_2 + 4H_2 \quad (\Delta H_o = +165.0 \text{ kJ/mol})$ (Eq. 3-20)

Pure methane from a gas cylinder and steam were simultaneously fed into the WGS reactor filled with 10g of HTS catalyst and 75-150μm of particle size. The activities were observed under temperature ranging between 350-450^{o}C and steam to carbon ratio of 3 for at least 3 hours each run. The results, in Figure 3-12, presents the deviation of the CH_4 flow rate as dry basis compared between the input and output flow. The change of CH_4 flow rate was insignificantly low in this range of reaction temperature. The average change of flow rate was less than 1%. Thus, CH_4 should be considered unreacted over the Fe-Cr based catalyst [50, 89].

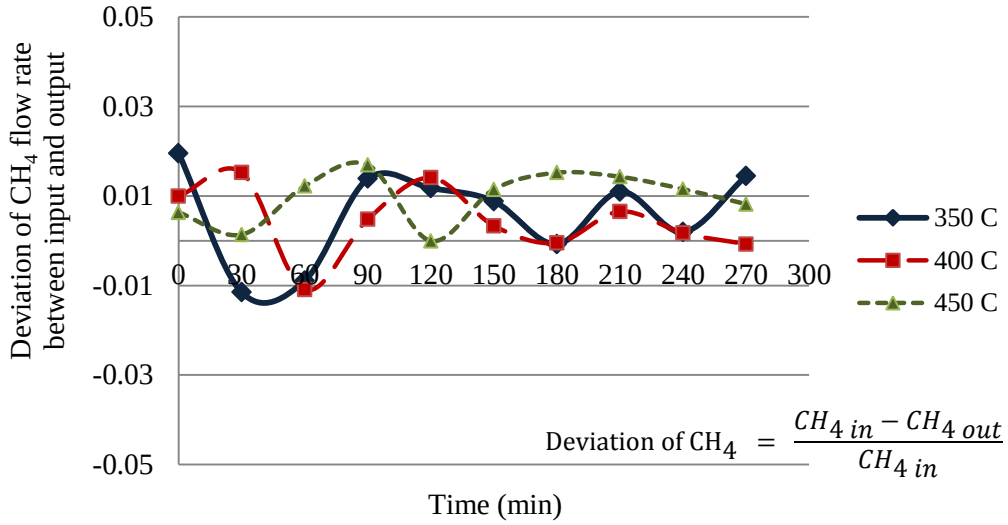

Figure 3-12 Deviation of CH_4 flow rate compared between input and output of WGS system at different temperature

3.3.5 Influences of gas composition on CO conversion

The sensitivity of the CO conversion on WGS reaction using different feedstock is presented here. Table 3-3 presents the composition of some feedstock used in the stirred batch reactor at 750^{o}C and high pressure.

Table 3-3 Chemical composition of some different feedstocks

	Compound	Biosolids mixed with woody biomass	Algae	Bituminous coal
Proximate	Volatile Matter	80.98	71.74	36.19
	Fixed Carbon	16.67	22.39	50.89
	Ash	2.35	5.87	9.75
Ultimate	C	48.37	47.84	67.35
	H	5.95	6.29	5.07
	O	42.72	31.31	13.28
	N	0.46	8.12	1.29
	S	0.16	0.57	3.26

Some of the experimental results were obtained previously from CE-CERT gasification laboratory. The gas composition from RGA analysis results and simulation are given in Table 3-4. Notice that results from the RGA and simulation are well matched except for the percentage of CO_2. This difference is the consequence of the Reverse Water Gas Shift (RWGS) reaction inside the batch reactor during the longer operation period. The reaction is shown in Eq. 3-21.

$$H_2 + CO_2 \Leftrightarrow CO + H_2O \qquad (\Delta H_o = +\ 41 kJ/mol) \qquad \text{(Eq. 3-21)}$$

Table 3-4 Composition of producer gas from SHR using different feedstocks

Feedstock	SHR-Method	H_2 (%)	CH_4 (%)	CO (%)	CO_2 (%)	References
Biosolids+biomass	Simulation	55	22	5	18	Aspen plus
	SHR-batch reactor	69	18	5	8	[90]
Algae	SHR-batch reactor	64	23	6	7	[91]
Bituminous Coal	SHR-batch reactor	60	22	15	3	[92]

These results guided the selection of a variety of input gas composition fed into the shift reactor to investigate the relationship between CO conversion and concentration of CO_2 in the producer gas from SHR. The selected gas compostion was averaged from the data given in Table 3-4. Thus, a new mixture gas, labeled as MG2, consisted of 20% of CH_4, 7% of CO, 7% of CO_2 and balanced by H_2 which normally exists as the highest portion of gas stream from SHR. S/C was maintained at 5.

The CO conversion could be further increased up to 75% at 30 sccm of MG2 using 5g of HTS catalyst reacted at 350^{o}C. This is shown in Figure 3-13. When the total flow rates were increased to 100 and 200 sccm at this reaction temperature and the particle size was increased from 75-150μm to 1-1.3 mm the CO conversion decreased to 72% and 67%, respectively. These results also can be interpreted that the similar level of CO coversion, about 65-67% compared with that of MG1 at 350^{o}C, could be successful using the same amount of catalyst (20g) even though the flow rate of mixture gas, MG2, was double (i.e., operation at the higher space velocity). The conversion was more influenced by the

content of CO_2 compared to that of H_2 when operating at these extreme concentrations of H_2. The lower concentration of CO_2 in mixture gas helped improve the conversion of CO due to the equilibrium was forward shifted. The result means that the volume of the shift reactor can be significantly reduced, by almost 50%, to accomplish the desired WGS conversion when there is approximately 50% lower content of CO_2. It is directly beneficial for a reduction of the captial cost of processing equipment. This result also supports the improvement of gasification efficiency by mitigation of CO_2 in the CE-CERT process using the sorption enhancement and catalytic reaction using biosolids in the CE-CERT gasifier [90, 93].

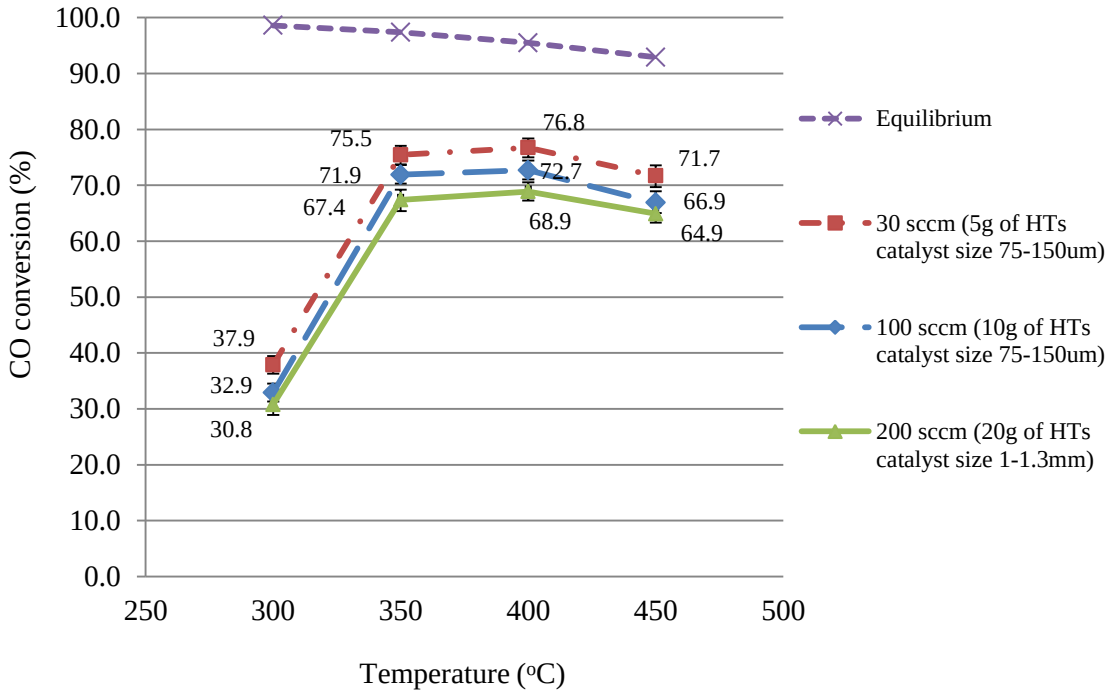

Figure 3-13 CO conversion of mixture gas, MG2, obtained from WGS reaction using various particle sizes and loading of catalyst at different temperature

Figure 3-14 shows the flow rate of output gas from the shift reactor achieved at 67% conversion when operating at the conditions described above. The methane content in the product stream was almost unchanged while the total gas volume incresed due to the amount of H_2 and CO_2 from the WGS reaction. The availability of H_2 for recycle is surplus. CO in the mixture gas, on the contrary, decreased from 7% to 2%.

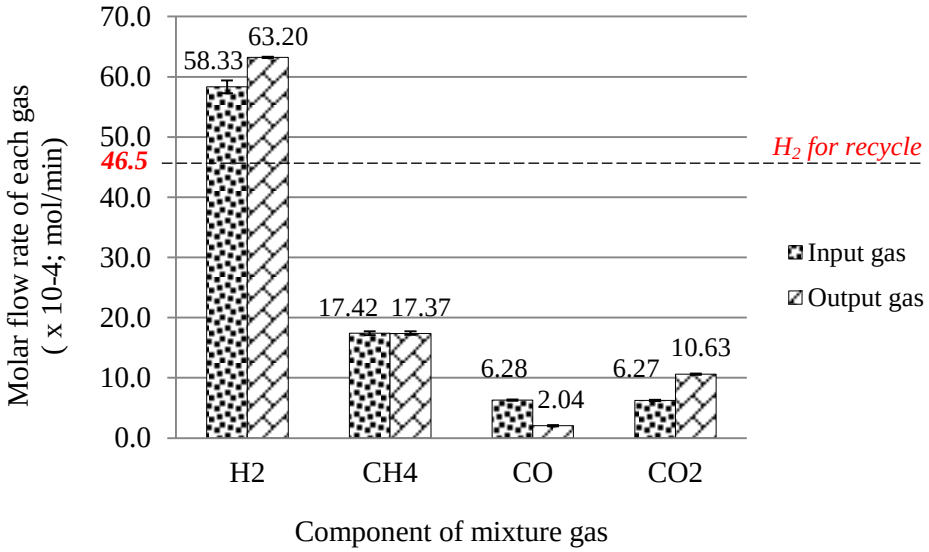

Figure 3-14 Gas species as dry basis of MG2 compared between input and output via WGS reaction at 350°C and space velocity of 4500 h^{-1}

In Figure 3-15, it presents the optimal conversion of CO in WGS reaction using producer gas generated from coal steam hydrogasification as input. The concentration of CO_2 in this mixture gas was even lower which caused of a higher CO conversion up to 85% at the WGS reaction temperature of 350°C. Based on this information, the ratio calculated from the concentration of CO and CO_2 in the producer gas from steam hydrogasification

could be hinted that the larger ratio of CO/CO_2 could be obtained, the higher conversion of CO could be accomplished as illustrated in Figure 3-16.

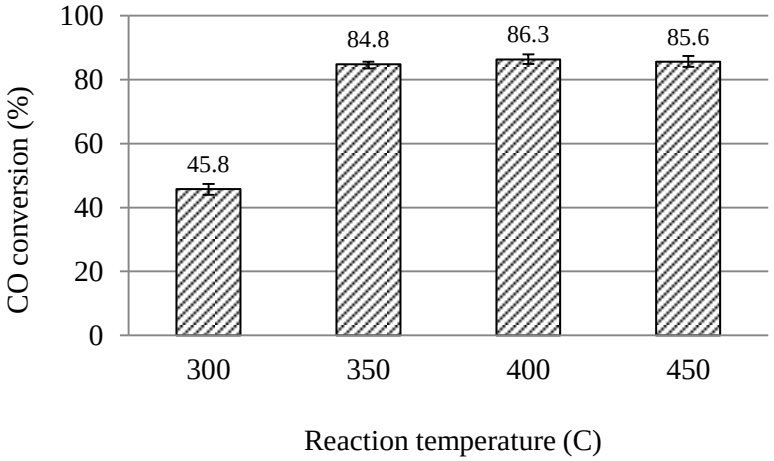

Figure 3-15 CO conversion of WGS reaction at different temperature of a mixture gas produced from steam hydrogasification of coal

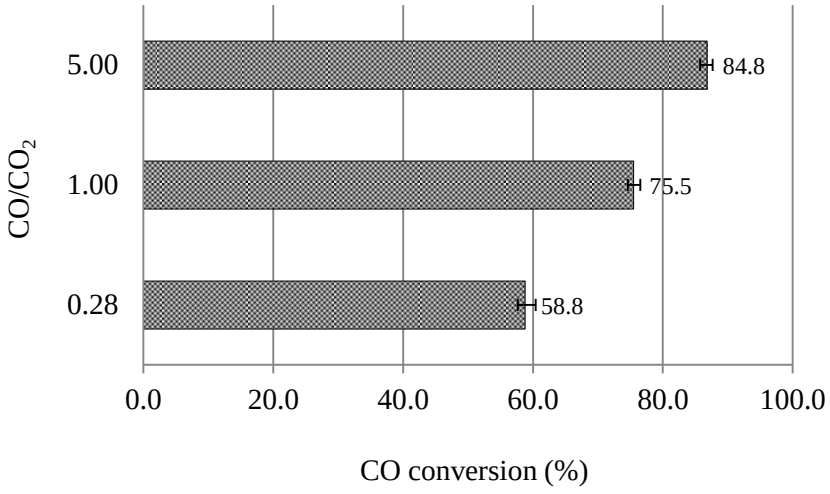

Figure 3-16 CO conversion of WGS reaction at 350^{o}C for different ratios of CO/CO_2 in mixture gas produced from steam hydrogasification

3.3.6 Influence of low steam to carbon ratio over HTS catalyst

For steam hydrogasification, the producer gas is normally carried a plenty of steam. Lacking of steam used to feed into the WGS reactor is rarely occurred. However, the additional investigation of the low steam to carbon ratio in product gas is an interesting issue to study prior to the scaling up of the shift convertor in the next chapter. In this study, the mixture gas, MG2, was simultaneously fed with steam into the shift reactor using HTS catalyst at space velocity of 4500 h^{-1} and atmospheric pressure. The ratio between steam and carbon was 1. Figure 3-17 shows the mole of gas distribution via WGS reaction at temperature between 350-450^{o}C at low content of steam. It was found that approximately 5-6% of CH_4 was generated in the shift reaction at 450^{o}C while the lower reaction temperature could not be clearly indicated. The flow rate of H_2 was slightly lower than the calculation based on the only stoichiometry of WGS reaction. However, the carbon balance was not equivalent. This is corresponded with several publications earlier studied on the operation of low steam ratios in WGS reaction [94, 95]. In the absence of steam, the formation of metallic iron can be existed using HTS catalyst in shift convertor. This would lead to methanation and also carbon formation deposited on the catalyst. As the low steam ratio is operated, it is possible to form iron carbides which is able to synthesize hydrocarbons from the carbon oxides and hydrogen (Fischer-Tropsch reaction) [73]. In such a case, the formation of hydrocarbons will consume the valuable H_2 in which it is undesirable for the RNG process even though more amount of methane can be obtained.

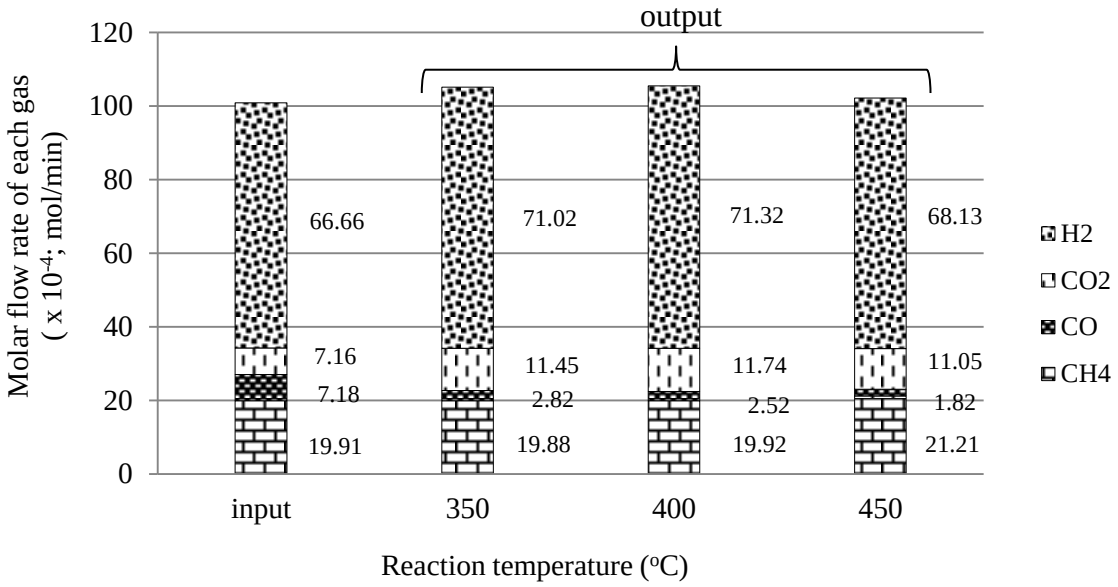

Figure3-17 Gas species as dry basis of MG2 compared between input and output via WGS reaction at S/C = 1 (at 350-450^{o}C and space velocity of 4500 h^{-1})

3.4 An alternative process of RNG production for a high sulfur feedstock

3.4.1 Experimental setup for WGS reaction using a sour gas shift catalyst

Some sulfur species are generally found in the producer gas generated from the conventional gasification process. Steam hydrogasification is not excluded. The amount and type of sulfur compounds (e.g., H_2S COS CS_2) are dependent on the type of feedstock used to gasify [92]. Coal usually has higher sulfur content than any biomass. The option for RNG production using CE-CERT technology is to include a sulfur tolerated catalyst in this process. The SHR product gas can be directly delivered into the shift reactor without first undergoing any cleanup process. In this case, the shift reactor is operated as a "sour gas shift" reactor with a special catalyst. The final product gas can then be subjected to cleanup under ambient conditions. In this section, a commercial

sulfur resistant catalyst, ShiftMax®820, supplied by the Clariant Corporation (SÜD-CHEMIE) was used to investigate its behavior and optimize the shift reactor. The process configuration shown in Figure 3-18 was used with a high sulfur content material as feedstock. The specification of the SGS catalyst is given in Table 3-5 [96].

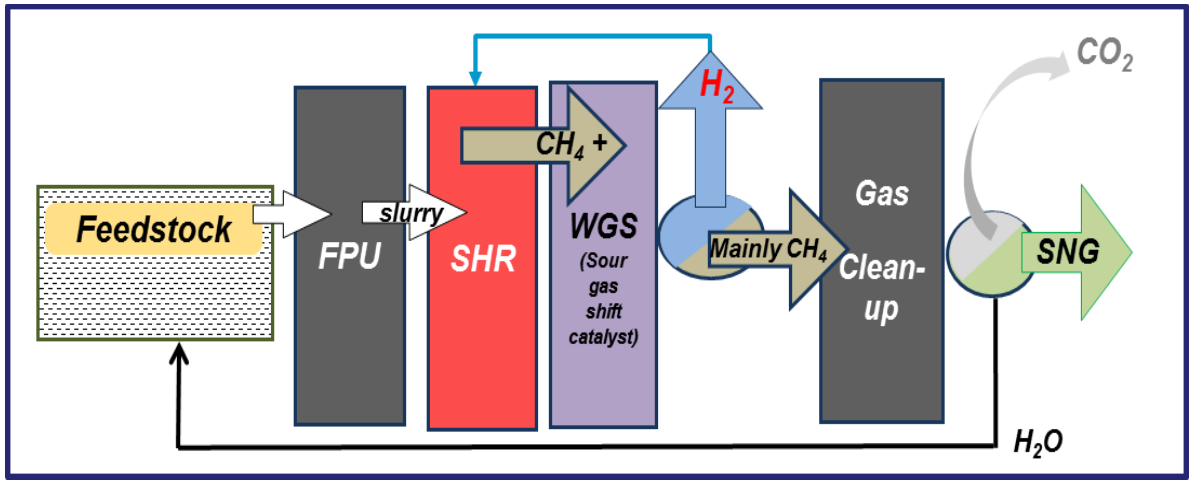

Figure 3-18 Schematic diagram of the RNG production using sour gas shift reactor

Table 3-5 Specification of ShiftMax®820

Composition	Content (wt.%)
CoO	4
MoO_3	10
Al_2O_3 support	Balance
Bulk density (kg/l)	0.8
Size (mm)	3.2
Shape	Extrusions

The ShiftMax®820, sour gas shift (SGS), catalyst in its oxide form was supplied in pre-sulfided form. Therefore, a sulfidation procedure is required to activate the catalyst following the procedure below [96].

1. After loading of catalyst in the stainless steel tubing reactor, it was heated from ambient condition to 150-180^{o}C under N_2 environment with the temperature ramp of 50^{o}C/h at atmospheric pressure.
2. Then H_2-contained gas (about 20% H_2) at a minimum space velocity of 200 $Nm^3/m^3/h$ of catalyst was introduced into the reactor.
3. Increase of temperature to 175-205^{o}C was set up to assure that water did not condense on catalyst bed.
4. 4% wt. of sulfur contained in the activation gas, H_2 and N_2, was then flowed through the reactor for activating the catalyst bed.
5. Temperature of the reactor was increased to 450^{o}C with the same heating rate.
6. The catalyst was continuously sulfided for 4 hours. After sulfidation, the desired gas stream was injected into the reactor for the investigation.

The normal operating inlet temperature range for the ShiftMax®820 is 235^{o}C to 275^{o}C with a maximum bed temperature of 510^{o}C. The pressure for typical operation was between atmospheric and 1422psi (100 kg/cm^2) [96]. Sulfur is present in the feed stream and must be keep at a certain level depended upon the operation conditions. Usually, it is above 100 ppm.

An additional pipeline and a MFC were added into the lab-scale WGS reactor to conduct the experiment as shown in Figure 3-19. In this study, a mixture of 10% H_2S in N_2 gas cylinder was simulated as a source of sulfur mixed in the producer gas. It was reported by an earlier study that only sulfur in form of H_2S was existing in the raw gas produced by the steam hydrogasification [92].

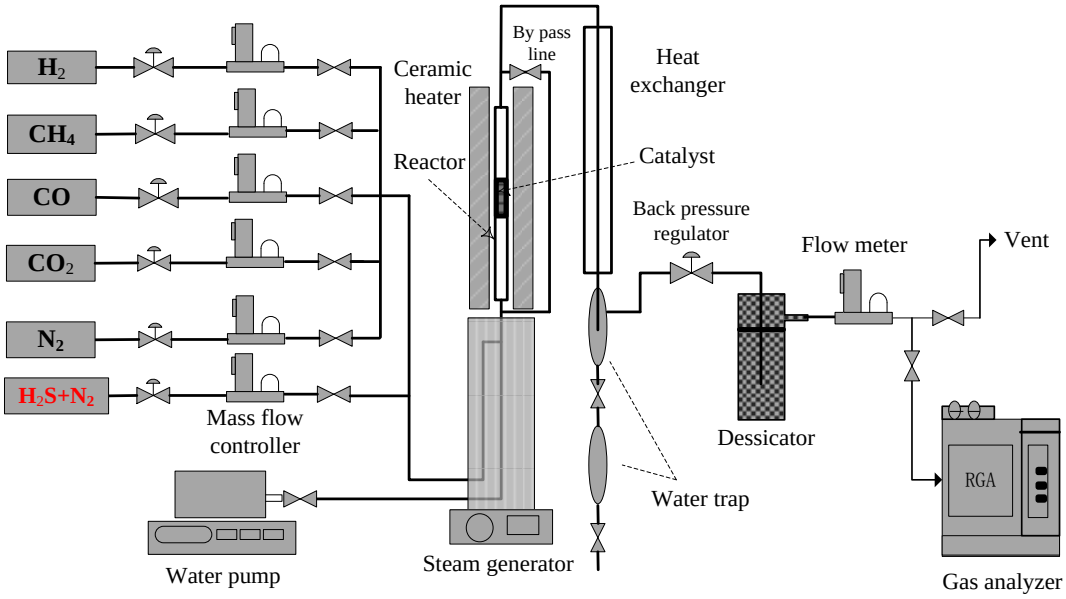

Figure 3-19 Schematic diagram of WGS reaction system using sour gas shift catalyst

It was calculated in a previous simulation given in Chapter 2 that the content of H_2S in the producer gas using biosolids co-mingled with pine wood as the feedstock is about 330 ppm. The content of H_2S in mixture gases (both MG1 and MG2) in these experiments were varied from 350 to 3400 ppm [76, 97] to observe the activity of the WGS reaction at

various concentration of sulfur. The experiments were carried out following the conditions given below from which the optimum condition would be determined.

- Temperature: 350 – 500^{o}C
- Pressure: Atmospheric
- Particle size of catalyst: 75µm – 1.3mm
- Catalyst loading: 5 – 20g
- Total flow rate of mixture gas: 30 – 200sccm
- Steam to C ratio: 5:1
- Concentration of H_2S in mixture gas: 350 – 3400ppm

3.4.2 Influences of H_2S concentration on the performance of SGS catalyst

H_2S was blended into the input gas (MG1) at the concentration of 350 ppm to represent the raw producer gas from the SHR. Total flow rate of input gas was about 100sccm as dry basis. The concentration of H_2S was confirmed by the H_2S detector tube (Matheson Kitagawa No.8014-120SF). Then, the CO conversion of the sour gas shift reaction at 450-500^{o}C was explored. Experiments were continued using higher levels of H_2S at concentrations of 960, 2100 and 3400 ppm to investigate the performances of the SGS catalyst.

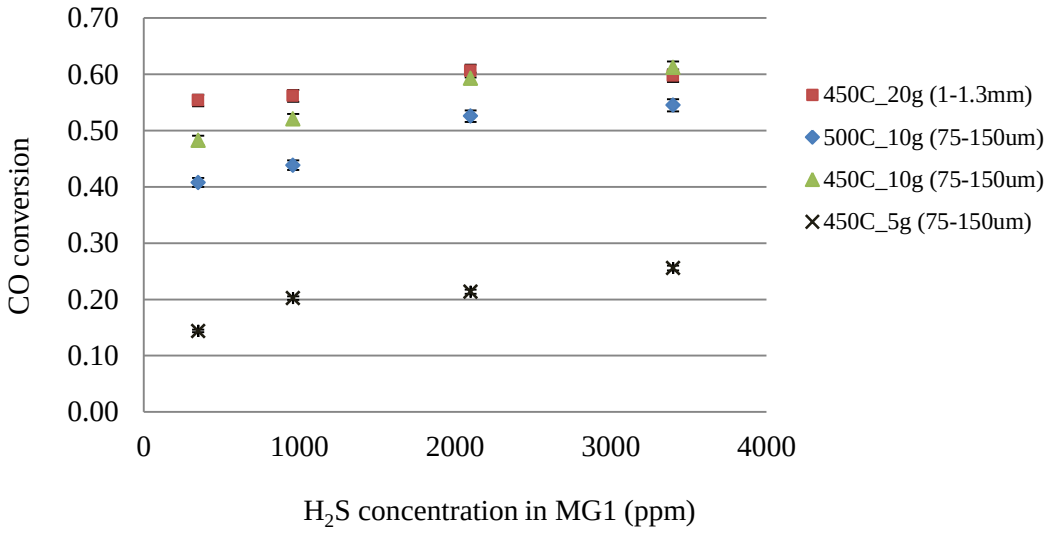

Figure 3-20 CO conversion of MG1 contained the different concentration of H_2S operated at various space velocities (2500-10000 h^{-1})

The results, shown in Figure 3-20, illustrate that the performance of SGS catalyst depends significantly on the concentration of H_2S in the feed gas. At each of space velocity, the CO conversion increased about 10-15% when the sulfur content was increased from 350 to 3400 ppm. These results point out the necessity of maintaining a certain level of H_2S in the raw gas to keep a high activity of the SGS catalyst. Frank [98] reported that the sulfur content of 550 ppm by volume at least was required to keep the catalyst active on the specified process at 440^{o}C.

At the low level of H_2S, 350 ppm, in the mixture gas, conversion was improved from 14% to 55% when the space velocity was reduced from 10000 to 2500 h^{-1} at the reaction temperature of 450^{o}C. However, CO conversion was lowered by 7-10% when the

reaction temperature was increased from 450 to 500°C at the same catalyst conditions. The maximum conversion obtained in this study was about 60% under the level of sulfur content in the range of 2000-3400 ppm.

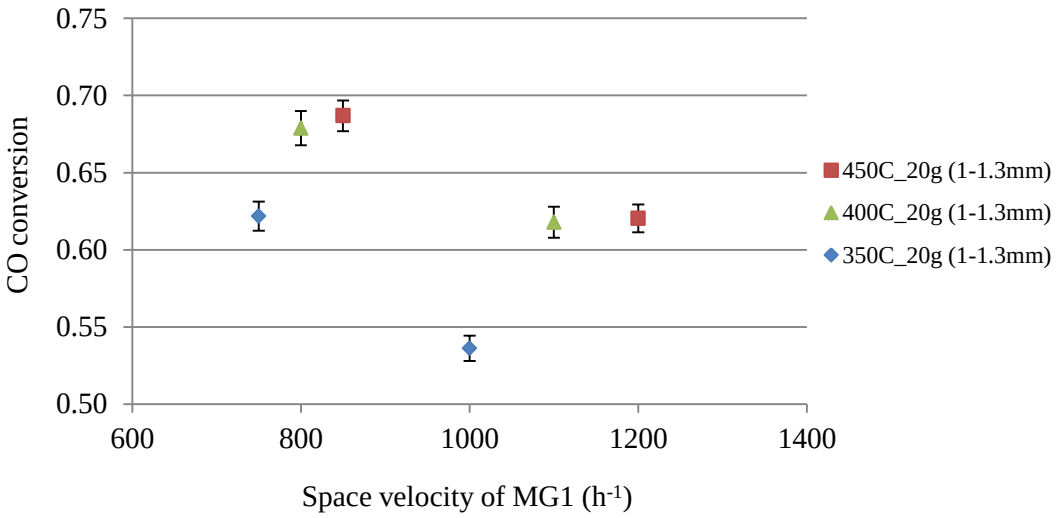

Figure 3-21 CO conversion of MG1 contained 350 ppm of H_2S at different temperature

More experiments of the activity of ShiftMax®820 catalyst were carried out at lower reaction temperature and space velocity using a low sulfur content at 350 ppm. Figure 3-21 shows that the CO conversions at temperature of 450°C were able to reach at 62-69% when the space velocities were lowered to 800-1200 h^{-1}. However, the activity of this catalyst was slightly lower at 400°C and the conversion was dropped to 54-62% when it was run at 350°C. This means that a longer residence time or a larger size of sour gas shift reactor is required if a low sulfur producer gas is applied to this process.

3.4.3 Influences of different gas distribution over sour gas shift reaction

The performance of the SGS catalyst was carried out comparing two types of input gases, MG1 and MG2 at reaction temperature of 450^{o}C and space velocity of 2500 h^{-1}. As seen in Figure 3-22, it indicates that the conversions of CO for MG2 were apparently higher than those of MG1 in all concentrations of H_2S. The conversion could be increased from 55-60% for MG1 to 71-79% for MG2 for the content of sulfur between 350-3400 ppm in gas. These results are consistent with the outcome of the WGS reaction using a HTS catalyst.

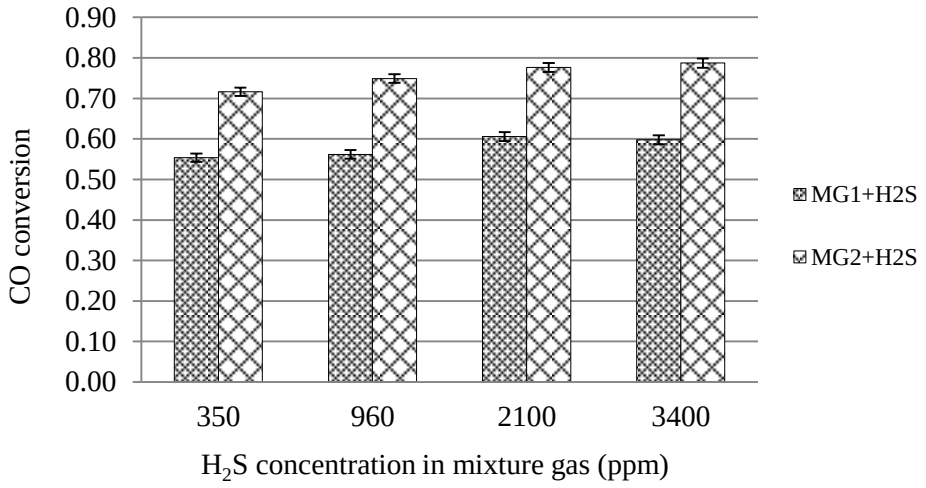

Figure 3-22 CO conversion of mixture gases contained the different concentration of H_2S operated at 450^{o}C and space velocity of 2500 h^{-1} (20g of SGS catalyst)

From the experimental result, CO conversion of MG2 with the content of H_2S at 350 ppm could be increased to 77% and 81% when the space velocity was decreased to 1200 h^{-1} and 800 h^{-1}, respectively, as presented in Figure 3-23. However, these results require a

much larger size shift reactor. To summarize, about 72% of sour gas shift conversion at space velocity of 2500 h^{-1} could be obtained.

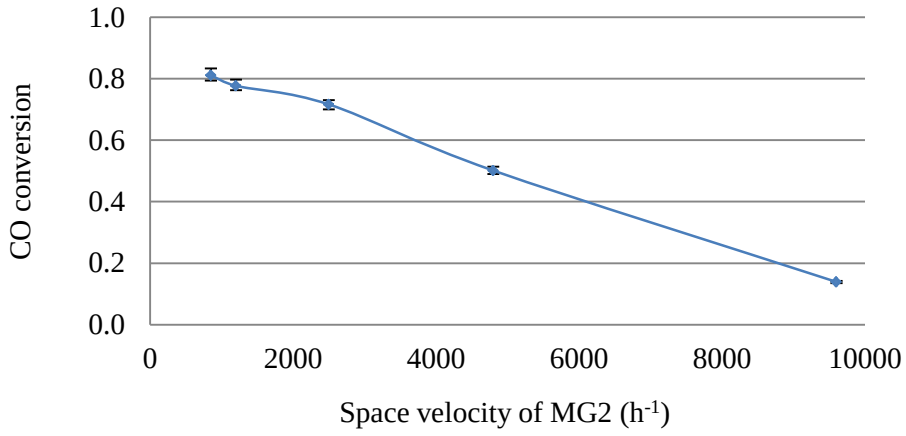

Figure 3-23 CO conversion of MG2 contained 350 ppm of H_2S at 450^oC

Figure 3-24 presents the gas distribution, at 72% of CO conversion, between the input and output streams at the optimum conditions derived from the above experiments. The flow rate of H_2 increased approximately 9% in which it could be used for recycle in SHR after purification. The content of CH_4 was almost unchanged at these conditions and the CO was reduced from 7.1% to 1.8% on a molar basis.

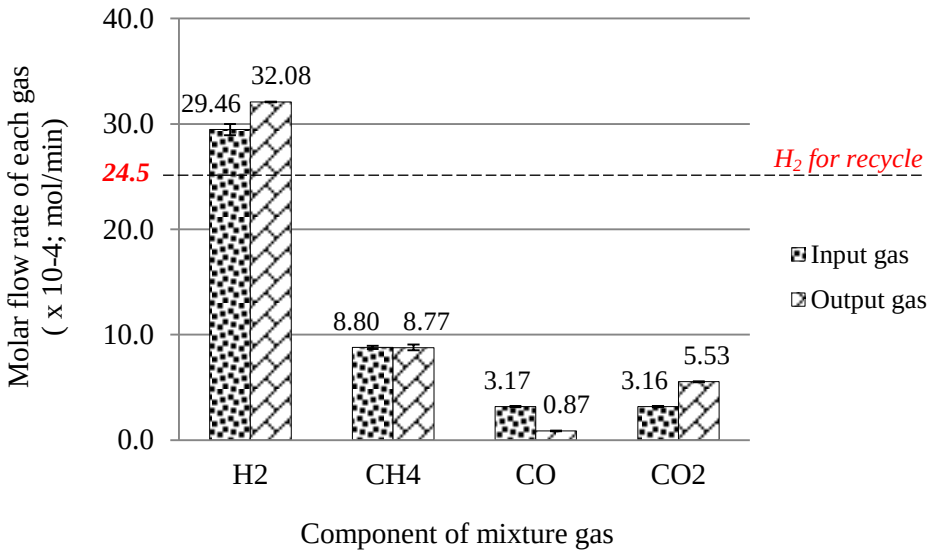

Figure 3-24 Gas distribution compared between input and output of sour gas shift reaction for MG2 contained 350 ppm of H_2S at 450°C and space velocity of 2500 h^{-1}

The SGS catalyst can be used successfully with a producer gas generated from high sulfur content such as coal. The sulfur content of sour gas generated from the co-mingled feedstock was approximately 350 ppm. The optimal conversion using the SGS catalyst was about 72% at space velocity of 2500 h^{-1}. On the other hand, the conversion was about 67.5% when a HTS catalyst was applied to the sulfur-free gas at space velocity of 4500 h^{-1}. These results led to further investigation of the performance of a shift reaction by directly applying a HTS catalyst in the sour gas. MG1 and MG2 were used to evaluate the performance of a shift reaction over the HTS catalyst using the different level of H_2S in the feed gas operated at 350°C and space velocity of 4500 h^{-1} (100sccm with 10g of HTS catalyst). Generally, H_2S negatively affects the activity of WGS reaction. The

sulfur species hinders the reaction by occupancy of the active sites on the surface of HTS catalyst following the reaction shown below (Eq. 3-22).

$Fe_3O_4 + 3H_2S + H_2 \Leftrightarrow 3FeS + 4H_2O$ (ΔH = -75.0 kJ/mol) (Eq. 3-22)

The loss of active site of catalyst caused the lower reaction rate on WGS reaction. Bohlbro [98] reported that the reaction rate using an HTS catalyst at 350^oC and atmospheric pressure was decreased approximately 50% with 1000ppmv of H_2S containing in syngas. Similarly, Hla et al. [99] studied the effect of 17-1100ppmv on the commercial Fe-Cr based catalyst at 450^oC and found the 3 different concentrations ranges of H_2S has negative impacts on the reaction rates. Figure 3-25 shows that the conversion of MG1 and MG2 were declined from 60% to 37% and 72% to 53%, respectively, when the H_2S in both mixture gases were increased from 0 to 3400 ppm. The decrease in conversion for MG1 and MG2, found in this study, could be predicted by the equations (Eq. 3-23 and Eq. 3-24) as shown below.

For MG1: CO conversion = $-7x10^{-5}$ x $[H_2S]$ + 0.6026, R^2 = 0.9721 (Eq. 3-23)

For MG2: CO conversion = $-5x10^{-5}$ x $[H_2S]$ + 0.7071, R^2 = 0.9702 (Eq. 3-24)

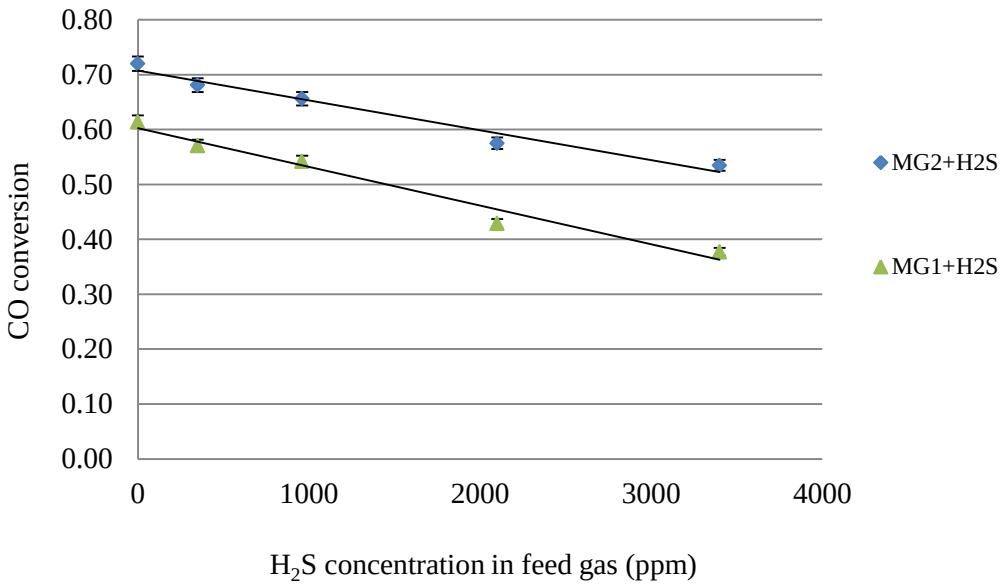

Figure 3-25 CO conversion at different level of H_2S in feed gas for WGS reaction using HTS catalyst at 350^oC (CO/CO_2 = 0.28 and 1.0 for MG1and MG2)

The shift reaction using an HTS catalyst to convert CO in the producer gas contained 350ppm of H_2S could be achieved at 57% and 68% for MG1 and MG2, respectively. Both result in the hydrogen surplus available for recycling as feed into the steam hydrogasification step. Mole balance and flow rate were illustrated in Figure 3-26 and 3-27. The flow rates of methane are fairly stable.

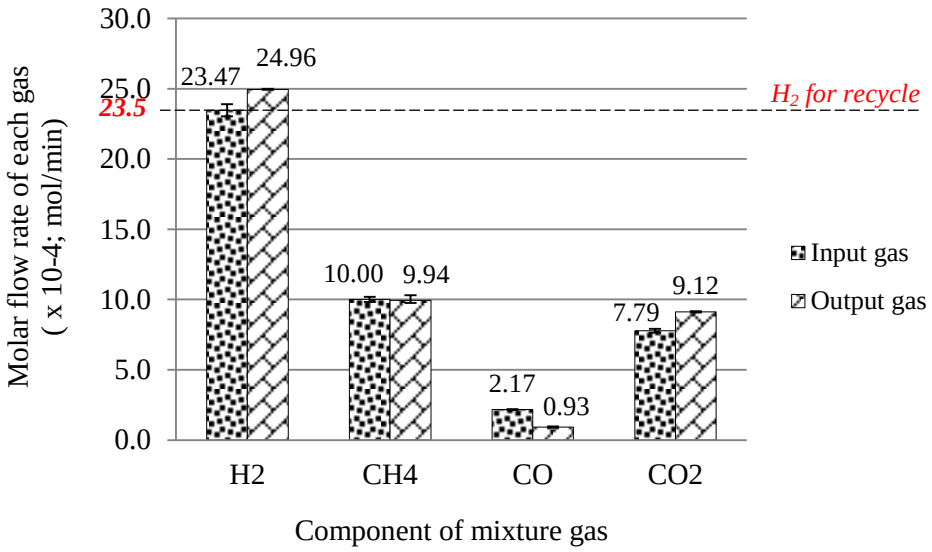

Figure 3-26 Gas distribution compared between input and output of WGS reaction using HTS catalyst for MG1 contained 350 ppm of H_2S at 350^oC and space velocity of 4500 h^{-1}

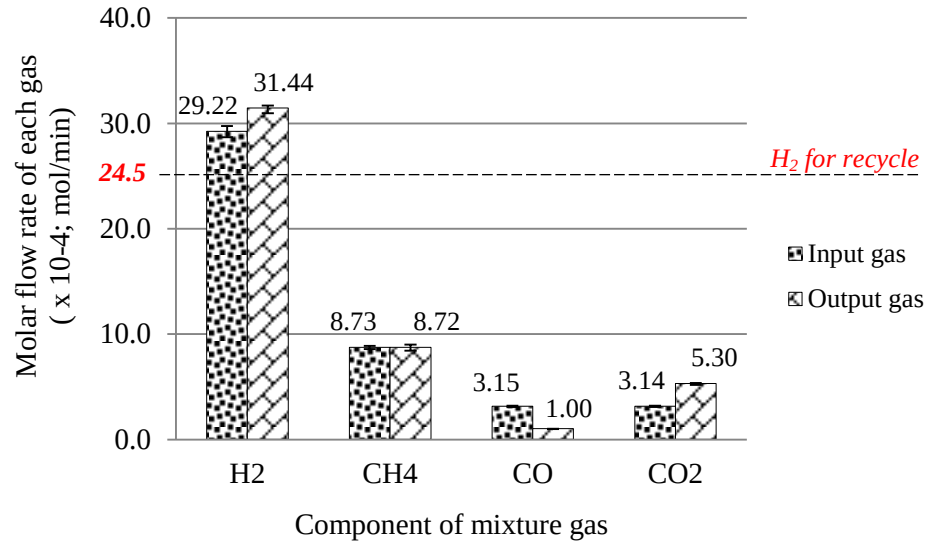

Figure 3-27 Gas distribution compared between input and output of WGS reaction using HTS catalyst for MG2 contained 350 ppm of H_2S at 350^oC and space velocity of 4500 h^{-1}

3.5 Summary

The performance of a commercial high temperature, Fe–Cr based, catalyst has been successfully evaluated under the specific conditions to determine the optimum conversion on the lab-scale WGS reaction system. The influence of the main operating parameters, including temperature, space velocity, feed composition, and steam to CO ratio, on the activity of the catalyst has been explored. The amount of steam in the system was found to be a critical parameter. The lower steam condition at 450^{o}C can promote the methanation in the shift reactor. It results in an increased fraction of CH_4 in final product gas but the availability of H_2 is suppressed and not sufficient to be recycled. Approximately 65-67% of CO conversion can be obtained at the reaction temperature of 350^{o}C and space velocity of 2500-4500 h^{-1}. This guarantees an adequate H_2 availability for recycling as feed into the SHR with the amount of CH_4 maintained relatively constant. In addition, the volume of the shift reactor can be reduced if the ratio of CO/CO_2 in the producer gas is increased. The parameters obtained from the experiments, given in Table 3-6, will be used to scale up a new WGS reactor to implement for RNG production with the CE-CERT technology. This will be presented in the next chapter.

Table 3-6 Summary of the optimum condition from the lab-scale WGS reactor

Amount of catalyst (g)	HTS catalyst	SGS catalyst	HTS catalyst
Particle size	1-1.3mm	1-1.3mm	75-150μm
Content of sulfur (ppm)	0	350	350
Space velocity (h^{-1})	2500-4500	1200-2500	4500
Temperature (^oC)	350	450	350
Pressure drop (psi)	1-2	1-2	7-10
CO conversion (%)	65-68	62-72	57-68

The commercial sulfur tolerant Co-Mo based catalyst has also been investigated in this research to optimize the conditions for a shift reactor using a sour gas produced from SHR. This catalyst performed well in a high sulfur atmosphere and is preferred for high sulfur applications. For the feedstock containing low sulfur, in this study, the reaction temperature of 450^oC with space velocity of 1200-2500 h^{-1} is the proper condition to operate. However, the HTS catalyst may be alternatively applied in this condition.

Chapter 4 Process demonstration unit for RNG production

4.1 Thermochemical processes for RNG/SNG production from organic waste

Many research groups have published results on the production of biomass derived syngas by several gasification technologies. The primary component of the product gas usually consists of H_2, CO and CO_2 with a small content of CH_4. The goals are to utilize the H_2 and CO output gas as a fuel, upgrade to methane by a Methanation process, provide a source of hydrogen for fuel cell or convert to a liquid fuel by a Fischer–Tropsch process. Elder and Groom [100] reported the performance of a pilot plant of a downdraft gasifier using pine wood and mixed-hardwood chips as the feedstock, at a rate of 17-30 kg/h, to produce a syngas with an energy content of 6MJ/m^3. The syngas consisted of 44% H_2, 46% CO, 7% CH_4 and 3% CO_2. Sheth and Babu [101] used a downdraft system for the gasification of wood-waste to study the relationship between the moisture in feed, the air flow rate and char production. The producer gas contained 26% H_2, 51% CO, 5% CH_4 and 18% CO_2 with an energy content ranging from 4.5 to 6.5 MJ/m^3 depending on the input ratio. Judex et al. [102] built two demonstration plants (at Balingen and Mannheim) of an air/steam fluidized bed gasifier under atmospheric condition operating temperature between 850-900^{o}C and using sewage sludge from the local municipal waste water treatment plant. The product gases contained 13% H_2, 8% CO, 2% CH_4 and 17% CO_2 with an energy content of 3.2 MJ/m^3 in Balingen and 13% H_2, 14% CO, 4% CH_4 and 13% CO_2 with energy content of 4.7 MJ/m^3 in Mannheim. Saw et al. [60] studied the effect of proportional ratio of biosolids blended with wood using steam gasification, at a 15.5 kg/h feed rate, to produce H_2-rich syngas at a temperature 720^{o}C. It was reported

that H_2 content in syngas increased with a higher ratio of biosolids loading in the fuel but the gas yield decreased. Blending 10-20% biosolids with wood had little impacted on the gas yield and cold gas efficiency. Mozaffarian and Zwart [103] produced SNG using a combination process of biomass hydrogasification and methanation. The properties of the SNG were comparable to standard natural gas. The final product gas comprised of 81.6% CH_4, 8.7% H_2 and 8.5% CO_2 with the energy content of 39 MJ/kg and an acceptable Wobbe-index number.

SHR is the hydrogasification reaction carried out in the presence of steam. The presence of steam enhances the rate of methane formation compared to conventional dry hydrogasification [44]. The hydrogen necessary for the SHR is generated internally and recycled back to the SHR. Thus, an external hydrogen supply is unnecessary in this process. The SHR configured with a WGS reactor has a potential to produce renewable or substitute natural gas (RNG/SNG) at a high percentage of methane. It is important to note that the WGS requires high temperature steam as a feed. Thus, the output stream of the SHR does not need to be dried. In this Chapter, the results of a process demonstration unit (PDU) for RNG production using SHR configured with a WGS reactor would be presented. In addition, a detailed process and equipment design would be introduced. Figure 4-1 shows the block diagram of the SHR-WGS system. Mass balance calculations compared with the real operation of the PDU would be presented in the next section.

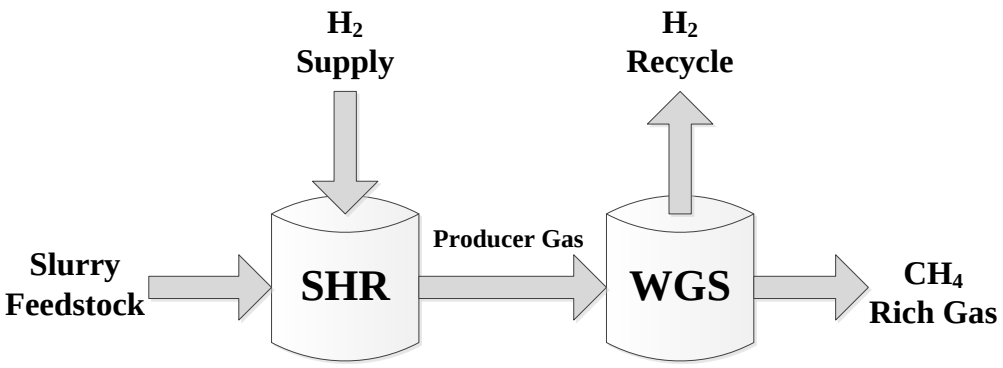

Figure 4-1 Simplified diagram of SHR-WGS configuration

4.2 Introduction of CE-CERT process demonstration unit (PDU) for RNG

4.2.1 Feedstock Pretreatment Unit (FPU)

The purpose of the FPU is to prepare the comingled feedstock so that it can be efficiently delivered to the downstream pressurized gasifier. A pumpable slurry using a progressive cavity pump can handle the feedstock in a cost and energy effective manner. Feedstock with high moisture content favors a wet feeding procedure. The biomass slurry is not simply formed by mixing the woody wastes and biosolids because of their highly hygroscopic and hydrophilic properties [61, 62]. A Hydrothermal Pretreatment (HTP) process has been developed in order to provide a high solid content of comingled slurry for the CE-CERT process [42, 68].

The hydrothermal reactor with a capacity of 5 gallons is made of 316-stainless steel. A magnetic stirrer powered by an electric motor is coupled with the agitator inside the

reactor. The vessel is wrapped with 3 sets of electric heaters to provide uniform heat. A serpentine cooling coil with a coolant circulating system is installed in order to quickly remove the heat from the reactor after the process. A control and monitor system was provided by Parr Instruments [42]. A flow diagram and a bench scale HTP reactor are described in Figure 4-2 and 4-3. A previous study stated that high pretreatment temperature had a major influence on carbon redistribution in the gas, liquid and solid phases of slurry after the process [43]. We found that the loss of carbon content in the slurry product was less than 1.0% of the original carbon loading. The increase of the flowability of the slurry in which its viscosity was determined to be only 1.0 Pascal-second at a 1/100 sec shear rate. This was the maximum value for a homogeneous form of pumpable slurry reported by earlier studies.

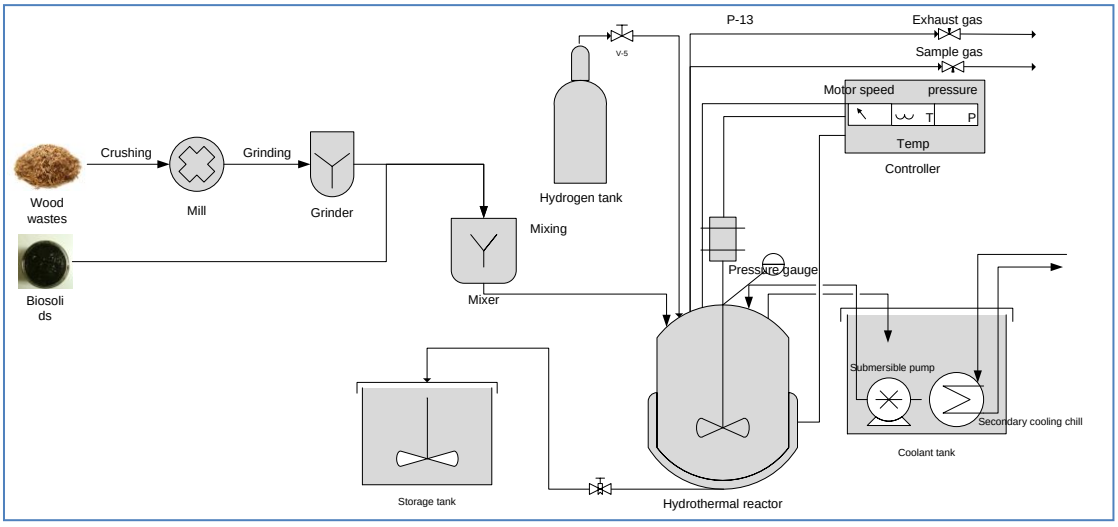

Figure 4-2 Flow diagram of CE-CERT Hydrothermal Pretreatment (HTP)

Figure 4-3 Stirred batch type hydrothermal reactor

The comingled feedstock in this study was prepared from pine wood sawdust mixed with sewage sludge or biosolids. The pine wood was initially crushed in a laboratory mill (Thomas–Willey model 4, Arthur H. Thomas Company) to reduce the size of particles. Then, the wooden pieces were pulverized in a grinder (Braun KSM-2W) and further sieved to particle size ranging of 150μm-180μm. It was then dried in a vacuum oven at 70^{o}C for 3 hours to eliminate any further moisture [43]. Dissolved Air Floatation Thickener (DAFT: discharged from the Wastewater Treatment Plant, Riverside, CA) was used as a source of biosolids for this research. A former study stated that the chemical composition of biosolids changed insignificantly relative to the season [42, 43]. The comingled slurry was formed using the batch type HTP system at the temperature of 240^{o}C and a pressure of 1420psi which resulted in a solid loading of over 40 wt% in

feedstock meeting the requirement of the CE-CERT process [104,105]. Examples of untreated and HTP treated mixture of woody waste (pine wood) and biosolids are shown in Figure 4-4. The chemical properties of the slurry are given in Table 4-1.

Figure 4-4 Untreated and HTP treated samples of biomass comingled with biosolids

Table 4-1 Composition of biosolids comingled with pine wood

Proximate	Volatile Matter	80.98
	Fixed Carbon	16.67
	Ash	2.35
Ultimate	C	48.37
	H	5.95
	O	42.72
	N	0.46
	S	0.16

4.2.2 Bubbling Fluidized Bed Gasifier

A Bubbling Fluidized Bed (BFB) Gasifier sponsored by the California Energy Commission (CEC) has been built in the CE-CERT gasification laboratory to demonstrate the steam hydrogasification process. This type of gasifier has a long history of being used for a number of chemical processes [106]. This type of reactor itself has a high heat transfer rate, and is also well-known for the reliability when used in biomass gasification [106]. The residence time is longer than 10 seconds and is favored due to the slower reaction rate of hydro-gasification compared to that of partial oxidation [106]. The capacity of the reactor for the SHR demonstration unit is 0.1TPD as dry basis. The reaction vessel is made of an Inconel pipe of 4 in. outside diameter. The heating source is provided by 5 sets of ceramic fiber heaters (WATLOW) which cover along the length of the reactor. They are controlled by a series of PID controllers (OMEGA) and can provide uniform heating up and cooling down. The design meets the nominal temperature of 750^{o}C and pressure of 400psi when operated in the environment of hydrogen and steam. Silica sand supplied by U.S Silica Company was used as the inert media in the fluidized bed gasifier and the sand particles are assumed to be uniformly spherical. The properties of sand are given in Table 4-2 [107]. There are four major parts assembled as part of the SHR of the PDU system following.

- A fluidized bed reactor where the main chemical reaction would be taken part.
- A distributor is used to control the inlet flow of gas.
- A cyclone is used to gather sands and other particles left of the reactor by gas flow.
- A gas chamber is used to collect the product gas.

The general information of design and specification of SHR are listed in Table 4-3.

Table 4-2 Specification of silica sand and ground silica

Component	**CAS#**	**%**
Crystalline Silica (quartz)	14808-60-7	98.7-99.9
Aluminum Oxide	1344-28-1	< 1.1
Iron Oxide	1309-37-1	< 0.1
Titanium Oxide	13463-67-7	< 0.1
Particle size		150 µm
Density		2.65 g/cm^3

Table 4-3 Summary of the bubbling fluidized bed gasifier design parameters

Parameter of Reactor	**Dimension/Value**
Inner diameter (cm)	9.40
Total height (m)	4.27
Stagnant bed height (m)	0.40
Bed height (m)	3.48
Particle size of sand (µm)	150
Volume of loaded sand (L)	2.3
Gas velocity (m/s)	0.019-0.086
H_2 density of (g/cm^3)	2.43×10^{-4}
H_2 viscosity (N-s/m^3)	1.90×10^{-5}
Temperature (°C)	750
Bed pressure (psi)	150

The detailed design drawing of the bubbling fluidized bed gasifier is shown in Figure 4-5. The equipment list is presented in Appendix A, (Table A-1).

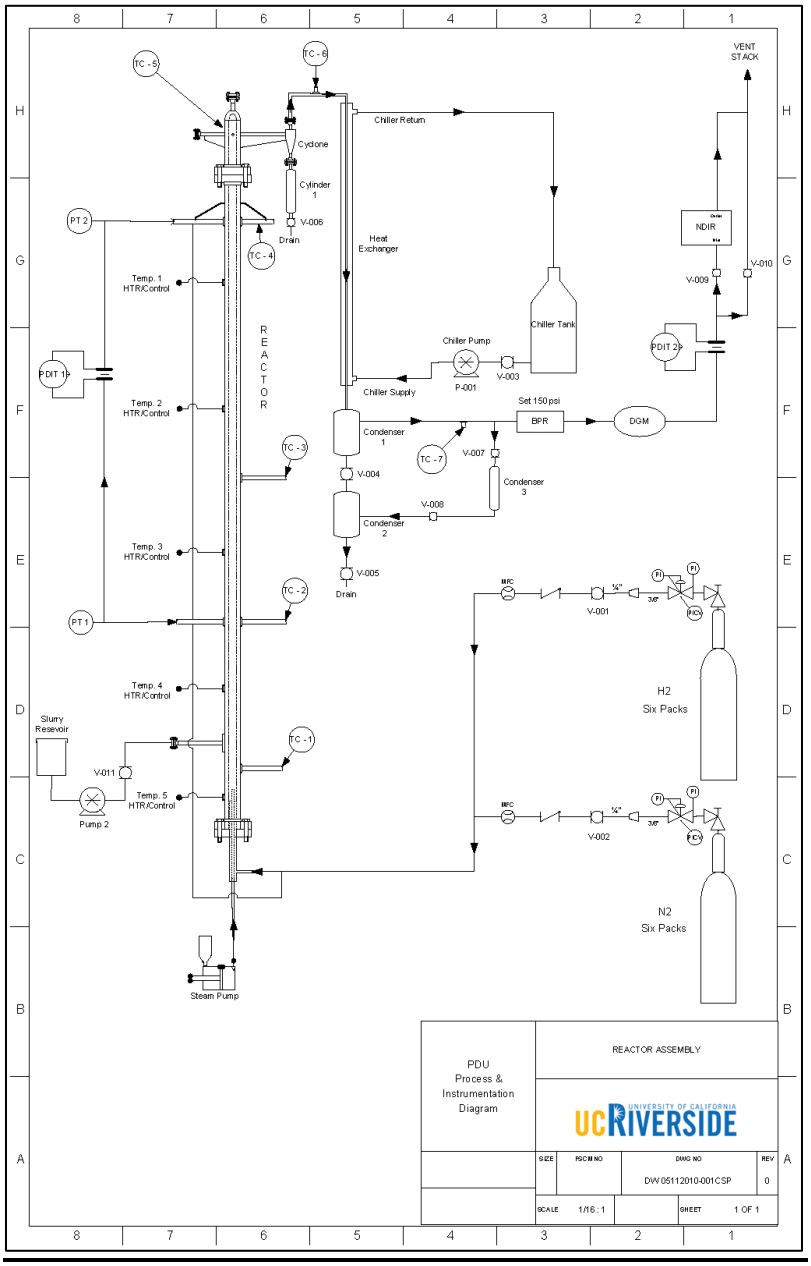

Figure 4-5 Detail of the process diagram for SHR-PDU

4.2.3 Design and construction of the water gas shift reactor

A new fixed bed reactor for the WGS reaction was built and tested the performance. The details are presented in this chapter. It was set up based on the experiments given in the previous chapter. The shift reactor is made of 316 stainless steel tube with 1 in. outside diameter in which it is covered by 2 sets of ceramic fiber heater (WATLOW 1100watt, 120volt) to provide sufficient heat during the reaction. Temperature of the reactor is controlled by a PID type controller and the catalyst bed temperature is monitored by a TC at the outlet of the bed. Two pressure transducers at the inlet and outlet of the reactor are able to monitor the pressure drop across the packed bed in order to be aware of the problem of coke formation in the bed. The loading of the catalyst is 400g using the particle size of 2.5-3mm. This amount is about 20 times of that determined by the optimum condition from a series of lab-scale experiments presented in Chapter 3. The particle size was picked to be a bit larger than that of the optimal one based on the relationship between the particle size of the catalyst and the inner diameter of the reactor. From the experimental result, the ratio of ID/d_p from the experimental results is approximately 8-11. This was selected for a safety reason to avoid the chance of getting too high pressure drop if clogging occurs in the reactor from carbon accumulation on the catalyst. A wet gas stream from the SHR is transferred to the shift reactor by a transfer line connected between the outlet of the cyclone located on the top of SHR and the inlet of WGS reactor. The system is also consisted of a blocked valve used to control the upstream flow rate fed into the shift reactor. The transfer line is wrapped by electric heating tapes to maintain the upstream temperature over the dew point. The detailed

drawing and design parameters of WGS reactor are shown in Figure 4-6 and Table 4-4, respectively. The process diagram and part list of the shift reactor are presented in Appendix A, (Figure A-1 and Table A-2). In addition, the remote controllers and monitoring systems, for both SHR and WGS, are set up to collect and record all real time data using LabVIEW software.

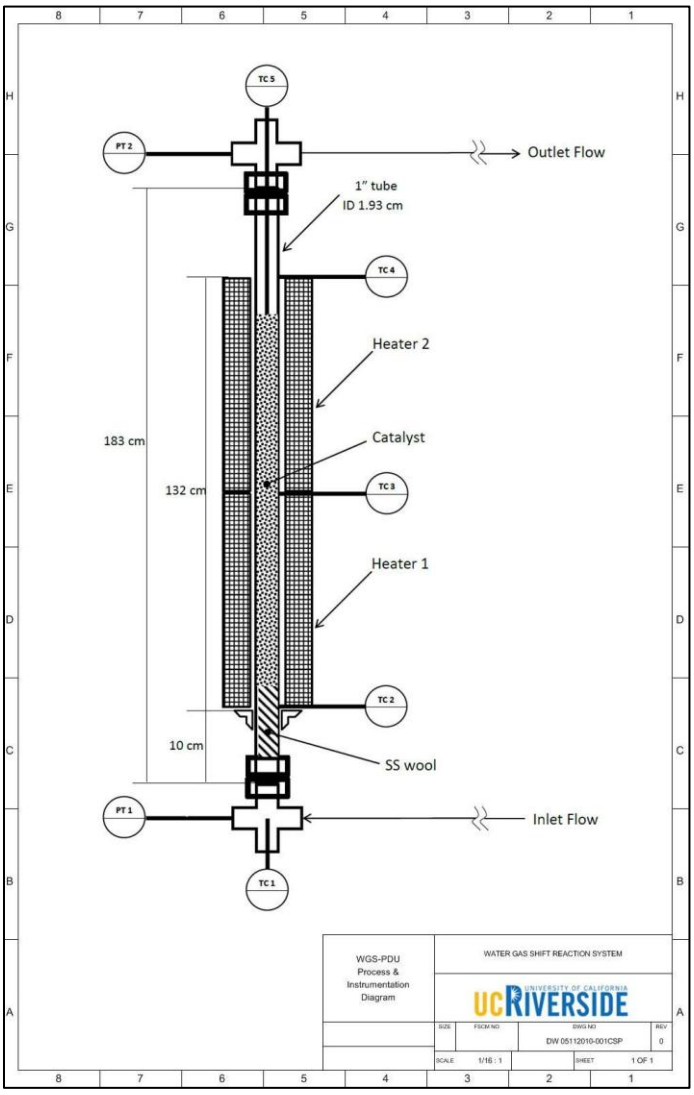

Figure 4-6 Detail of the water gas shift reactor for the PDU

Table 4-4 WGS fixed bed reactor design summary

Parameter of Reactor	**Dimension/Value**
Inner diameter (cm)	1.93
Total height (m)	1.83
Bed height (m)	1.30
Catalyst weight (kg)	0.4
Particle size of catalyst (mm)	2.5-3
Bed temperature (°C)	350
Bed pressure (psi)	150

4.2.4 Product gas separation and analysis

The downstream is cooled down after shift reaction to the ambient temperature by a double pipe exchanger to condense the unreacted water in the product stream. A series of water and gas separators are provided to eliminate the excess water and moisture. The volumetric flow rate of the final product gas is measured by a mass flow meter (MFM) and the composition is determined by non-dispersive infrared analyzer (NDIR).

NDIR is used for online gas analysis of CO, CO_2 and CH_4 produced from the process demonstration unit. It is named non-dispersive because the gas wavelength that passes through the sampling chamber is not pre-filtered, while other infrared sensors have filters used before the detector. The main components of the NDIR are an infrared lamp, a sample chamber, and a wavelength sample chamber. The infrared light is directed through the sample chamber towards the detector, and gas concentration is measured electro-optically by its absorption of a specific wavelength in the infrared light. There is

another chamber in parallel, which houses a reference gas, typically nitrogen. The detector has an optical filter which eliminates all light except the wavelength that the selected gas can absorb. A gas concentration is calculated by the amount of light reaching the detector compared with that in reference gas chamber [110].

Figure 4-7 shows the overview of the PDU of RNG production with the capacity of 0.1 TPD of feedstock developed by the research team of the CE-CERT gasification laboratory. This system is used to assess the performance and feasibility of the RNG process presented in the next section.

Figure 4-7 Pictures of Process demonstration unit of RNG production at CE-CERT

4.3 Performance of PDU scale of RNG process

4.3.1 Computational result from a modified Aspen simulation model

Data and operational information from the process demonstration unit was estimated prior to the real operation by a modified computational model using previous experimental results. H_2S and NH_3 were assumed to be completely removed by the cleanup unit and the char was set to 17.9% related to the gasification temperature as

discussed in Chapter 2. The limitation of the gas flow rate required to properly fluidize the sand bed and avoid the accumulation of char clogging the injection zone, an increase of the H_2 flow rate was necessary. It was needed to adjust the molar ratio between H_2 and C in the feed to 2 instead of 1 as mentioned in the former simulation. The heating rate of the input zone was also limited to the feed rate of slurry in order to keep maintaining the appropriate gasification temperature as desired. The operating pressure was restricted by a leak test at the high temperature operation and capability of the progressive cavity pump to deliver slurry into SHR. Thus, the operating pressure was set at 150psi.

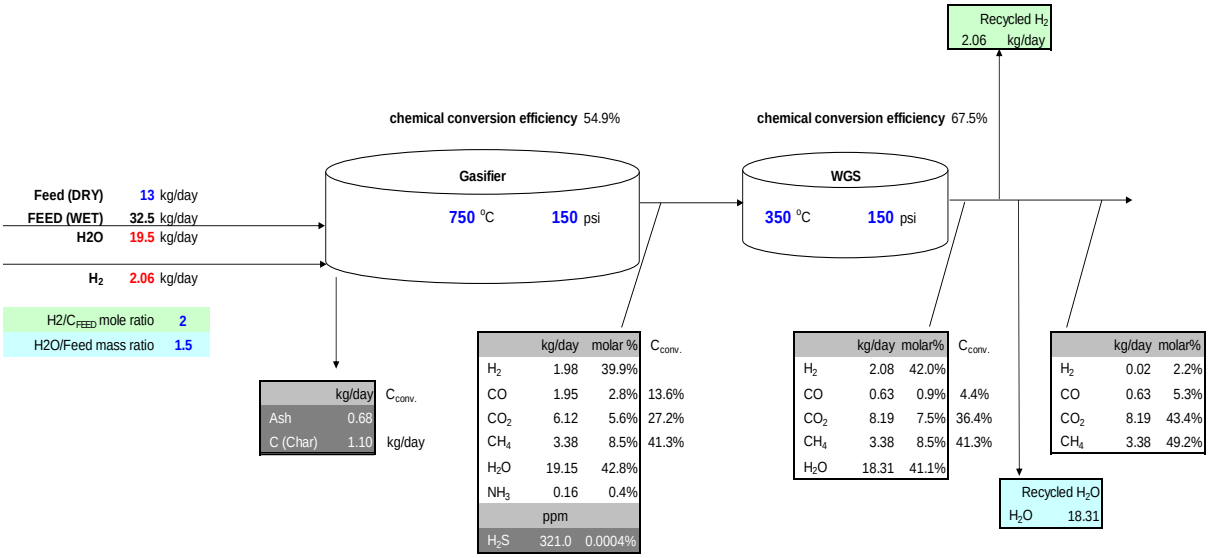

Figure 4-8 Mass balance of the SHR-WGS process demonstration unit operated at 750^{o}C for gasification and 350^{o}C for water gas shift reaction underneath 150psi

The mass balance of the process demonstration unit at this realistic condition results in a feed rate of 32.5 kg/day with the proportional input ratio operated at 750^{o}C and 150psi in the gasifier coupled with 350^{o}C in WGS reactor under the same pressure as given in Figure 4-8. The chemical conversion was achieved at 54.9% using the SHR and 67.5% of CO by mole were shifted to CO_2 and H_2 using the HTS reactor. The maximum production yield was 41.3% of carbon converted to be CH_4, about 3.4 kg/day. In this process condition, 87% of CH_4 as a dry basis can be obtained after recycle of H_2 and separation of CO_2. Approximately 178 MJ/day or 32.6 MJ/m^3 of energy could be obtained from the RNG product. This calculation would be substantiated by the practical operation of PDU performed in the next section.

4.3.2 PDU performance of SHR only operation

Initially, the temperature of the SHR was gradually increased to 750^{o}C to avoid the thermal shock on the reactor. Nitrogen initially flowed through the system as the fluidizing and purging gas during the starting process and for maintaining the operating pressure about 150psi. Later, nitrogen was switched to hydrogen when the temperature of the bottom of reactor reached 750^{o}C. After that, the slurry of comingled feedstock prepared by the hydrothermal process, stated in 4.2.1, was continuously injected into the gasifier using a progressive cavity pump when the reactor temperature and pressure were uniform at steady state. Figure 4-9 shows the controlled parameters and acquired data displayed on panel screen during the real operation.

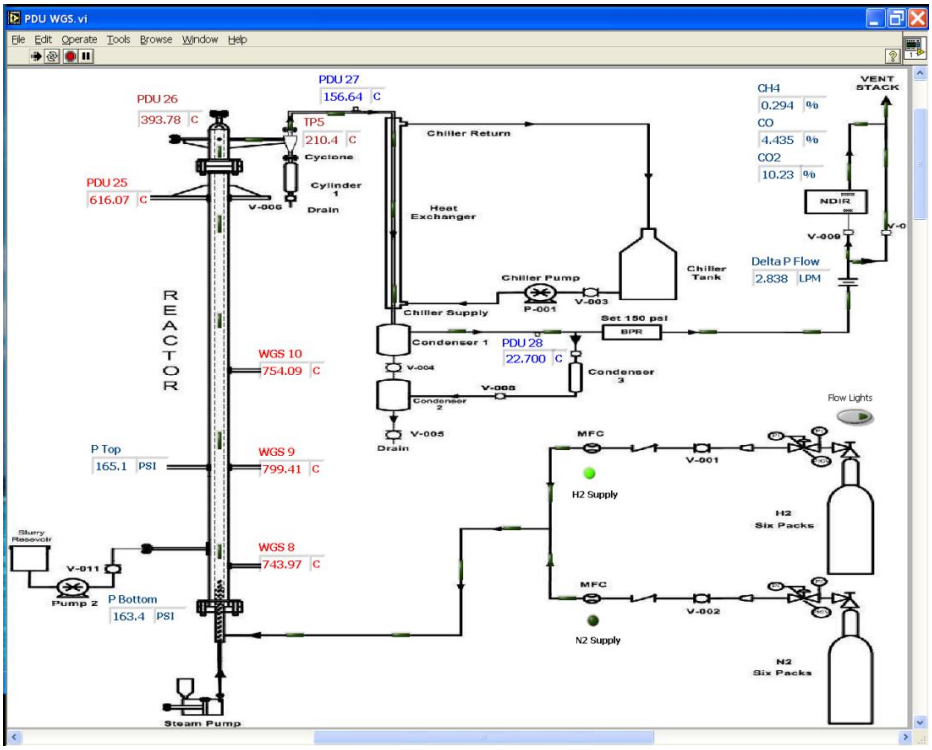

Figure 4-9 Front panel display of SHR-PDU operating system

H_2 as a gasifying agent was continued pressurizing the system and fluidizing the sand while the gasifier was working. After feeding the slurry for about 10 min, the evolution of carbonaceous gases in the product stream was detected by NDIR. The concentration of each gas kept increasing until it was relatively stable for 40 min. As seen in Figure 4-10, the reaction temperature dropped slightly from the desired temperature to less than 700^{o}C due to the heater at the gasifying region could not provide enough heat during the loading of fresh feedstock. The average flow rate of CH_4, at steady state, was about 2.8 lpm which accounted for 63% of the total carbon gas. CO and CO_2 flow rates were approximately 1.2 lpm and 0.6 lpm which were about 25% and 12%, respectively. However, the total carbonaceous gas produced from this operation was only 58%, at 6.6

kg/day, of the production yield estimated by the simulation process, at 11.5 kg/day, as explained in 4.3.1. More information of these tests is presented in Table 4-5 and 4-6. The carbon conversion at steady state condition of the steam hydrogasification using BFB gasifier achieved approximately 30-35%. This low conversion was probably caused by an insufficient heating supply during gasification. In these experimental results, the concentration of CO_2 was apparently lower than the simulation. It could be explained by the effect of catalytic performance or sorption enhancement resulted from some minerals contained in blended biosolids. The results were corresponded to the previous results done by other students in this group [90, 93]. Similarly, the literature review, studied by Saw W., el [60], indicated that CO_2 was rationally decreased in steam gasification when the higher proportion of biosolids was added in wood feedstock. It was influenced by sorption enhancement of Calcium Oxide (CaO) contained in biosolids.

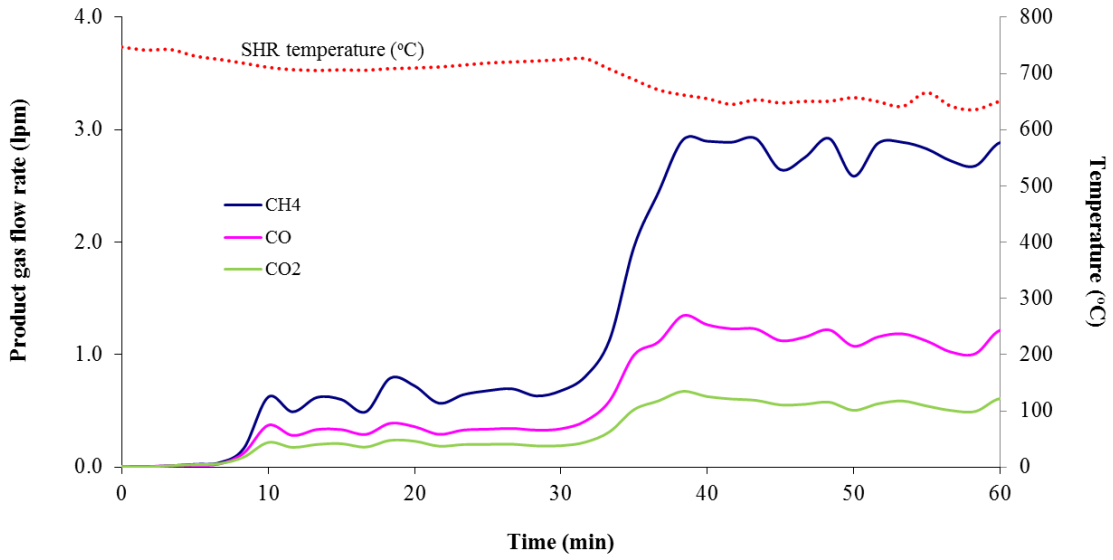

Figure 4-10 Real time of producer gas generated from SHR using biosolids comingled with pine wood as feedstock

Table 4-5 Composition of carbonaceous gas produced from SHR using comingled feed

Component	Average composition of carbon gas (% volume)		
	Test 1	Test 2	Test 3
CH_4	63	67	66
CO	25	22	23
CO_2	12	11	11

Table 4-6 Overall performance of SHR only operation using comingled feed

Testing conditions	Average results
Rate of Carbon input (mole/min)	0.46
Total flow rate of product gas (liter/min)	16.4 - 20.2
Total flow rate of product gas (mole/min)	0.75 - 0.90
H_2 (mole/min)	0.60 – 0.74
CH_4 (mole/min)	0.09 - 0.11
CO (mole/min)	0.026 – 0.037
CO_2 (mole/min)	0.019 – 0.021
Carbon conversion (%)	30 - 35

4.3.3 PDU performance of the SHR integrated with the WGS reactor

The performance of the SHR configured with a new shift reactor is presented in this part. Figure 4-11 shows both of the operating conditions for the SHR and WGS. The shift reactor using the HTS catalyst was activated using the procedure outlined in Chapter 3. Activation gas (H_2, CO and N_2) was provided by compressed gas cylinders and steam was generated by the SHR when the temperature was over the dew point. After 1 hour of

activation, the shift reactor was continuously purged by pure N_2 to prevent the oxidation occurred on the catalyst and the temperature of the reactor was increased to 350^{o}C.

Because of the difference in the volume of the SHR and WGS reactor, we split only 20% of the total gas flow produced from the SHR to enter the new shift reactor in order to investigate the catalytic activity of the WGS reactor and the overall performance of the process demonstration unit of RNG. According to this is only a demonstration process, the warm gas cleanup was not set up in this experiment. However, the concentration of H_2S in this raw producer gas was only 200 ppm. It was confirmed by the H_2S detector tube (Matheson Kitagawa No.8014-120SF). Based on the study in Chapter 3, the performance of ShiftMax®120 was good enough to perform in a lean sulfur atmosphere.

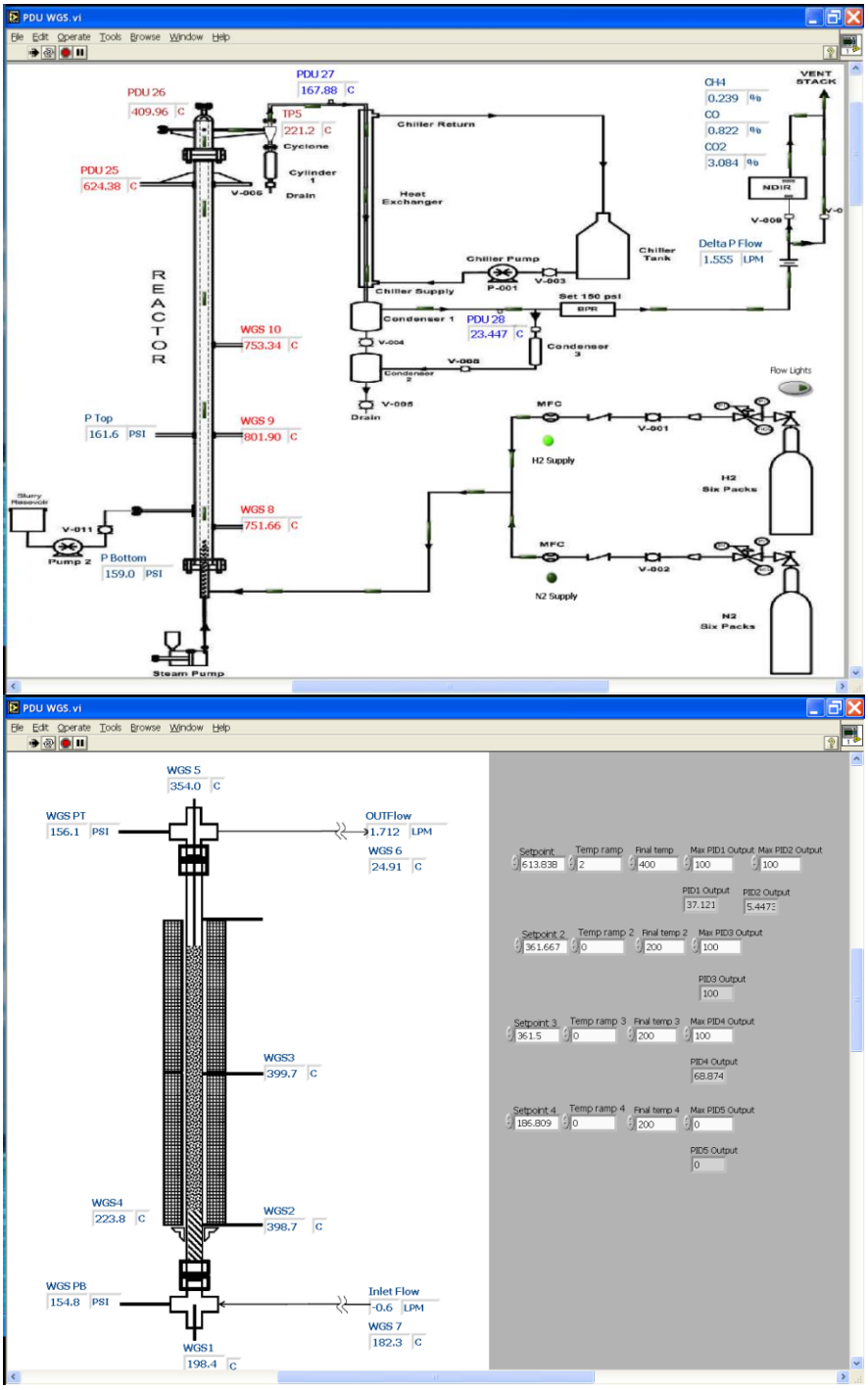

Figure 4-11 Front panel display for SHR-WGS operating system

The SHR operated at 750^{o}C and 150psi using slurry feed of comingled pine wood and biosolids. The WGS reactor was operated at 350^{o}C at the catalyst bed and the pressure was slightly lower than that of the SHR. The temperature profile of real time operation and online results from SHR-WGS system is presented in Figure 4-12. The SHR system stabilized after 1 hour of re-starting slurry pump and then, the raw gas stream from SHR was directly fed to the WGS reactor. By this result, the flow rate of CO_2 was increased from 0.065-0.069 lpm to 0.125-0.131 lpm while that of CO was decreased from 0.099-0.115 lpm to 0.031-0.044 lpm via the shift reaction. The flow rate of CH_4 was fairly stable about 0.35-0.37 lpm at steady state condition. Consequently, the CO conversion was accomplished in 58-60% which was a little bit lower than the design conversion, at 67.5%. This could be caused by the larger particle size of catalyst resulting in a channeling effect in the shift reactor. The pressure drop through the reactor was less than 1-2psi even though the height of catalyst bed was longer. The smaller particle size of catalyst could help eliminate this effect and improve the CO conversion. The concentration of steam during the operation might be lower than the expectation due to the condensation in the transfer line between SHR and WGS. In addition, the lean content of sulfur species contained in the raw producer gas could be slightly suppressed on the CO conversion as well.

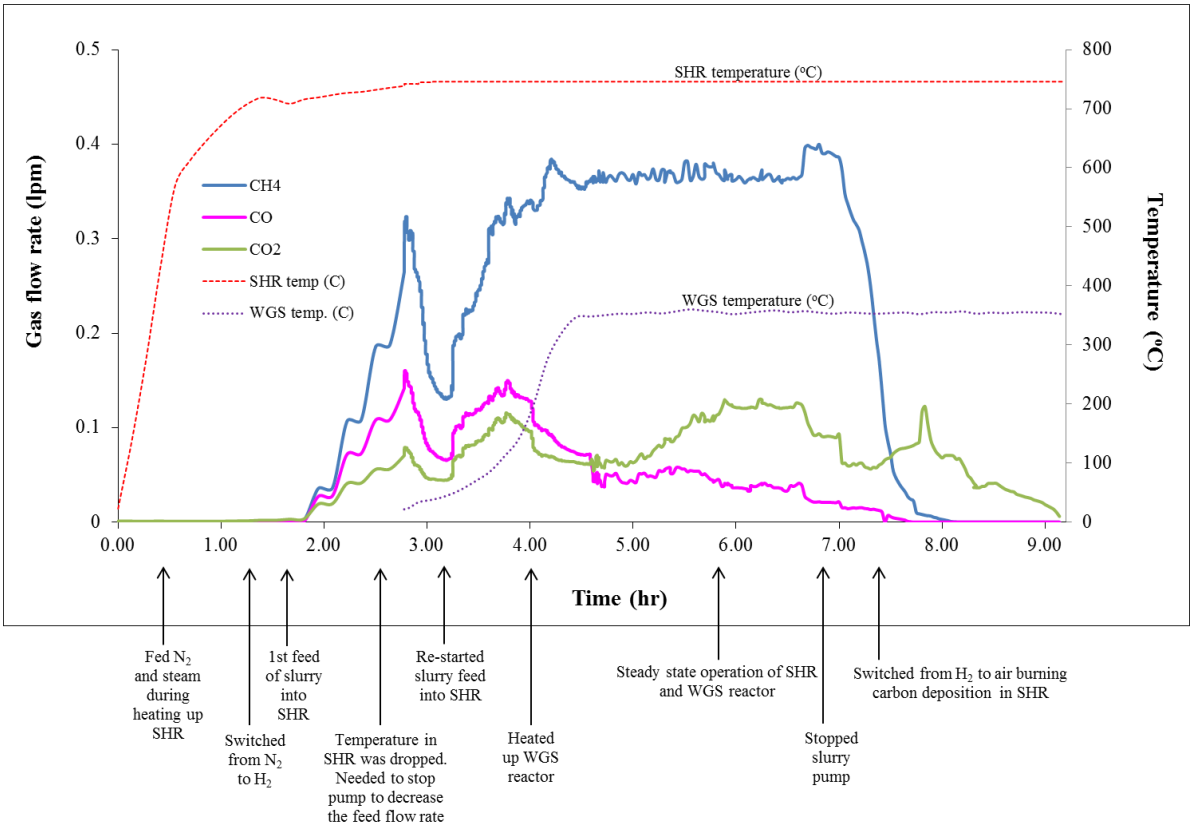

Figure 4-12 Real time operation of the demonstration unit of SHR-WGS using biosolids comingled with pine wood as feedstock

Percentage of gas distribution and mole balance compared between input and output of WGS are presented in Table 4-7 and Figure 4-13. It was comparable with the information obtained from the simulation. However, the feed rate performed in this test was needed to be decreased to 50% of the calculation basis to keep maintaining the gasification temperature at 750^{o}C in order to accomplish in the higher conversion. This run was succeeded in 42% of carbon conversion for SHR and 60% CO conversion in WGS.

Table 4-7 Percentage of gas component compared between input and output of WGS

Component	Experiment		Simulation	
	% Gas input from SHR	% Gas output from WGS	% Gas input from SHR	% Gas output from WGS
H_2	74.4 - 75.7	75.9 - 76.3	70.3	71.2
CH_4	16.0 - 16.6	15.9 - 16.2	15.0	14.5
CO	4.0 - 4.4	1.7 - 2.0	4.9	1.5
CO_2	3.0 - 3.4	5.6 - 6.0	9.9	12.8

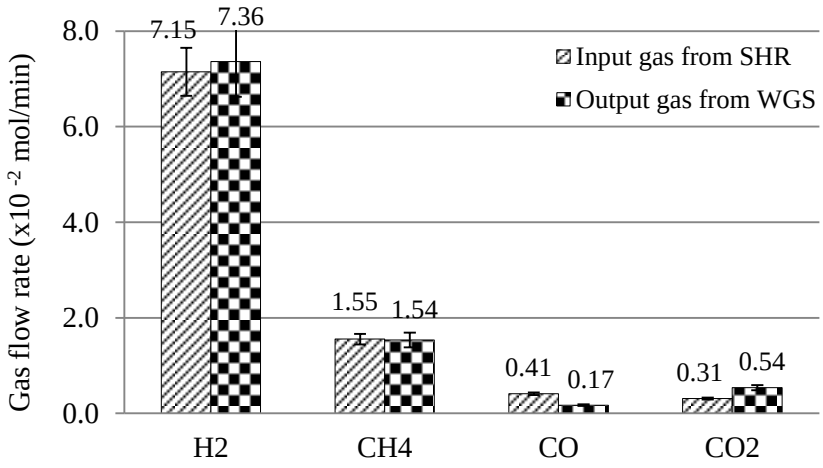

Figure 4-13, Comparison of the gas distribution between input and output of WGS reactor at 350^{o}C resulted from the operation of the PDU

From the experimental result, the amount of H_2 was sufficient for recycling back to feed in the gasifier. After separation process, it revealed that molar concentration of the final product gas was approximately contained 86.5 % by mole of CH_4, 9.6% by mole of CO and 3.9% by mole of H_2 in which 85 MJ/day or 32.6 MJ/m^3 of energy could be produced.

4.4 Summary

A process demonstration unit for RNG production was built and operated. It was shown that this facility could be properly worked at the operating condition of 750^{o}C and 150psi. The carbon conversion obtained from the SHR only operation was achieved approximately 30-35%. The low carbon conversion was caused by the lower heating rate supplied in the gasifier. To maintain to reaction temperature, the feed rate of slurry was necessary to be slower for improving the carbon conversion at desired gasification temperature. The CO conversion performed by the new WGS reactor was also investigated in this process. About 60% of CO conversion could be achieved using HTS catalyst to convert CO to H_2 and CO_2. The overall performance is almost similar with the simulation results, especially CH_4 content in the product gas. This process using biosolids co-mingled with woody biomass as feedstock has a potential to produce the RNG contained over 85% by mole of CH_4 as a final product following the objectives. The results were supported the conceptual design and feasibility of the configuration process for the production of renewable natural gas via the CE-CERT steam hydrogasification technology. However, the capability of the shift reactor should be increased to match with the production yield of SHR to be capable of handling the whole product gas to confirm full mass balance. Also, the heating facilities for the gasifier are necessary to be improved so that the gasification temperature can be well maintained.

Chapter 5 Estimation of RNG Production by CE-CERT Technology

The steam hydrogasification technology configured with a water gas shift reactor was shown in the previous chapter to be able to produce energetic gases that can be upgraded to high levels of renewable natural gas. These results were encouraging enough to perform an initial technical evaluation of a commercial scale plant using the CE-CERT technology with a water gas shift reactor. This chapter will present the possible scenarios of the RNG production using the CE-CERT technology simulated by Aspen software and using experimental results presented earlier. The production of RNG using the available biomass resources in California will be estimated to determine potential locations of gasification facilities there.

5.1 Process design methodology and evaluation

Aspen Plus version 7.3 was used for the process simulation as outlined in Chapter 2. The model includes solid, liquid and gas phases which require various modules to represent different chemical processes. The feedstock used was comingled biomass and biosolids, was defined in Aspen as non-conventional component. HCOALGEN and DCOALIGT were established as the enthalpy and density module for the feedstock. All the properties for the liquid and gas phases were obtained from the default database in Aspen. The detailed operation units used in the simulation for the CE-CERT process are given in Table 5-1.

Table 5-1 Unit operations specified in Aspen simulation

Unit operation	Aspen plus module	Specifications
Pretreatment unit	RYield	Simulation of feedstock decomposition to elemental C, H, O, N, S, Cl
Gasification	RGibbs	Specification of the possible products: H_2O, H_2, Cl_2, HCl, C, CO, CO_2, CH_4, COS, H_2S, CS_2, ash
Combustor	Rstoic	Simulation of char combustion with air
Solid separation	Sep	Simulation of product gas and sand separation
Warm gas cleanup	Sep	Simulation of H_2S and chloride removal
WGS reactor	Rstoic	Empirical simulation of WGS reaction
H_2 separation	Sep	Simulation of H_2 split from the product gas
CO_2 Removal	Sep	Simulation of CO_2 removal

A commercial scale 400 TPD plant using steam hydrogasification configured with a WGS reactor is simulated here. The design consists of 5 major steps: Feedstock pretreatment, Steam hydrogasifier (SHR), Gas cleanup system, WGS reactor, H_2 separation and CO_2 removal. Some unit operations used in the design such as, warm gas clean up system, WGS reactor, H_2 separation and CO_2 removal are available commercial systems. Some units, i.e., warm gas cleanup and solid or gas separation unit used in the simulation are simplified empirical equations and the requirements of the chemical kinetic reactions are not specified. The gasification temperature was set at 750^{o}C. The carbon conversion defined the amount of leftover char remaining in the residue. The optimum H_2O/feed mass ratio was defined as 1.5 based on previous studies. The H_2/C_{Feed} molar ratio should be at least 1 or higher in order to provide enough gas flow for the fluidized bed circulation and, also promote the formation of CH_4. Any simulation must have condition that provides sufficient availability of H_2 for the internal recycle into the

SHR. A brief summary of the important unit operations used in the simulation is described below to provide a picture of the commercial scale facility.

- *Feedstock pretreatment section*

Biosolids comingled with green waste is used as a feedstock. It is mixed as a certain ratio in order to be a pumpable slurry. A solid content over 40% in the feedstock can be achieved in order to meet this requirement [42]. A hydrothermal pretreatment step is employed due to the hygroscopic and hydrophilic property of feedstock to ensure slurry formation. A batch type pretreatment reactor is operated at 270^{o}C and 400 psi for 30 min [43]. A stable and homogeneous slurry can be obtained after the hydrothermal pretreatment and is directly pumped into the gasifier. Two reactors in parallel could be utilized in the pretreatment process to keep the slurry feed constant and continuous.

- *Gasification section*

Feedstock is injected via a slurry pump into a bed of sand operated at 150-400psi which uses recycled H_2 flow for fluidization. The additional energy source for the SHR is recirculated sand heated by the combustion of char with pressurized air in an external fluidized bed combustor. An additional 20% of air flow is added in order to assure the complete combustion of char. It is recognized that if the heat requirements of the gasification could not be met just with the combustion of char it would require additional fuel. The char leftover percentages are corresponding to different gasification conditions.

These data are used to determine the percentage of char in the gasifier using the Gibbs model.

The inventory of sand depends on the hydrodynamics performance in the circulating system. Based on the preliminary study, the optimum bed inventory to feedstock mass ratio in the circulating fluidized bed is about 250 for gasifier system [109]. Assuming the residence time of feedstock in the gasifier is 30 seconds, the feedstock mass in the gasifier is 0.14 tons for the feeding rate of 400 tons/day. Thus, the total bed inventory is 35 tons of sand. The sand in the gasifier is fluidized and the gas bubbles leaving the fluidized bed enter a large expanded section of the vessel where larger char particles can be disengaged from the gas. Fine char and ash produced in the gasifier flows with the gas to the cyclone where disengaged solids falls into a standpipe back into the fluidized bed. It was assumed that ash and sand particles were completely recovered by gasifier and combustor with no loss.

- *Gas cleanup section*

The steam in the SHR producer gas needs to be cooled down to 350ºC in the downstream WGS reaction part after contaminants are removed. In this study, a warm gas cleanup is applied because the performance of the high temperature shift catalyst is more efficient than the sour gas shift catalyst in the low level sulfur conditions. Product gas generated from biosolids and biomass contained low sulfur content compared to that from coal. Initially the gas contacts a bed containing HCl adsorbents. The second step is a compact Transport Desulfurization Reactor (TDR) system that utilizes a regenerable ZnO sorbent

for sulfur removal and conversion into SO_2. The SO_2 is converted into elemental sulfur via a reaction with hydrogen. A third step is the use of a regenerable sorbent for fixed bed ammonia/HCN conversion. Finally, trace elements (Hg, As, and Se) can be removed at temperatures above 250°C [110].

- *Water gas shift reaction section*

The capacity of the shift reactor for the commercial facility is assumed to adequately support the commercial HTS catalyst without any modification. The limitations of particle size of catalyst related to the drawback of the reaction, i.e., channeling effect or the surface contact, are not taken into account. The temperature of reactor is controlled at 350^oC as the same operating pressure. CO is reacted with the internal steam in the fixed bed reactor filled with a commercial high temperature, Fe-Cr based, catalyst. Approximately 65-75% of CO conversion would be expected to achieve a sufficient amount of H_2 to recycle after the separation step. CH_4 generated in the gasification step is approximately 20-23% content of dry gas. The amount of CH_4 is almost unchanged during the shift reaction.

- *Hydrogen separation section*

After leaving the WGS unit, the product gas flows into a series of heat exchangers, Heat Recovery and Steam Generation (HRSG), and cool the gas down to 30°C to condense the remaining H_2O before entry into the Pressure Swing Adsorption (PSA) process. The

Pressure Swing Adsorption (PSA) unit is utilized for H_2 separation to provide the necessary enriched hydrogen stream for recycle to the SHR [66].

- *CO_2 removal section*

The clean syngas is processed in an amine unit to remove the CO_2. The removal process utilizes methyldiethanolamine (MDEA) as solvent and CO_2 is removed by counter-current contact with MEDA solution in an absorption tower [92].

A detailed diagram of simulation was created and presented in the Appendix A-2 and A-3. In this study, three scenarios were simulated based on the plausibility of the practical operation related to the experimental results obtained from Chapter 3 and 4.

Case 1 represented the preliminary result of the simplified process demonstration unit in which it could produce the energetic gas at the conversion of 40% under the operating pressure of 150psi. The char remaining in the residue was approximately 60% and assumed to be burnt in the combustor to recover the energy for the SHR. The WGS reactor was operated at 60% conversion of CO to produce the sufficient amount of H_2 for recycle.

Case 2 showed the best RNG production for the base case following the assumptions mentioned in Chapter 2. The operating pressure and temperature was set at 400psi with

the char ratio of 17.9%. The CO conversion was set at 75% following the best condition of the shift reactor operated at 350^{o}C.

Case 3 was simulated at the medium scenario proposed to compare between current operation and the best scenario. The inert char production was set at 35% to reflect experiments done on the steam hydrogasification of biomass [90-93].

Material and carbon balances were given for each case study and no detailed chemical kinetic models were considered in the simulation. The simulation results are given in Table 5-2. The optimum scenario showed the balance of mass and energy was described in Figure 5-1. Some definitions shown in this list are following below.

- CH_4 Conversion (%) = CH_4 moles in RNG/Carbon moles in feed
- Cold gas efficiency (%) = HHV of Product gas/HHV of Feed
- Power generated (Mw) = Electricity can be produced by Fuel (30% as usual)
- Overall thermal efficiency (%) = HHV of Net product gas/HHV of Feed

Table 5-2 Plant performance of three scenarios

RNG production plant	Case 1	Case 2	Case 3
Feedstock (Dry, ton/day)	400	400	400
Gasifier operating pressure (psi)	150	400	400
Gasifier exit temperature (^{o}C)	750	750	750
Char ratio (%)	60	17.9	35
CO conversion of WGS at 350^{o}C (%)	60	75	75
Gasifier exit gas composition (Vol%)			
H_2	34.2	25.6	26.4
CO	1.8	2.2	1.7
CO_2	5.5	8.5	6.8
CH_4	2.7	10.8	8.5
H_2O	55.6	52.5	56.3
H_2S	0.03	0.03	0.03
NH_3	0.21	0.21	0.21
Product gas composition (Vol%)			
H_2	13.9	5.2	5.1
CO	12.4	4.7	4.6
CO_2	0.02	0.01	0.01
CH_4	73.6	90.1	90.3
CH_4 Conversion (%)	10.7	41.2	32.4
RNG production (ton/day)	36.5	116.6	91.5
Cold gas efficiency (%)	22.2	79.1	62.2
Power generated (Mw)	17.8	80.6	60.0
Plant overall thermal efficiency (%)	22.2	68.2	40.9

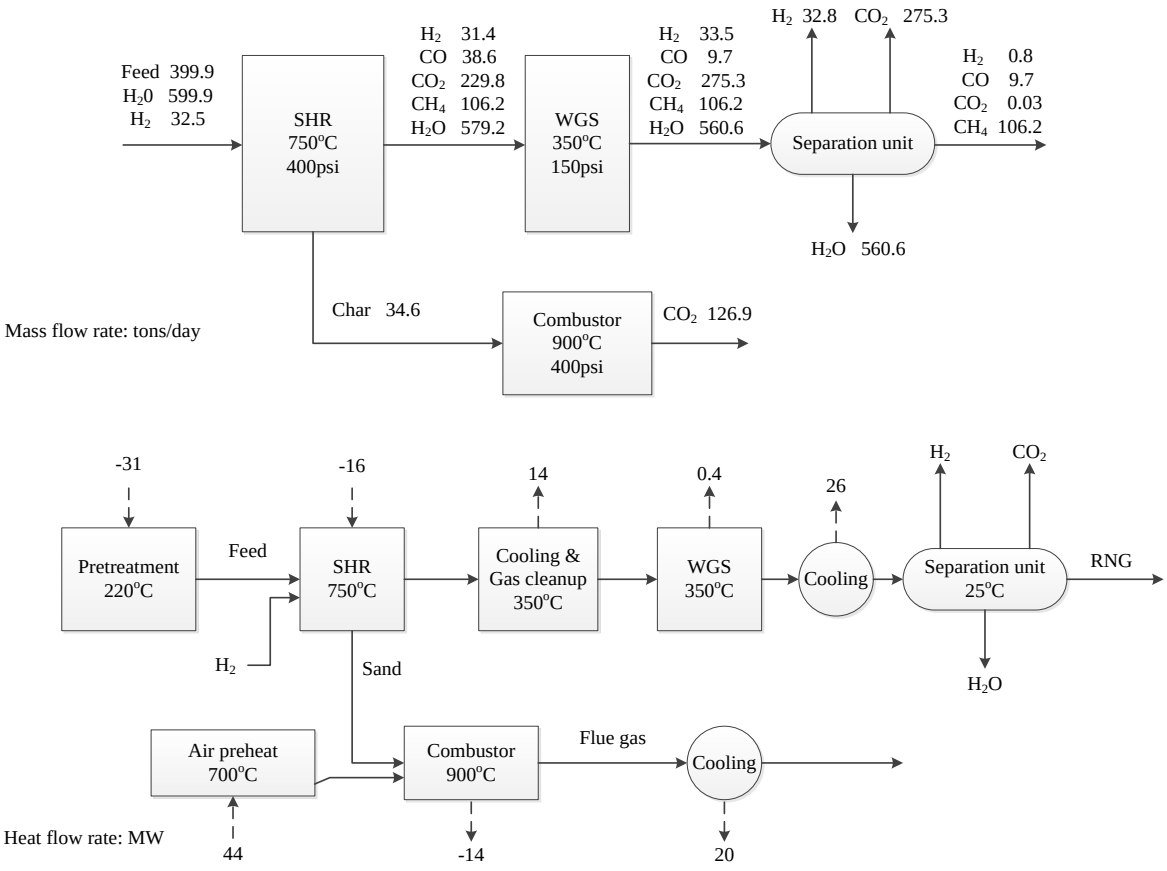

Figure 5-1 Mass and energy balance of main processing units of SHR-WGS based process for RNG production in Case 2

The result from the simulation shows that the key performance aspect of this process is the efficiency of the SHR. To increase the production of RNG, the gasification step is needed to convert the carbon in the feed to gas as much as possible. For the case 2, the production of 400 TPD of comingled feedstock can produce 117 TPD of combustible gas with the CH_4 conversion of 41% which is the best scenario in this study. The content of CH_4 in RNG can be higher than 90% and the process thermal efficiency is expected 68%

based on the heating value. However, the overall efficiency can be decreased to 41%, in case 3, with the production of 92 TPD when the remained char in SHR is about 35%.

5.2 Availability of feedstock in Southern California

The information required to estimate the availability of feedstock found in Southern California is from the California Energy Commission (CEC) Public Interest Energy Research (PIER) collaborative report and Statewide Waste Characterization Study [111-113]. The available feedstock in California is specifically focused in the Southern California region, as seen in Figure 5-2, and includes Los Angeles County, Orange County, Riverside County and San Bernardino County. In this study, resources considered for the production of RNG include biosolids and biomass or green waste. The availability of both resources is observed for the purposes of estimating the potential quantities utilized for RNG production. Practically, not all of the feedstocks produced in this region can or should be used for industrial purposes. For example, not all green waste should be harvested where it is needed to maintain soil fertility and/or for erosion control. Similarly, terrain limitations, environmental and ecosystem requirements, collection inefficiencies, and a number of other technical and social constraints limit the amount of feedstocks that can be used. For these reasons, amounts that can technically be supplied to utilization are substantially less than gross production.

Figure 5-2 Map of California with county lines defining Southern California

5.2.1 Biosolids availability

Biosolids, also refers to as treated sludge, is generated from both aerobic and anaerobic waste water treatment process during sewage and wastewater treatment. Estimates of biosolids production were adapted from PIER biomass resources report. Biosolids generation and the amounts landfilled and diverted in this region are listed in Table 5-3 [114]. Based on the available fraction, 80% is practically assumed to be utilized for technical conversion. The normal unit generally used to determine the availability of biomass is Bold Dry Ton (BDT) per year.

Table 5-3 Gross biosolids production and availability for conversion in 2010

Region	Generation (BDT/year)	Landfilled (BDT/year)	Diverted (BDT/year)	Available for Production (BDT/year)
Orange County	64,830	6,570	58,260	46,608
Los Angeles County	258,560	38,160	220,400	176,320
Riverside County	59,410	-	59,410	47,528
San Bernardino County	38,960	1,120	37,840	30,272
Southern CA Total	421,760	45,850	375,910	300,728
CA Total	872,000	128,000	744,000	595,000
S. CA Total/CA Total	48.4%	35.8%	50.5%	50.5%

To address the contributions to RNG production from biosolids and to provide information needed for the economic assessments, projections from the base 2010 year data are made for the years 2017, 2020. The gross biosolids production and availability for conversion in the year mentioned above are shown in Table 5-4 [114].

Table 5-4 Gross biosolids production and availability for conversion in CA

Region	Generation (BDT/year)	Landfilled (BDT/year)	Diverted (BDT/year)	Available for Production (BDT/year)
2017				
Orange County	67,500	6,800	60,700	48,560
Los Angeles County	266,300	39,300	227,000	181,600
Riverside County	66,000	-	66,000	52,800
San Bernardino County	42,000	1,200	40,800	32,640
Southern CA Total	441,800	47,300	394,500	315,600
CA Total	921,100	133,000	788,100	631,000
S. CA Total/CA Total	48.0%	35.6%	50.1%	50.0%

2020				
Orange County	69,500	7,000	62,500	50,000
Los Angeles County	271,400	40,100	231,300	185,040
Riverside County	71,600	-	71,600	57,280
San Bernardino County	44,400	1,300	43,100	34,480
Southern CA Total	456,900	48,400	408,500	326,800
CA Total	954,300	136,300	818,000	654,000
S. CA Total/CA Total	47.9%	35.5%	49.9%	50.0%

5.2.2 Biomass or green waste availability

Green waste includes leaves, grass, pruning and stumps that can be categorized as municipal solid waste (MSW). Green waste can be collected and used for recycle material production and power generation via combustion or anaerobic digestion. Estimates of green waste production were also adapted from PIER biomass resources report. The total green waste yield in Southern California is 371,980 BDT/year in 2010. Detailed green waste generation data is given in Table 5-5 [113]. Based on the available fraction in green waste, 50% is assumed to be used for this conversion. Projections from the base 2010 year data are made for the years 2017, and 2020.The gross green waste production and availability for conversion in the year mentioned above is shown in Table 5-6 [113].

Table 5-5 Gross green waste production and availability for conversion in 2010

Region	Leaves, Grass (BDT/year)	Prunings& Trimmings (BDT/year)	Branches & Stumps (BDT/year)	Available for Production (BDT/year)
Orange County	69,640	482,330	7,460	279,715
Los Angeles County	208,680	521,230	22,360	376,135
Riverside County	50,380	245,990	5,400	150,885
San Bernardino County	43,280	191,560	4,630	119,735
Southern CA Total	371,980	1,441,110	39,850	926,470
CA Total	760,000	2,330,000	80,000	1,585,000
S. CA Total/CA Total	48.9%	61.9%	49.8%	58.5%

Table 5-6 Gross green waste production and availability for conversion in CA

Region	Leaves, Grass (BDT/year)	Prunings& Trimmings (BDT/year)	Branches & Stumps (BDT/year)	Available for Production (BDT/year)
2017				
Orange County	72,500	502,300	7,800	291,300
Los Angeles County	214,900	536,800	23,000	387,350
Riverside County	55,900	273,100	6,000	167,500
San Bernardino County	46,700	206,600	5,000	129,150
Southern CA Total	390,000	1,518,800	41,800	975,300
CA Total	802,100	2,466,300	86,000	1,677,200
S. CA Total/CA Total	48.6%	61.6%	48.6%	58.2%
2020				
Orange County	74,700	517,400	8,000	300,050
Los Angeles County	219,000	547,000	23,500	394,750
Riverside County	60,800	296,600	6,500	181,950
San Bernardino County	49,300	218,400	5,300	136,500
Southern CA Total	403,800	1,579,400	43,300	1,013,250
CA Total	833,000	2,563,900	88,900	1,742,900
S. CA Total/CA Total	48.5%	61.6%	48.7%	58.1%

The estimation of green waste and biosolids yield that can be practically converted to RNG is concluded in Table 5-7.

Table 5-7 Technical available feedstock yields for RNG production in Southern California

Year	Feedstock	BDT/yr	BDT/day
2010	Biosolid	300728	824
	Green waste	926470	2538
	Total	1227198	3362
2017	Biosolid	315600	865
	Green waste	975300	2672
	Total	1290900	3537
2020	Biosolid	326800	895
	Green waste	1013250	2776
	Total	1340050	3671

If the entire available portion of feedstock listed above is used for RNG production via the proposed technology, 48.5 Million cubic feet per day (MMcfd) can be generated using the feedstock yield in 2010 which accounts for about 6.6% of the Natural Gas produced in CA [115]. As the yields of biosolids and green waste increased in next 10 years, the RNG yield can be expected to increase to 53 MMcfd in 2020 that counts on 7.8% of the Natural gas produced in CA [115].

5.3 Cost comparison with other RNG productions

The capital cost estimation required for the life cycle cost is mainly based on economic analysis made by National Energy Technology Laboratory (NETL) within the Department of Energy (DOE). NETL has reviewed the SHR process through a Cooperative Research And Development Agreement (CRADA) by validating the equilibrium model, process flow sheet for FT (Fischer Tropsch) liquids production and power generation with IGCC using SHR technology using bituminous coal as feedstock (4000 TPD) in 2008. Although the feedstock used in this study is biosolids and green waste instead of coal, the same number was used in assessment the cost of the facilities, utilities and chemicals. The major assumptions used in the economic model are given in Table 5-8 [68].

Table 5-8 Assumptions for the production cost calculation

Description	value
Average inflation (%)	3.0
Discount rate (Debt, %)	4
Discount rate (Equity, %)	4
Ratio of debt (%)	50
Nominal interest rate (%)	4
Economic life of facility	20
Operation cost (% of total capital cost)	3
Operation cost (M$)	3.78
Feedstock cost ($/ton)	-80
Annual operation day (day)	365

Estimation of process economic parameters of 400TPD biosolid-biomass plant was performed. Tipping fee credit of $60 per ton and the additional credit for the drying cost saving of $20 per ton were applied [68]. Total Plant Cost (TPC) was estimated by ASPEN Economic Analyzer. TPC for the steam hydrogasification based process is shown in Table 5-9 [68].

Table 5-9 TPC of Steam Hydrogasification Process

Equipment	Reference Coal (4000TPD) in 2008	Biomass (400TPD) in 2014	Cost (%)
Feed water & Misc. BOP	34.098	7.240	5.93
Steam hydrogasifier, Combustor & Accessories	256.069	54.373	44.56
Ash handling	26.761	5.682	4.66
Gas cleanup & Piping	81.202	17.242	14.13
Air supply	9.97	2.117	1.73
HRSG Ducting & Stack	36.853	7.825	6.41
Water Gas Shift		2.574	2.11
CO2 Removal and Compression	37.338	7.018	5.75
Hydrogen Purification (PSA)		5.892	4.83
Accessories Electric Plant	2.33	2.828	2.32
Instrument & Control	1.44	1.748	1.43
Cooling Water System	12.222	2.595	2.13
Fuel BOP	23.068	4.898	4.01
Total Plant Cost (TPC)		122.032	100.00

It was presented that about 45% TPC is assigned to the SHR unit, followed by 14% cost for Gas cleanup. The Return on Invest (ROI) was estimated to 8% over the 15 years discounted cash flow. The production cost of the RNG for a 400 BDT per day plant using green waste and biosolids as feedstock is 6.45 $/MMBtu [68].

Based on the literature review for the production of RNG studied earlier, Table 5-10 summarizes some limitations and performances of different processes for producing the RNG. Steam hydrogasification has the higher performances and relative faster rate of RNG production compared to other competing processes. For application of smaller sized, distributed feedstock such as biosolids or biomass, SHR process definitely shows benefit in its process economics. Also, the production cost compared to the other RNG process is concluded in Table 5-11 [68].

Table 5-10 Comparison of the RNG producing processes

	Anaerobic Digestion	Hydrogasification	Methanation of Syngas	Steam Hydrogasification
Limitation in the Feedstock?	Yes (cannot process Lignin)	No	No	No
Can process Wet feedstock	Yes	No	No	Yes
Minimum Process size for economics	~ 10 TPD	Large	Large	~100 TPD
Reaction Rate	10-25 day	~ 1 min.	~ 10 sec	~ 30 sec
Producer Gas Pressure	Atmospheric Pressure	High Pressure	High Pressure	High Pressure
Waste water treatment facility requirement	High	Low	Low	Very Low (Can produce clean water by-product)
Capital cost	Low	High	High	Low

Table 5-11 Production cost of the different RNG producing processes

	Anaerobic Digestion	Indirect Gasification/ Methanation	POX Gasification/ Methanation	POX Gasification/ Methanation	Steam Hydrogasification
Production Cost ($/MMBtu)	$7.56	$7.05	$11.2	$8.42	$6.45
Feed	Diary Waste	Biomass	Biomass	Illinois Coal	Biosolids mixed with Biomass
Capacity	807,000 ft^3/day	1000 MWth		1000 TPD	400 TPD
Reference	[118]	[119]	[120]	[121]	[68]

5.4 Summary

RNG has the potential to make a significant contribution as an alternative fuel and help the State of California achieve stated fossil fuels replacement and emissions reduction goals. The potential RNG supply available in the United States and in California has been estimated in a number of studies. A topic paper on RNG by the National petroleum Council (NPC) estimates the practical potential of RNG to be approximately 4.8 Trillion Cubic Feet (TCF) or 40 billion gasoline gallon equivalents (GGE) per year [28]. This is approximately equal to 20% of the US Natural gas consumption. Most of the natural gas used in California comes from out-of-state natural gas basins. In 2008, the total natural gas consumption in CA was 2,405,266 Million Cubic Feet. Based on the data provided by CA Public Utilities Commission, CA produced only 13% of the total natural gas consumed, around 312,685 Million Cubic Feet [115]. Developing in-state resources would result in considerable economic benefit to the State's natural gas consumers in the form of increased sustainable energy production at reduced costs. Also the initial

economic analysis provides considerable confidence to move forward with the pilot plant design and evaluation. This technology has the potential to enable RNG production in a commercially viable manner so as to benefit the ratepayers and can also contribute towards achieving the State of California's conventional fuel replacement and emissions reduction goals. The implementation of this technology could result in cost-effective and environmentally friendly RNG production from California's local waste resources, which can then be used as a clean burning transportation fuel or for electricity generation. For the commercial sized process, an estimated size of 400TPD. Production cost to final product from the result of current project will be ~6-7$/MMBtu. If California converted the technically available biosolids waste stream from waste water treatment facilities to renewable natural gas using SHR technology, it could replace up to 6% of the state's total natural gas consumption and reduce an estimated 10 million tons of GHG emissions [116].

Chapter 6 Conclusions and Recommendations

6.1 Conclusions

The results and conclusions derived from the research performed in this thesis and some recommendations for research are presented in the Section. This research investigated the performance of the water gas shift reaction to increase the availability of recycled hydrogen when it is integrated with the steam hydrogasification process for the production of renewable natural gas. A bench scale unit for RNG production by the CE-CERT technology is also demonstrated. The main tasks were completed with these following conclusions.

Chapter 2

An equilibrium model of the steam hydrogasification process and water gas shift reaction was developed using Aspen software to calculate the product gas from carbonaceous materials. Reaction temperature, pressure and feed mass ratio was varied to determine the distribution of the product gases. A H_2/C molar ratio of 1.0 and H_2O/feedstock mass ratio of 1.5 were determined to be optimum conditions when using comingled biosolids and green waste as the feedstock. The gasification temperature and pressure were set at 750^oC and 400psi, respectively. The operating condition for the WGS reactor is set at 350^oC and 150psi. The carbon conversion obtained from the steam hydrogasification at these conditions was about 80% and the CO conversion obtained from WGS reaction was over 90%. The operation pressure has no effect on the conversion in the WGS reactor. The distribution of the product gases and steam obtained from the SHR model was used

to determine the input conditions for the lab-scale WGS reactor to further investigate the performance of the commercial shift catalysts and determine the optimum condition of the WGS reaction used to apply in the RNG process.

Chapter 3

A series of experiments performed using a lab-scale facility of a high temperature shift Fe-Cr based catalyst. Approximately 65-67% of CO conversion can be obtained at the reaction temperature of 350^{o}C and space velocity of 4500 h^{-1}. A sufficient amount of H_2 after removing potential contaminants was available for recycling. Methane reforming effects at these conditions using the HTS catalyst were negligible. Methanation can be promoted over the HTS catalyst when the molar ratio of steam to carbon is below 1 and the reaction temperature is 450^{o}C.

Different levels of sulfur in the product gas was studied via the shift reactor using a commercial sour gas shift, Co-Mo based, catalyst. The activity of the WGS reaction was favored in a higher amount of sulfur. This catalyst is preferred for this process when there is a high content of sulfur in the feedstock such as coal. The CO conversion is lower when compared to a low level of sulfur environment. The steam hydrogasification using biosolids comingled with biomass as a feedstock produces a combustible gas containing 350ppm of sulfur. The optimum conditions for the SGS catalyst in this condition is a reaction temperature of 450^{o}C and the space velocity of 2500h^{-1}. The conversion of CO was about 70% with no change of CH_4 flow. The capacity of the reactor using the SGS

catalyst was about twice the size used for the HTS catalyst. Similarly, for both types of catalysts, the lower content of CO_2 in the producer gas can help improve the conversion. Thus, the sizing of the shift reactor can be reduced to obtain the same level of conversion.

Chapter 4

A new shift reactor was designed and built to implement with the bench scale BFB gasifier to demonstrate the production of RNG using the CE-CERT process. The performance of the process demonstration unit (PDU) of RNG was evaluated using a slurry feedstock of the comingled biosolids and green waste. The carbon conversion of SHR was between 35-40%. The producer gas contained 16.0-16.6% of CH_4, 4.0-4.4% of CO, 3.0-3.4% of CO_2 and 74.4-75.7% of H_2. Approximately 58-60% of CO conversion was obtained from the shift reactor using the HTS catalyst. The content of CO was decreased to 1.7-2.0% and that of CO_2 increased to 5.6-6.0%. The flow rate of CH_4 was fairly stable and the amount of H_2 increased about 3%. Based on this performance, the PDU was able to produce an energetic gas contained over 85% of CH_4.

Chapter 5

The experimental results obtained from the laboratory and PDU facilities were used to modify the Aspen simulation of the RNG process. The model of a commercial scale RNG production facility was built to observe the potential production of RNG using CE-CERT technology. For the capacity of 400 TPD of dry feed, about 117 TPD of RNG can be produced with the overall thermal efficiency of 68%. The availabilities of biosolids and

biomass in Southern California were determined to estimate the feasible supply of RNG in Southern California. If California converted the available biosolids waste stream from waste water treatment facilities to the renewable natural gas using SHR technology, it could replace up to 6% of the state's total natural gas consumption. While that may not seem large it also diverts carbonaceous matter that would be landfilled at high costs.

6.2 Recommendations

One potential area for continued research on the WGS reaction in the CE-CERT process would be to investigate LTS catalysts. A higher conversion of shift reaction could be obtained and the level of CO minimized. However, an efficient warm gas cleanup system must be applied because the catalyst is easily poisoned and deactivated.

Another area for continuation of this research is to improve the quality of the RNG to meet the natural gas pipeline specification by integrating the methanation step after the recycle of hydrogen. This process can help minimize the level of CO content in the final product gas by conversion to CH_4. Also, CO_2 can be utilized for this process which would improve climate change issues.

The problem of insufficient heat supply for the BFB gasifier needs to be investigated. A CFB gasifier should be applied for the better heating circulation and heat recovery in order to help maintain the gasification temperature and improve the carbon conversion in the SHR.

References

1. Annual Energy Outlook 2011, April, 2011, US Energy Information Administration: Washington.

2. Annual Energy Outlook 2013 with Projections to 2040, April, 2013, US Energy Information Administration: Washington.

3. World total energy consumption by region and fuel, Reference case. http://www.eia.gov/oiaf/aeo/tablebrowser/#release=IEO2013&subject=0-IEO2013&table=2-IEO2013&region=0-0&cases=Reference-d041117

4. Annual Energy Outlook 2014, Early Release Overview.

5. Natural Gas Unlocking the Low Carbon Future, International Gas Union (IGU) News, views and knowledge on gas – worldwide, September 2010.

6. Mintz, M., and Wegrzyn, J., Renewable Natural Gas: Current Status, Challenges, and Issues, A Discussion Paper for Clean Cities Coalitions and Stakeholders to Develop Strategies for the Future, September 2009.

7. Natural gas processing, http://naturalgas.org/naturalgas/processing-ng/

8. Overview of Natural Gas, http://naturalgas.org/overview/background/

9. Chemical Composition of Natural Gas, NATURAL GAS SPECS SHEET, http://www.naesb.org/pdf2/wgq_bps100605w2.pdf.

10. Ibrahim, N.K., Gas Technology Lectures 4thYear/Petroleum Refinery Engineering Branch, University of Technology Chemical Eng. Department.

11. Safe & Responsible Development, The Science Behind America's Natural Gas Production, America's Natural Gas Alliance. http://www.anga.us/media/content/F7D1441A-09A5-D06A-9EC93BBE46772E12/files/hydraulic%20fracturing%20101.pdf.

12. The Facts about Hydraulic Fracturing and Seismic Activity, Chesapeake Energy Corporation, 2012. http://www.api.org/~/media/Files/Policy/Hydraulic_Fracturing/Facts-HF-and-Seismic-Activity.pdf.

13. Warpinski, N.R., Du, J. and Zimmer, "U. Measurements of Hydraulic-Fracture Induced Seismicity in Gas Shales." Paper SPE 151597 presented at the SPE

Hydraulic Fracture Technology Conference, The Woodlands, Texas. 6-8 February 2012.

14. Pless, J., Natural Gas Development and Hydraulic Fracturing, A Policymaker's Guide, Revised June 2012.

15. Higman C. Gasification. 2nd edition. Boston: Gulf Professional; 2008. (700-1000 C)

16. Demirbas, A., Progress and recent trends in biofuels. Progress in energy and combustion science, 2007. 33(1): p. 1-18.

17. Yuan, J.S., et al., Plants to power: bioenergy to fuel the future. Trends in plant science, 2008. 13(8): p. 421-429.

18. Zidansek, A., et al., Climate changes, biofuels and the sustainable future. International Journal of Hydrogen Energy, 2009. 34(16): p. 6980-6983.

19. Low Carbon Fuel Standard State of California (USA), http://www.fao.org/bioenergy/28166-0875f073cf34442758e99e61d688c8fe2.pdf.

20. Carbon Intensity Lookup Table for Gasoline and Fuels that Substitute for Gasoline, Revised 01/06/2011.

21. McKendry, P., Energy production from biomass (part 1): Overview of biomass, Bioresource Technology, 2002, 83, 37-46.

22. Advancing Security and Sustainability through Collaboration and Diversification, America Biofuels Council, http://www.americanbiofuelscouncil.com.

23. Perlack, R.D., Stokes, B.J., Billion-ton update: Biomass supply for a bioenergy and bioproducts industry, U.S. Department of Energy, ORNL/TM-2011/224, 2011.

24. Wolfgang H. Schwarz, et al., Scientific Assessment in support of the Materials Roadmap enabling Low Carbon Energy Technologies, STRATEGIC ENERGY TECHNOLOGY PLAN, EUR 25154 EN – 2011.

25. Elbehri, A., Segerstedt, A., and Liu, P., Biofuels and the sustainability challenge: A global assessment of sustainability issues, trends and policies for biofuels and related feedstocks, FOOD AND AGRICULTURE ORGANIZATION OF THE UNITED NATIONS ROME, 2013.

26. Abboud, S., et al.,"Potential Production of Methane from Canadian Wastes," Canadian Gas Association, October 2010: http://www.cga.ca/publications/documents/PotentialProductionofMethanefromCanadianWastes-ARCFINALReport-Oct72010.pdf.

27. Ahman, M., "Biomethane in the Transport Sector – An Appraisal of the Forgotten Option," Energy Policy 38, no. 1 (January 2010): 208-217.

28. Hamberg, K., Renewable Natural Gas for Transportation, An Overview of the Feedstock Capacity, Economics, and GHG Emission Reduction Benefits of RNG as a Low-Carbon Fuel, March 2012.

29. Perry's Chemical Engineers' Handbook, 1964.

30. https://en.wikipedia.org/wiki/Anaerobic_digestion#cite_note Anaerobic_digestion-11.

31. Liu, G., et al., Biogasification of Green and Food Wastes Using Anaerobic-Phased Solids Digester system, Applied Biochem Biotechnology, 2011.

32. Rutledge, B., California Biogas Industry Assessment, WestStart-CALSTART, April 2005.

33. Hagen, M., et al., Adding Gas from Biomass to the Gas Grid, Final Report Contract No: XVII/4.1030/Z/99-412, 2001.

34. Hagen, M., et al., Adding Gas from Biomass to the Gas Grid, Final Report Contract No: XVII/4.1030/Z/99-412, 2001.

35. Reed TB, Gaur S. A Survey of Biomass Gasification, 2nd Ed. The National Renewable Energy Laboratory and Biomass Energy Foundation, Golden, CO. John Wiley & Sons; 2001.

36. Tennant JB. Overview of DOE's Gasification Program. National Energy Technology Laboratory, Department of Energy. 2012.

37. Joshi MM, Lee S. Integrated Gasification Combined Cycle-A review of IGCC technology. Energy Sources. 1996; 18: 537–568.

38. Bell D, Towler B. Coal Gasification and Its Applications. Elsevier; 2010.

39. Rezaiyan J, Cheremisinoff NP. Gasification Technologies: A Primer for Engineers and Scientists. Danver: CRC Press, Taylor and Francis Group; 2005.

40. Grieg C. ZeroGen project update: Commercial scale IGCC with CCS demonstration, managing risks and uncertainties. Gasification Technologies; 2009. Annual Conference.

41. Spath, PL, Dayton DC. Preliminary Screening-Technical and Economic Assessment of Synthesis Gas to Fuels and Chemicals with Emphasis on the Potential for Biomass-Derived Syngas. NREL/TP-510-34929. Golden, CO: National Renewable Energy Laboratory; 2003.

42. Rezaiyan J, Cheremisinoff NP. Gasification Technologies: A Primer for Engineers and Scientists. Danver: CRC Press, Taylor and Francis Group; 2005.

43. Park, C.S., et al., Bench Scale Demonstration of Substituted Natural Gas Production from Co-minlged Biosolids with Biomass Waste Using Steam Hydrogasification Process, SC-AQMD Clean Fuels Program, Final Report Contract Number: 10125 CE-CERT, March 2011.

44. Park, C.S., et al., Production of Substituted Natural Gas from the Wet Organic Waste by utilizing PDU-scale Steam Hydrogasification Process, Final Report PIER, October 2012, CEC-500-2013-104.

45. Jeon, S., et al., Characteristics of steam hydrogasification of wood using a micro-batch reactor. Fuel, 2007. **86**(17-18): p. 2817-2823.

46. Gray, D., et al., Increasing Security and Reducing Carbon Emissions of the U.S. Transportation Sector: A Transformational Role for Coal with Biomass, National Energy Technology Laboratory, 2007.

47. Callaghan, C. A., Kinetics and Catalysis of the Water-Gas-Shift Reaction: A Microkinetic and Graph Theoretic Approach. 2006.

48. Ertl, G. K., H. Weitkamp, J., Water Gas Shift and COS removal. Handbook of Heterogeneous Catalysis, 4: 1831-1841.

49. Liu, K. S., C. and Subramani, V., Hydrogen and Syngas Production and Purification Technologies, 2010: 311-328.

50. Luengnaruemitchai, A. O., S. Gulari, E., Comparative studies of low temperature water-gas shift reaction over Pt/CeO2, Au/CeO2 and Au/Fe2O3 catalysts. Catalysis Communication, 2003, 4: 215-221.

51. Ratnasamy, C. a. W., J.P., Water Gas Shift Catalysis. Catalysis Reviews, 2009, 51(3): 325-440.

52. National Association of Clean Water Agencies (NACWA), Renewable Energy Resources: Banking on Biosolids, 2010.

53. Rulkens, W. H., Bien, J. D., Recovery of energy from sludge-Comparison of the various options. Water Science Technology, 2004, 50, 213-221.

54. Lu, X., Development and Application of Advanced Models for Steam Hydrogasification: Process Design and Economic Evaluation, [dissertation]. California: University of California Riverside; 2012.

55. D.Fytili, A. Z., *Utilization of sewage sludge in EU application of old and new methods-a review.* Renewable and Sustainable Energy Reviews, 2008, 12: 116-140

56. U.S. Environmental Protection Agency, Biosolids generation, use, and disposal in the United States, EPA530-R-99-009, 1999.

57. U.S. Environmental Protection Agency, Emerging Technologies for Biosolids Management, EPA 832-R-06-005, 2006.

58. Claassen, P.A.M., et al., Utilization of biomass for the supply of energy carriers, Applied Microbiology Biotechnology, 1999, 52, 741-755.

59. Nipattummakul, N., et al., Hydrogen and syngas production from sewage sludge via steam gasification, International Journal of Hydrogen Energy, 2010, 35(21), 11738–11745.

60. Woei, S., et al., Production of hydrogen-rich syngas from steam gasification of blend of biosolids and wood using a dual fluidised bed gasifier, Fuel, 2012. 93, 473–478.

61. Wei He, C. S. P., Norbeck, J.M., Steam hydrogasification of comingled municipal sewage sludge and biomass to produce synthetic fuels. Report for public works department, Riverside, 2009.

62. Wei He, C. S. P., Norbeck, J. M., Rheological study of comingled biomass and coal slurries with hydrothermal pretreatment. Energy Fuels, 2009, 23: 4763–4767.

63. Manual of Aspen Physical Property System, Physical Property Models, Version Number: V7.3, March 2011.

64. C.S. Park, S.P. Singh, J.M. Norbeck, Steam hydrogasification of carbonaceous matter to liquid fuels, Proceedings of the 24th Annual International Pittsburgh Coal Conference, Johannesburg, South Africa, 2007.

65. Hakkarainen, R., S. T. and Keiskib, R.L., *Comparison of the dynamics of the high-temperature water-gas shift reaction on oxide catalysts*. Catalysis Today, 1994, 20: 395-408

66. Lu, Xiaoming, Development and Application of Advanced Models for Steam Hydrogasification: Process Design and Economic Evaluation, Dissertations for Ph.D of Chemical and Environmental Engineering UC Riverside December 2012.

67. Hakkarainen, R., S. T. and Keiskib, R.L., *Water-gas shift reaction on a cobalt-molybdenum oxide catalyst*. Applied Catalysis A: General, 1993, 99: 195-215.

68. Park, C.S., Kim, S., Thanmongkhon Y., Investigation of a New Process for SNG Production using Steam Hydrogasification, Final Report Grant #: 57237A/11-02G, October 2013.

69. Callaghan, C. A., *Kinetics and Catalysis of the Water-Gas-Shift Reaction: A Microkinetic and Graph Theoretic Approach*. 2006

70. Ladebeck, J. R. a. W., J.P., *Catalyst development for water-gas shift*. Handbook of Fuel Cells – Fundamentals, Technology and Applications, 2003, 3(2): 190-201.

71. Demirbas, A., *Biomass resource facilities and biomass conversion processing for fuels and chemicals.* Energy Conversion & Management, 2001, 42(11): 1357-1378

72. Gray, D., *Increasing Security and Reducing Carbon Emissions of the US Transportation Sector: Transformational Role for Coal with Biomass*. 2010: DIANE Publishing

73. Twigg, M.V., Catalyst Handbook, 2ed., Wolfe Publishing Ltd., 1989.

74. Rhodes, C., Hutchings, G.J., Ward, A.M., Water gas shift reaction: finding the mechanistic boundary, Catalysis Today, 23, 1995, 43-58.

75. Srinivas, G., Gebhard S.C., Selective Catalysts for Hydrogen Sulfide Oxidation in Natural Gas – Concept to Commercialization, TDA Research, Inc.

76. Osa de la, A.R., et al., Performance of a sulfur-resistant commercial WGS catalyst employing industrial coal-derived syngas feed, International Journal of Hydrogen, 36(1), 2011, 44–51.

77. General catalogue from SUD-CHEMIE catalyst: 97-99.

78. Catalyst Specification Sheet for ShiftMax120.

79. C12-4 Start-up/Shut-down operation manual from SUD-CHEMIE: 1-10.

80. Scott, A., et al., Improving the detection limit of a quadrupole mass spectrometer, J. Vacuum Science & Technology, 2001, A19, 1032.

81. Singh, H., et al., Mass spectrometric detection of reactive neutral species: Beam-to background ratio, Journal of Vacuum Science & Technology, 1999, A17, 2447.

82. K. Kim, S.K. Jeon, C.Vo, Removal of hydrogen sulfide from a steam-hydrogasifier product gas by zinc oxide sorbent. Ind. Eng.Chem.Res. 2007,46,5848-5854.

83. San Shwe Hla, G. J. D., D.Park, Kinetics of high temperature water-gas shift reaction over two iron-based commercial catalysts using simulated coal–derived syngas. Chemical Engineering Journal, 2009, 146: 148-154.

84. San Shwe Hla, G. J. D., Catalysts for water gas shift processing of coal-derived syngas. ASIA Pacific Journal of Chemical Engineering, 2010.

85. U.S. Energy Information Administration. Improvement in power generation with post-combustion capture of CO_2. IEA Greenhouse Gas R&D Programme, November 2004. Report PH4/33.

86. Park, C.S., Kim, S., Thanmongkhon Y., Investigation of a New Process for SNG Production using Steam Hydrogasification, Final Report Grant #: 57237A/11-02G, October 2013.

87. Ross, J.R.H., Metal Catalysed Methanation and Steam Reforming.

88. Munster, P. and Grabke,H.J., Kinetics of the Steam Reforming of Methane with Iron, Nickel and Iron-Nickel Alloys as Catalysts, Journal of Catalysis 72, 1981, 279-287.

89. Singh, H., et al., Mass spectrometric detection of reactive neutral species: Beam-to background ratio, Journal of Vacuum Science & Technology, 1999, A17, 2447.

90. Liu, Zhongzhe, Development of a Sorption Enhanced Steam Hydrogasification Process for In-situ Carbon Dioxide (CO2) Removal and Enhanced Synthetic Fuel Production, Dissertations for Ph.D of Chemical and Environmental Engineering UC Riverside March 2014.

91. Lu X., Suemanotham A., Park C. S., Norbeck J.M., Techno-economic Analysis of Synthetic Fuel Production from Microalgae by Steam Hydrogasification, California Energy Commission, Algae biofuel life cycle analysis project, December 2011.

92. Luo, Qian, The Development of Warm Gas Cleanup Technologies for the Removal of Sulfur Containing Species from Steam Hydrogasification, Dissertations for Ph.D of Chemical and Environmental Engineering UC Riverside December 2012.

93. Fan, Xin, Investigation of the Effect of In-Situ Catalyst on the Steam Hydrogasification of Biomass, Dissertations for Ph.D of Chemical and Environmental Engineering UC Riverside December 2012.

94. Maroño, M., Sánchez, J.M., Ruiz E., Hydrogen-rich gas production from oxygen pressurized gasification of biomass using a Fe–Cr Water Gas Shift catalyst, International Journal of Hydrogen Energy, 35(1), 2011, 37–45.

95. Sanjaya, D., at el., Water gas shift and CO Methanation reactions over Ni-CeO2(111) catalyst. Top Catalyst, 2011, 54, 34-41.

96. Operating Manual ShiftMax820/821/822, Clariant International, 2013.

97. Hla S.S,, Investigation into the performance of a Co–Mo based sour shift catalyst using simulated coal-derived syngases, International Journal of Hydrogen Energy, 36(11), 2011, 6638–6645.

98. Frank P., Sulfur tolerant shift catalyst-dealing with the bottom of the barrel problem, 2003, Johnson Matthey Rep 659W/099/REF.

99. Boon, J., et al., Water-Gas Shift Kinetics over FeCr-based Catalyst: Effect of Hydrogen Sulphide, Hydrogen & Clean Fossil Fuels, Rnrg research Centre of the Netherlands.

100. Elder, T. and Groom L.H., Pilot-scale gasification of woody biomass, Biomass and Bioenergy, 35, 2011, 3522-3528.

101. Sheth, P.N. and Babu, B.V., Production of hydrogen energy through biomass (waste wood) gasification, International Journal of Hydrogen Energy, 35(19), 2010, 10803–10810.

102. Judex et al., Gasification of dried sewage sludge: Status of the demonstration and the pilot plant, Waste Management, 32(4), 2012, 719–723.

103. Mozaffarian, M., Zwart, R.W.R., Production of Substitute Natural Gas by Biomass Hydrogasification, Netherlands Energy Research Foundation, ECN.

104. Reed TE. Biomass gasification: Principles and technology. Energy Technology, Review. 1981; 67: 401.

105. Raju ASK, Park CS, Norbeck JM. Synthesis gas production using steam hydrogasification and steam reforming. Fuel Processing Technology. 2009; 90(2): 330–336.

106. Basu, P., Combustion and Gasification in Fluidized Beds, CRC Press, 2006.

107. MSDS: Silica Sand and Ground Silica.

108. Non-dispersive infrared analyzer Manual.

109. Yun MY, Bae DH, Park CS, Norbek JM. Development of circulating fluidized bed reactor for the steam hydrogasification of low ranked fuel. US-Korea Conference on Science, Technology and Entrepreneurship. 2012.

110. Larry A. Bissett. Hot/Warm Gas Cleanup. U.S. DOE Technical report.

111. California 2008 Statewide Waste Characterization Study. California Integrated Waste Management Board, 2009.

112. Williams, R., Gildart, M., California Biomass Reporting System, database from California Biomass Collaborative and California Energy Commission, Davis, CA, 2007. http://biomass.ucdavis.edu/tools.html.

113. Jenkins, B., Williams, R.B., Kaffka, S., An Assessment of Biomass Resources in California, 2007: Draft Report, report contract number 500-01-016 prepared for California Energy Commission, Davis, CA, March 2008, http://biomass.ucdavis.edu/materials/reports%20and%20publications/2008/CBC_Biomass_Resources_2007.pdf.

114. California Waste Stream Profiles, database from California Integrated Waste Management Board, Sacramento, CA, October 2007, http://www.ciwmb.ca.gov/Profiles/

115. U.S. Energy Information Administration (U.S.E.I.A), California Natural Gas Consumption. 2012.

116. An Assessment of Biomass Resources in California, by CEC Mar 2008.

117. Management, W. NGVs Run on Low-Carbon Renewable Fuel. 2012; Available from: http://cngvc.org/why-ngvs/renewable-fuel.php.

118. Krich, K., Augenstein, D., etc. Biomethane from Dairy Waste: A Sourcebook for the Production and Use of Renewable Natural Gas in California. Western United Dairymen. 2005.

119. Zwart, R.W.R., Boerrigter H., Production of Synthetic Natural Gas (SNG) from Biomass: Development and operation of an integrated bio-SNG system. Energy Research Center of the Netherlands. 2006.

120. Chandel, M., Williams, E., Synthetic Natural Gas (SNG): Technology, Environmental Implications, and Economics. Duke University, 2009.

121. Bartone, L.M., White, J. Industrial Size Gasification for Syngas, Substitute Natural Gas and Power Production. National Energy Technology Laboratory (NETL). 2007.

Appendices

Table A-1 Description of the process demonstration unit of SHR system

Item	Part No.	Description
1	TC-1	Thermal couple measured temperature at the bottom of the reactor
2	TC-2	Thermal couple measured temperature in the middle of the reactor
3	TC-3	Thermal couple measured temperature in the middle of the reactor
4	TC-4	Thermal couple measured temperature in the middle of the reactor
5	TC-5	Thermal couple measured temperature at the top of the reactor
6	TC-6	Thermal couple measured temperature before the heat exchanger
7	TC-7	Thermal couple measured temperature after the heat exchanger
8	V-001	Valve used to isolate Hydrogen supply
9	V-002	Valve used to isolate Nitrogen supply
10	V-003	Valve used to isolate Chiller tank
11	V-004	Valve use to isolate condenser 2
12	V-005	Valve used to drain condenser 2
13	V-006	Valve used to drain cylinder 1
14	V-007	Valve used to isolate condenser 3
15	V-008	Valve use to isolate condenser 2
16	V-009	Valve used to isolate NDIR
17	V-010	Valve used to close vent
18	V-011	valve used to isolate Pump 2
19	PT-1	Pressure transducer used to measure pressure at the bottom of the reactor
20	PT-2	Pressure transducer used to measure pressure at the top of the reactor
21	PDIT-1	Pressure differential used to measure different pressure between the top of bottom of the reactor
22	PDIT-2	Pressure differential used to measure the volume flow rate of product gas when it passed through a venturi flow meter
23	BPR	Back Pressure Regulator used to keep reactor at desired pressure
24	NDIR	Non Dispersive Infrared Sensor for measuring the percentage of CH_4, CO, CO_2
25	DGM	Dry Gas Meter for measuring flow rate of gas
26	Condenser 1	Condenser for collecting condensate water
27	Condenser 2	Condenser for collecting condensate water

28	Condenser 3	Condenser for collecting condensate water
29	Cyclone	Cyclone used to separate solid particles from the gases
30	Cylinder 1	Collect all the solid particles from the cyclone
31	Chiller Tank	Water tank used to hold the water that will be pump through heat exchanger
32	Heat Exchanger	Heat Exchanger used to cool down gases and also convert steam back to water
33	HTR/control	Thermal couple/heater controller control the temperature of all heaters
34	Steam Pump	Water pump for injecting steam into the reactor
35	Pump 2	Slurry feed pump for handling the feedstock to the reactor
36	Reactor	3.5" ID with 14 ft. long of the reactor made from Inconel pipe

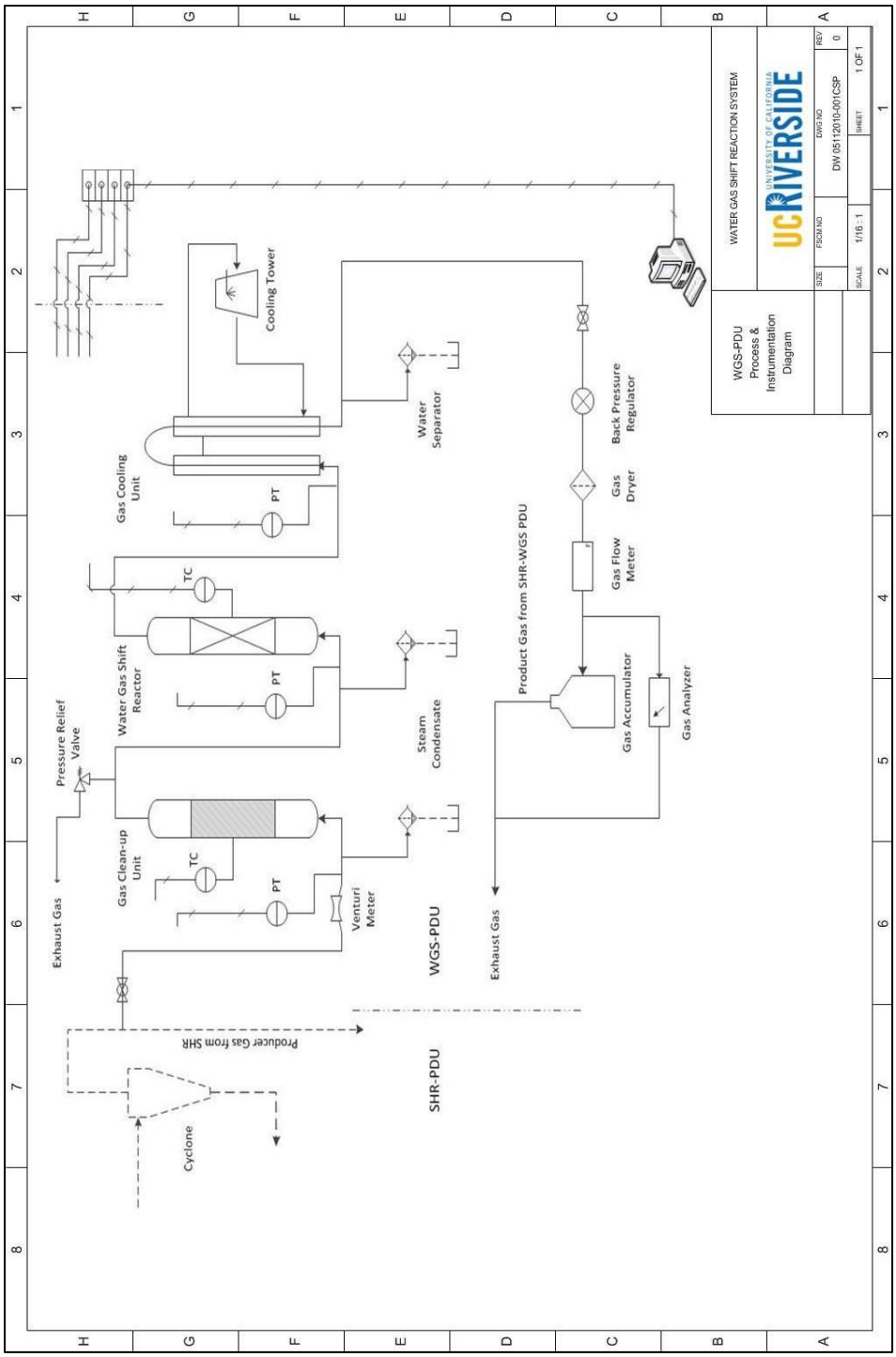

Figure A-1 Process diagram of WGS reactor system

Table A-2 Description of the process demonstration unit of WGS system

Item	Part No.	Description
1	TC1	Thermal couple measured temperature of gas inlet
2	TC2	Thermal couple measured temperature at the bottom the reactor
3	TC3	Thermal couple measured temperature at the middle of the reactor
4	TC4	Thermal couple measured temperature at the top of the reactor
5	TC5	Thermal couple measured temperature at the top of catalyst bed
6	PT1	Pressure transducer measured pressure at the bottom of the reactor
7	PT2	Pressure transducer measured pressure at the top of the reactor
8	Reactor	1" ID with 6 ft. long of the reactor made from 316 stainless steel tube
9	HE	Heat Exchanger for cooling down gases and convert steam back to water
10	BPR	Back Pressure Regulator for maintaining desired pressure in reactor
11	GWS	Gas and Water separator
12	DGF	Dry gas flow meter
13	RGA	Residue gas analyzer for analysis the composition of product gas

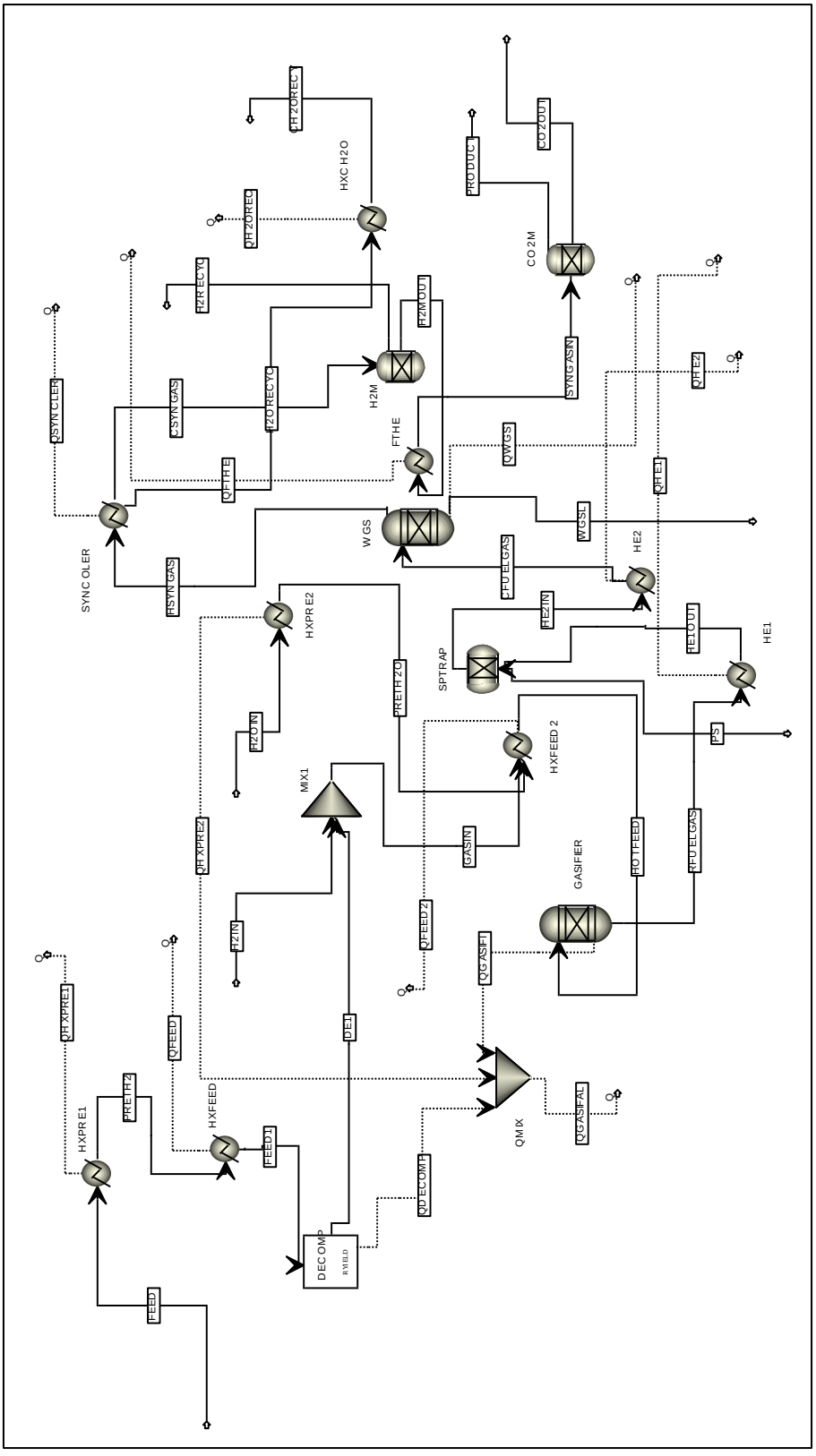

Figure A-2 Block flow diagram of Aspen simulation for RNG production based on SHR-WGS

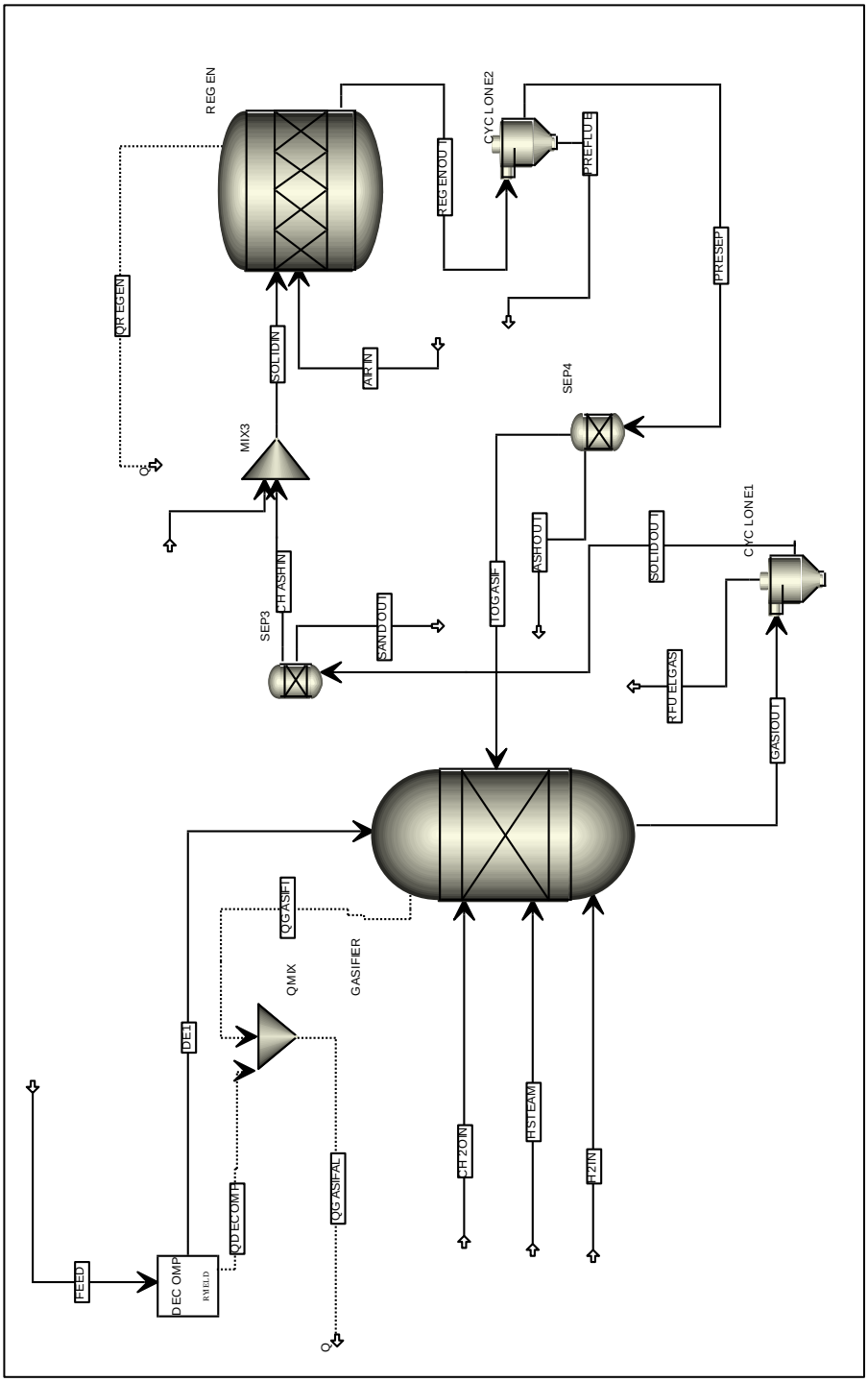

Figure A-3 Block flow diagram of Aspen simulation for a circulating fluidized bed gasifier